

University of Groningen

Glutamate Transporter Inhibitors with Photo-Controlled Activity

Hoorens, Mark W. H.; Fu, Haigen; Duurkens, Ria H.; Trinco, Gianluca; Arkhipova, Valentina; Feringa, Ben L.; Poelarends, Gerrit J.; Slotboom, Dirk J.; Szymanski, Wiktor

Published in:
Advanced Therapeutics

DOI:
[10.1002/adtp.201800028](https://doi.org/10.1002/adtp.201800028)

IMPORTANT NOTE: You are advised to consult the publisher's version (publisher's PDF) if you wish to cite from it. Please check the document version below.

Document Version
Final author's version (accepted by publisher, after peer review)

Publication date:
2018

[Link to publication in University of Groningen/UMCG research database](#)

Citation for published version (APA):

Hoorens, M. W. H., Fu, H., Duurkens, R. H., Trinco, G., Arkhipova, V., Feringa, B. L., Poelarends, G. J., Slotboom, D. J., & Szymanski, W. (2018). Glutamate Transporter Inhibitors with Photo-Controlled Activity. *Advanced Therapeutics*, 1(2), [1800028]. <https://doi.org/10.1002/adtp.201800028>

Copyright

Other than for strictly personal use, it is not permitted to download or to forward/distribute the text or part of it without the consent of the author(s) and/or copyright holder(s), unless the work is under an open content license (like Creative Commons).

The publication may also be distributed here under the terms of Article 25fa of the Dutch Copyright Act, indicated by the "Taverne" license. More information can be found on the University of Groningen website: <https://www.rug.nl/library/open-access/self-archiving-pure/taverne-amendment>.

Take-down policy

If you believe that this document breaches copyright please contact us providing details, and we will remove access to the work immediately and investigate your claim.

Downloaded from the University of Groningen/UMCG research database (Pure): <http://www.rug.nl/research/portal>. For technical reasons the number of authors shown on this cover page is limited to 10 maximum.

DOI: 10.1002/ ((please add manuscript number))

Article type: Full Article

Title Glutamate Transporter Inhibitors with Photo-controlled Activity

*Mark W. H. Hoorens[#], Haigen Fu[#], Ria H. Duurkens, Gianluca Trinco, Valentina Arkhipova, Ben L. Feringa, Gerrit J. Poelarends, Dirk J. Slotboom, Wiktor Szymanski**

[#] These authors contributed equally to this work

M. W. H. Hoorens, Dr. W. Szymanski

1 Department of Radiology, University of Groningen, University Medical Center Groningen, Hanzeplein 1, 9713 GZ, Groningen, The Netherlands

E-mail: w.szymanski@umcg.nl

M. W. H. Hoorens, Prof. B. L. Feringa, Dr. W. Szymanski

2 Centre for Systems Chemistry, Stratingh Institute for Chemistry, Faculty of Science and Engineering, University of Groningen, Nijenborgh 7, 9747 AG Groningen, The Netherlands

H. Fu, Prof. G. J. Poelarends

3 Department of Chemical and Pharmaceutical Biology, Groningen Research Institute of Pharmacy, University of Groningen, Antonius Deusinglaan 1, 9713 AV, Groningen, The Netherlands

R. H. Duurkens, G. Trinco, Dr. V. Arkhipova, Prof. D. J. Slotboom

4 Department of Biochemistry, Groningen Biomolecular Sciences and Biotechnology Institute, Nijenborgh 4, 9747 AG Groningen, The Netherlands

Keywords: Glutamate transport, photopharmacology, azobenzene, photo-controlled inhibitor

Abstract

Glutamate is an important signaling molecule in the nervous system and its extracellular levels are regulated by amino acid transporters. Studies on the role of glutamate transport have benefitted from the development of small molecule inhibitors. Most inhibitors, however,

cannot be remotely controlled with respect to the time and place of their action, which limits their application in cell and tissue studies. Here we show the development and evaluation of inhibitors of the prokaryotic transporter Glt_{TK} with photo-controlled activity, enabling the remote, reversible and spatiotemporally resolved regulation of transport. Based on a known inhibitor, **TFB-TBOA**, seven **azo-TBOAs**, bearing a photoswitchable azobenzene moiety, were designed and synthesized. The most promising photo-controlled inhibitor, ***p*-MeO-azo-TBOA**, showed in its non-irradiated form an IC_{50} of $2.5 \pm 0.4 \mu\text{M}$ for transport by Glt_{TK}. Photoswitching resulted in a reversible drop of potency to an IC_{50} of $9.1 \pm 1.5 \mu\text{M}$. This 3.6-fold difference in activity was used to demonstrate that by irradiation the transporter function can be switched on and off reversibly. The photo-controlled inhibitors reported here could be a powerful tool in studying the role of glutamate transport by precisely controlling at which time and in which tissue or groups of cells the inhibitor is active.

1. Introduction

Glutamate transporters belong to a large family of membrane proteins that catalyze co-transport of the substrate (glutamate/aspartate/neutral amino acid) and cations.^[1,2] Glutamate is an important precursor in the biosynthesis of purines, glutamine, proline, arginine, alpha-ketoglutarate and glutathione.^[3,4] Most importantly, in the human Central Nervous System (CNS), glutamate is a neurotransmitter: In order to pass a signal, the pre-synaptic neuron releases glutamate via exocytosis, upon which glutamate is sensed by receptors on the post-synaptic neuron.^[5] Subsequently, glutamate is removed by glutamate transporters, known as Excitatory Amino Acid Transporters (EAATs), to attenuate the signal.^[6] Accumulation of glutamate in the synapse results in elevated neuroplasticity and is involved in the development of several neuro-degenerative diseases.^[7]

Mammalian glutamate transporters belong to the SLC1 family of membrane proteins, which is present in all the kingdoms of life, and includes the archaeal aspartate transporters Glt_{Ph} and Glt_{Tk}.^[1,2] Much of our understanding of the transport mechanism of the glutamate transporters has come from structural studies of Glt_{Ph} and Glt_{Tk}^[8–16] that are structurally and mechanistically similar to the mammalian proteins,^[17,18] however can transport only aspartate, while EAATs can use both aspartate and glutamate as a substrate.^[19]

Mechanistic studies on the role of glutamate transport are facilitated by the use of small molecule inhibitors.^{[6][20,21]} *L-threo*- β -Benzyloxyaspartate (**TBOA**) and (*L-threo*)-3-[3-[4-trifluoromethyl)benzoylamino]benzyloxy]aspartate (**TFB-TBOA**) are aspartate derivatives that are most commonly used to study the role of glutamate transporters in the CNS.^[22,23] An impressive example was published by Xie *et al*,^[24] where a window was installed in the skull of a mouse that was genetically modified with a fluorescent glutamate reporter protein. Upon delivering a light pulse to the eye of the mouse, increased glutamate levels were observed shortly in the visual cortex. After injection of glutamate transporter inhibitor **TBOA**, the level of glutamate was higher and clearance was slower.^[24]

However, in experiments such as the one described above, the inhibition of glutamate transport by **TBOA** and **TFB-TBOA** is systemic and it cannot be excluded that compensation effects occur. Furthermore, due to systemic inhibition, it is difficult to study the physiology of glutamate transporters in a specific organ, tissue or group of cells of interest. To overcome this limitation, control over the activity of the inhibitor with an external stimulus would be highly desirable as it would allow to reversibly turn the inhibitor on and off at specific organs, tissues and cells at any chosen time and in a reversible manner. Such a remotely-controlled inhibitor would contribute to a better understanding of the role of the glutamate transporters in health and disease, as also exemplified by a recent report by Trauner and Kavanaugh in which one of the molecules reported here was evaluated on human EAATs.^[25]

In recent years, bio-active molecules have been developed that can be switched on and off with light as an external stimulus (**Figure 1**), along the principles of photopharmacology.^[26–28] Photo-control over biological activity can be achieved by the introduction of a molecular photoswitch, such as azobenzene,^[29] into the structure of the molecule. Thermally stable *trans*-azobenzene (See **Figure 2** in blue) is a linear, (near) flat molecule; irradiation with UV light results in the isomerization of the azo bond and gives *cis*-azobenzene, which is less stable, non-planar, has a higher dipole moment^[29,30] and is more soluble in aqueous solutions than the *trans* isomer.^[31] *Trans* to *cis* isomerization can be reversed by irradiation with visible light, however the *cis-trans* isomerization also happens spontaneously on a time-scale of milliseconds to years, depending on the azobenzene structure.^[29,30] Since *trans*-azobenzene and *cis*-azobenzene strongly differ in structure and polarity, they have the potential to differently influence the activity of a bio-active molecule into the structure of which they have been incorporated. This enables the reversible photoswitching between the forms of a photo-active molecule with different potency.^[26–28] A schematic view of possible photo-control over glutamate transporter activity using a photo-controlled inhibitor is shown in Figure 1. The glutamate transporter facilitates the transport of substrate, together with sodium ions.^[12,16] The inhibitor has two states, an inactive state (yellow) that does not bind to the transporter and an active state (green) that blocks transport. Light of specific wavelengths can be used to switch between the two states of the inhibitor and hereby a reversible photo-control over transport can be achieved, offering additional advantages of high spatiotemporal resolution possible in light delivery and the low toxicity of photons to biological systems.^[27] This approach has been successfully demonstrated in developing photo-controlled antibiotics,^[32,33] anticancer drugs^[17–22] and receptor ligands,^[40–49] among others.

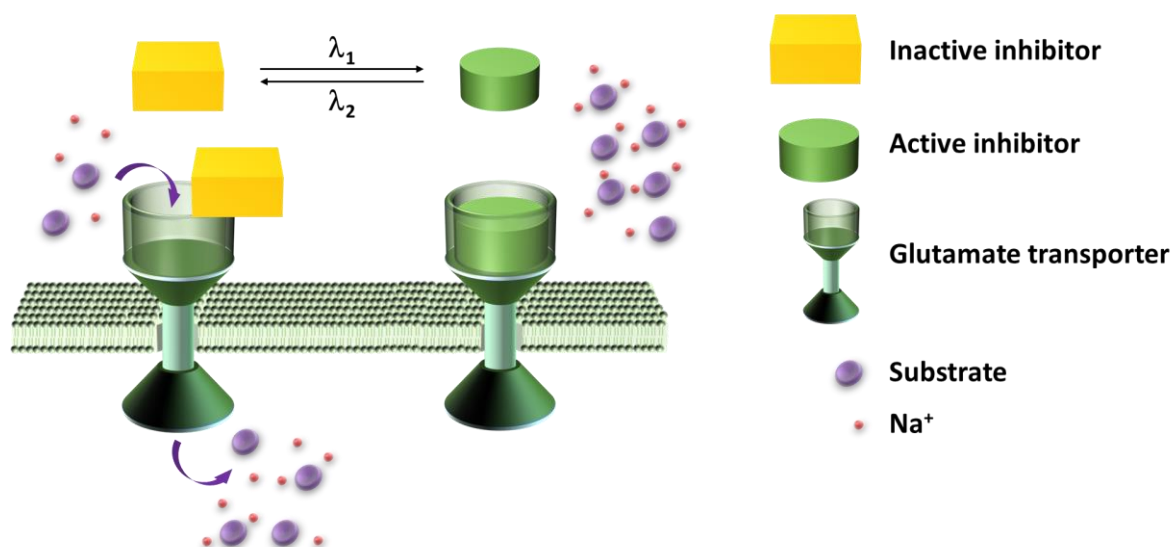


Figure 1: Schematic view of photo-control over glutamate transporter activity, along the principles of photopharmacology. The yellow box represents an inactive inhibitor, which does not block the transport of the substrate (purple). By irradiation with light of λ_1 , the active inhibitor can be locally formed (green cylinder), which blocks substrate transport. This process is reversible by irradiation with wavelength λ_2 .

Here we present the synthesis and evaluation of seven analogues of **TBOA** and **TFB-TBOA** with photo-controlled activity. The compounds were prepared using a key enzymatic step to ensure high stereocontrol in the synthesis of enantiopure precursor. Subsequently, the photochemical properties were studied and biological activity was determined using the archaeal aspartate transporter Glt_{TK}. ***p*-MeO-azo-TBOA** and ***p*-HexO-azo-TBOA** showed the best photochemical properties, in which nearly full conversion from *trans* to *cis* isomer can be achieved upon irradiation. The largest difference in activity between *trans* and *cis* isomers was observed for ***p*-MeO-azo-TBOA** and this difference was successfully used to reversibly control the transport rate by light *in situ*.

2. Results and Discussion

2.1 Design and synthesis of glutamate transporter inhibitors

Our design of photoswitchable inhibitors is based on a known EAAT inhibitor **TFB-TBOA** (Figure 2),^[50] which has been widely used to study glutamate transport in the CNS.^[20,21] To render **TFB-TBOA** photoresponsive, we replaced the amide bond by a diazo moiety (Figure 2), in a photopharmacological approach known as azologization.^[51] An extensive SAR of **TBOA** has been described^[50] on EAAT2 and EAAT3 and it demonstrated that substituents at the *para* position are beneficial for the potency. **TFB-TBOA** (*p*-CF₃) has an affinity of 1.9 nM and 28 nM for EAAT2 and EAAT3, respectively. Other potent inhibitors disclosed in the SAR study have either *p*-HexO (1.2 nM for EAAT2, 18 nM for EAAT3), *p*-MeO (12 nM for EAAT2 and 266 nM for EAAT3) or *p*-CF₃O (7 nM for EAAT2 and 128 nM for EAAT3) substituents at the *para* position. With those high potencies in mind, ***p*-CF₃-azo-TBOA**, ***p*-HexO-azo-TBOA**, ***p*-MeO-azo-TBOA** and ***p*-CF₃O-azo-TBOA** (Figure 2) were synthesized and evaluated in our study. The choice of MeO and HexO substituents was further expected to be beneficiary, since alkyloxy substituents in the *para* position of azobenzene often result in good band separation of the isomers, enabling nearly full isomerization to *cis* upon irradiation.^[52] To evaluate the importance of the position on the ring, further **azo-TBOAs** with methyl substituents on the *ortho*, *meta* and *para* position were designed (Figure 2). Due to the difference in electronic properties and structure, all the substituents likely influence both the biological activity of *cis* and *trans* isomers and the photochemical properties such as the maximum wavelength of absorption, photo-stationary states (PSS) and half-life of the *cis* isomer. Finally, we also sought to evaluate the *p*-CF₃ substituted compound, which is the closest to the original **TFB-TBOA** structure, inspired by a recent report by Trauner and Kavanaugh.^[25] In their study, differences in activity between *trans* and *cis* isomers were observed on oocytes overexpressing either EAAT1, EAAT2 or EAAT3 by measuring membrane voltage. The photo-controlled glutamate transporter inhibitor was more potent in the *trans* configuration than in *cis* form.

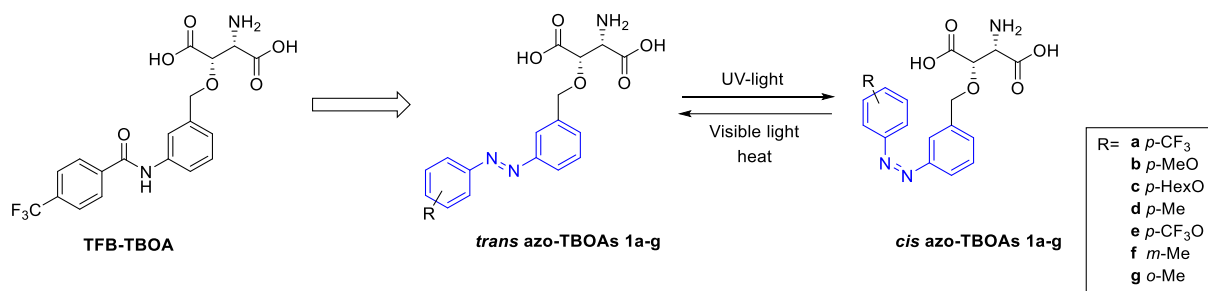


Figure 2: TFB-TBOA and designed photoswitchable glutamate transporter inhibitors azo-TBOAs, with the photoswitch azobenzene marked in blue.

The **azo-TBOAs** were prepared in a convergent synthesis, where the alkylating agents **4a-g** and the chiral building block **17** were synthesized separately and coupled at a late stage in the synthetic route (**Figure 3**). The alkylating agents **4a-g**, containing the azobenzene photoswitch, were synthesized using standard procedures, as described in Figures S2, S3 and S4. The chiral building block **17** was synthesized using an enzymatic reaction, in which an optimized mutant of methylaspartate ammonia lyase (MAL)^[53,54] stereoselectively aminates 2-(benzyloxy)fumaric acid **13** to (2*S*,3*S*)-2-amino-3-(benzyloxy)succinic acid **14**.^[55] Subsequently, the free amine and carboxylic acid groups of compound **14** were protected and, after debenzylation, the reaction of the alcohol moiety in **17** with bromides **4a-g**, followed by global deprotection, gave final compounds **1a-g** (**azo-TBOAs**).

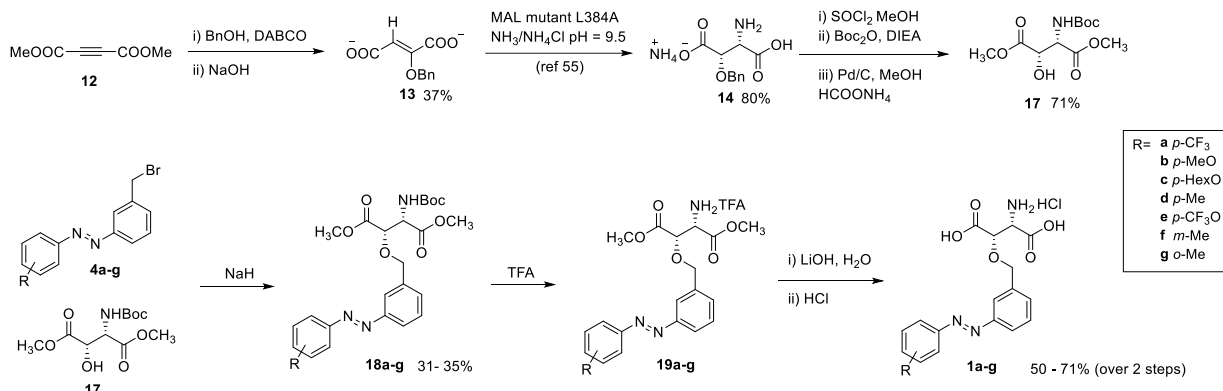


Figure 3: Synthesis of azo-TBOAs

2.2 Photochemical properties of photoswitchable glutamate transporter inhibitors

Next, the photochemical properties of the **azo-TBOAs** were analyzed (**Figure 4**). As determined by UV/VIS spectroscopy, all compounds absorb in the UV region, where *trans-p*-**MeO-azo-TBOA** and *trans-p*-**HexO-azo-TBOA** have an absorption maximum in DMSO of 355 nm and 353 nm, respectively (Figures 4B, S46 and S53). All other *trans-azo-TBOAs* have an absorption maximum in the 317 - 332 nm region (Figures S41, S57, S61, S65 and S69), slightly more blue-shifted than *p*-**HexO-azo-TBOA** and *p*-**MeO-azo-TBOA**. All **azo-TBOAs** could be switched for several cycles in DMSO with little fatigue observed (Figures 4C, S51, S55, S59, S63, S67 and S71). Using ^1H NMR spectroscopy, the photo-stationary states (PSS) of all **azo-TBOAs** in DMSO were determined, providing information on how much of the compound can be switched to the *cis* isomer upon irradiation in DMSO as a solvent. As expected, *p*-alkyloxy substituted azobenzenes *p*-**MeO-azo-TBOA** and *p*-**HexO-azo-TBOA** showed excellent PSS: irradiation with 365 nm light results in nearly full isomerization to the *cis* isomer (Figure 4D, S56). In contrast, *p*-**CF₃O-azo-TBOA** shows a PSS with only 71% *cis* present upon irradiation with 312 nm light. Irradiation of *p*-**Me-azo-TBOA**, *m*-**Me-azo-TBOA** and *o*-**Me-azo-TBOA** resulted in a PSS containing 93%, 86% and 90% of the *cis* isomer, respectively (Figure S60, S68 and S72).

Surprisingly, *p*-**CF₃-azo-TBOA**, reported earlier,^[25] was in our hands unstable and small shifts in the spectra upon five cycles of irradiation were observed (Figure S45). When determining the PSS upon irradiation in DMSO by ^1H NMR spectroscopy, formation of side products was observed (Figures S43 and S44), which was not reported before.^[25] However, it must be noted that we used different wavelengths of irradiation (312 nm and 365 nm vs. 350 nm^[25]) and the shifts in the spectrum are mainly observed for switching in DMSO and not in 50 mM KPi buffer (pH 7.4). For all other compounds, no photodegradation was observed. To confirm that the excellent switching behavior extends to biologically relevant solvents, *p*-**MeO-azo-TBOA** was dissolved in 50 mM KPi buffer (pH 7.4) and switching was studied with UV/VIS spectroscopy, showing very similar properties to those in DMSO (Figure S49,

S50 and S51). To evaluate the rate of thermal *cis-trans* relaxation, half-lives for all compounds were determined in DMSO at 37 °C. For all **azo-TBOAs**, a half-life at 37 °C in DMSO of > 10 h was observed, showing that the *cis* isomer is relatively stable. The half-life of the *cis* isomer of ***p*-MeO-azo-TBOA** in 50 mM KPi buffer (pH 7.4) at 37 °C is approximately 6 h (Figure S50), which is shorter than in DMSO, but the isomer is still relatively stable on the timescale (4 -12 min) of the experiments that were used to evaluate the biological activity of **azo-TBOAs** (*vide infra*).

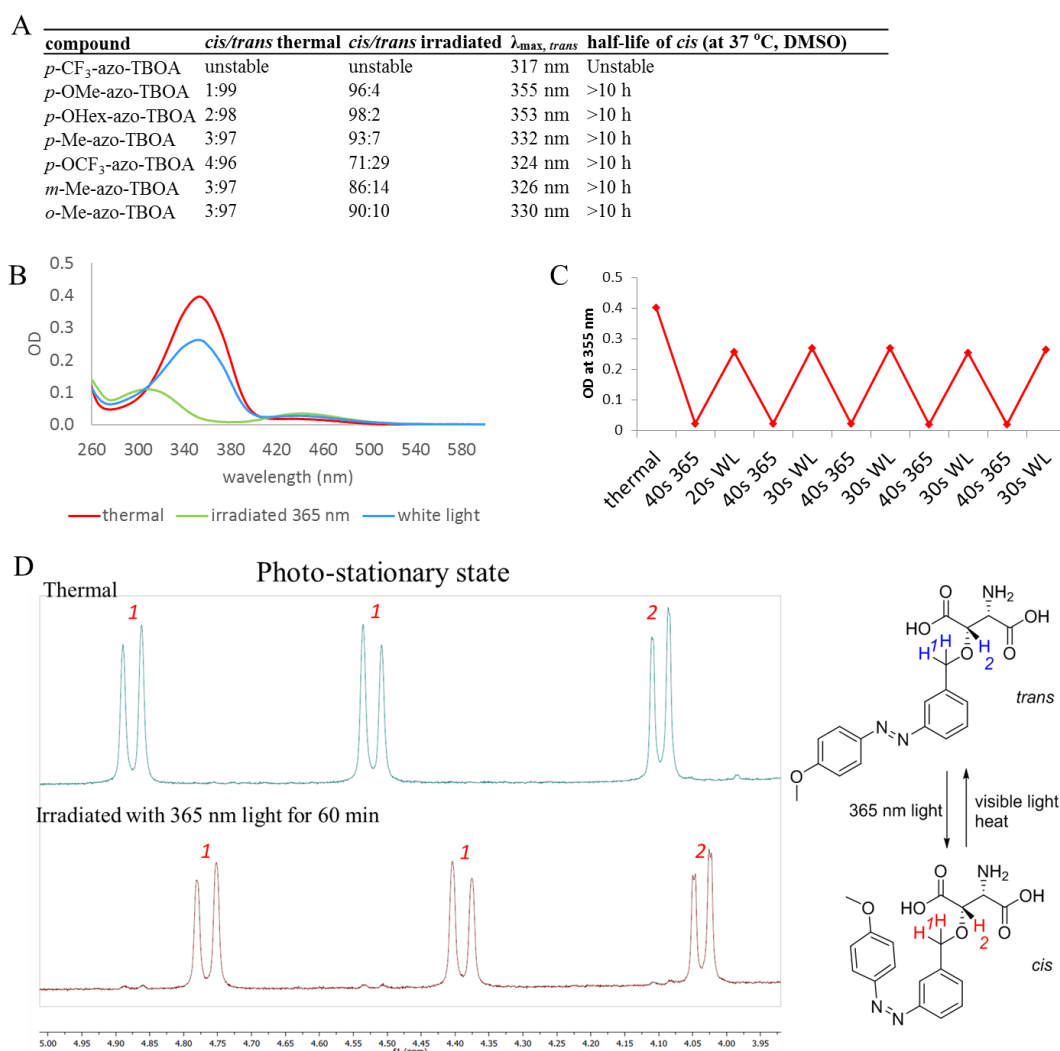


Figure 4: Photochemical properties of **azo-TBOAs**. **A:** Photochemical properties of **azo-TBOAs** in DMSO. **B:** UV/VIS spectra of ***p*-MeO-azo-TBOA**, 20 μ M in DMSO, thermally adapted, irradiated with $\lambda = 365$ nm light for 40 s and white light for 20 s. **C:** UV/VIS

absorbance of **p-MeO-azo-TBOA** at $\lambda = 355\text{ nm}$, $20\text{ }\mu\text{M}$ in DMSO, irradiated with 365 nm light and white light (WL). **D**: ^1H NMR spectrum (for full spectrum, see Figure S30) of **p-MeO-azo-TBOA**, 1 mg in $500\text{ }\mu\text{l}$ DMSO- d_6 , *cis-trans* ratio's calculated from the ^1H signals of Ar-CH₂-O (1) and O-CH-R₂ (2). Top: thermal, *cis-trans* ratio 1:99. Bottom: irradiated with $\lambda = 365\text{ nm}$ light for 60 min, *cis-trans* ratio 96:4. Right: structure of **p-MeO-azo-TBOA** in *trans* and *cis* configuration.

2.3 Biological evaluation of light-switchable glutamate transporter inhibitors

Next, the biological activity of the synthesized **azo-TBOAs** was determined on the aspartate transporter Glt_{TK} from the archaeon *T. kodakarensis*, that shows 32% sequence identity with human EAATs with even higher conservation of amino acid residues in the substrate/cation binding site and therefore Glt_{TK} has been used for structural and mechanistic studies.^[12] Glt_{TK} catalyzes uptake of aspartate coupled to the symport of three Na⁺ ions.^[16] To study the inhibition of uptake by **azo-TBOAs**, Glt_{TK} was purified, incorporated in liposomes and the rate of uptake of ^{14}C -labeled aspartate into the lumen of the liposomes was assayed^[1] in the presence and absence of the photoswitchable inhibitors.

For initial screening, [^{14}C]aspartate was used at a concentration of $1\text{ }\mu\text{M}$, and all **azo-TBOAs** were tested at $10\text{ }\mu\text{M}$ concentration, both in the dark (full *trans*) or irradiated (PSS) state, together with a negative control (no inhibitor) and a positive control (**TFB-TBOA**) (**Figure 5A**). The uninhibited uptake rate was set at 100% transporter activity. At $10\text{ }\mu\text{M}$ concentration, all *para*-substituted **trans-azo-TBOAs** showed activity in the same range as **TFB-TBOA**, while **trans-m-Me-azo-TBOA** and **trans-o-Me-azo-TBOA** were less potent. This shows that for a better inhibitor in the *trans* configuration, a substituent on the *para* position is preferred, in agreement with previously reported SAR for **TFB-TBOA**^[50]. In general, the irradiated *cis* **azo-TBOAs** had less inhibitory effect than the corresponding *trans* isomers. For **p-MeO-azo-TBOA**, we have observed the largest difference in inhibitory activity between the *cis* and

trans forms at 10 μM and therefore the IC_{50} values for both *cis* and *trans* isomers were determined (**Figure 5B**), showing $IC_{50} = 2.5 \pm 0.4 \mu\text{M}$ for *trans* and $IC_{50} = 9.1 \pm 1.5 \mu\text{M}$ for *cis*, which represents a statistically significant 3.6-fold drop in activity upon irradiation. As compared to **TFB-TBOA** (IC_{50} of $0.4 \pm 0.1 \mu\text{M}$), ***p*-MeO-azo-TBOA** lost one order of potency due to the azologization. Since ***p*-MeO-azo-TBOA** and ***p*-HexO-azo-TBOA** have nearly identical photochemical properties, also IC_{50} was determined for ***p*-HexO-azo-TBOA**. Surprisingly, for ***p*-HexO-azo-TBOA** we observed no differences in activity between *trans* and *cis* isomers, giving IC_{50} values of $0.7 \pm 0.1 \mu\text{M}$ and $0.6 \pm 0.1 \mu\text{M}$, respectively. This result cannot be explained by differences in photoswitching between the *p*-MeO- and *p*-HexO-substituted molecules, since in both cases the *trans* isomer can nearly completely be switched to the *cis* isomer. Interestingly, both isomers of ***p*-HexO-azo-TBOA** are nearly as active as **TFB-TBOA** (Figure 5b). To demonstrate that the lower activity of *cis* compared to *trans* is not because of an unexpected photodegradation effect, ***p*-MeO-azo-TBOA** was switched in several cycles in DMSO to confirm the recovery of the activity of the *trans* isomer (Figure S90).

Besides the biological activity in the uptake assay, dissociation constants (K_d) were determined using Isothermal Titration Calorimetry (ITC)^[16] (**Figure 5C**). The affinity of the transporter substrate aspartate and the inhibitor **TFB-TBOA** were determined with K_d values of $0.12 \pm 0.03 \mu\text{M}$ and $0.86 \pm 0.19 \mu\text{M}$, respectively. For **TFB-TBOA**, the affinity of $0.86 \pm 0.19 \mu\text{M}$ is in the same order as the IC_{50} of $0.4 \pm 0.1 \mu\text{M}$, as determined by the uptake assay. The isomers of ***p*-MeO-azo-TBOA** have K_d of $1.89 \pm 1.26 \mu\text{M}$ (Figure S93) and $3.19 \pm 0.49 \mu\text{M}$ (Figure S94), for the *trans* and *cis* form respectively, with no statistically significant difference between the values. Also for ***p*-HexO-azo-TBOA** no significant difference in binding was observed for the two isomers, where *trans* binds with an affinity of $2.56 \pm 0.77 \mu\text{M}$ (Figure S95) and *cis* with $4.99 \pm 3.05 \mu\text{M}$ (Figure S96). Although the error in the ITC measurements is too large to determine whether the *cis* and *trans* isomers bind with different

affinity to the transporter, the K_d values in the low micromolar range are consistent with the uptake assays. Furthermore, we expect that the observed differences in the inhibitory activity between the two different photoisomers may not only originate only from differences in binding affinity, but possibly also binding kinetics.^[56]

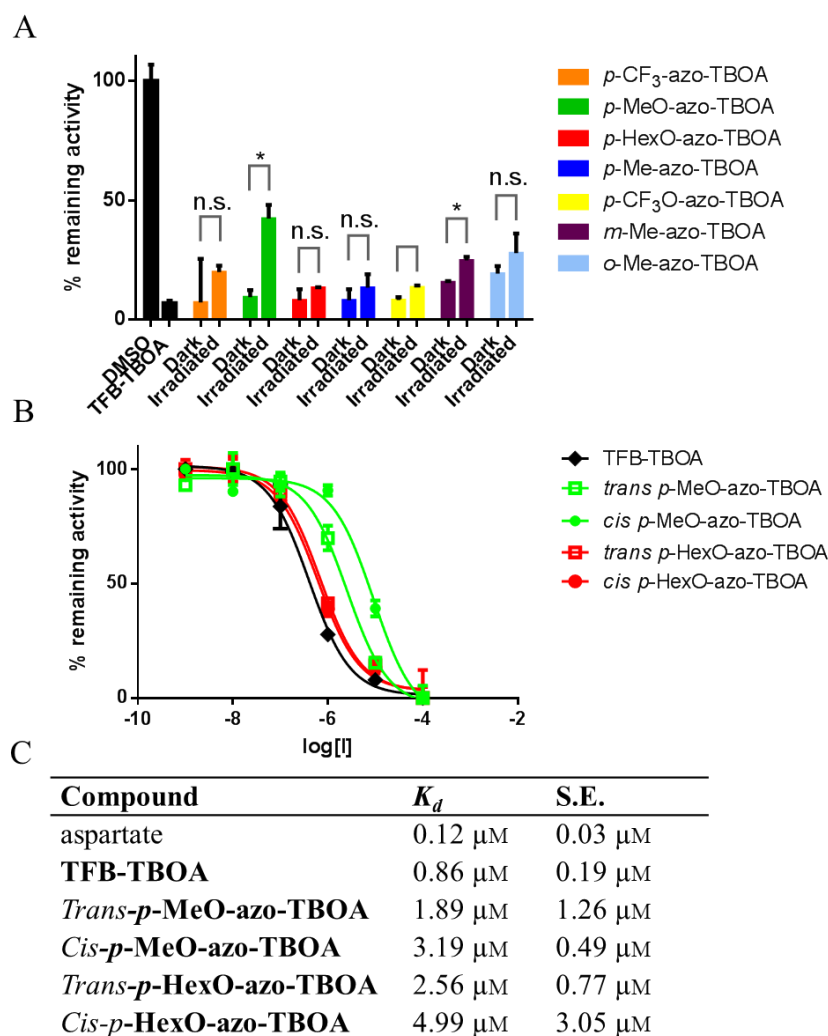


Figure 5: Biological evaluation of **azo-TBOAs**. **A:** Screening of the Glt_{Tk} inhibitory activity of **azo-TBOAs** at 10 μ M, dark and irradiated, error bars represent the range obtained in duplicate experiments, n.s. not significant, * $p < 0.05$. **B:** IC_{50} curves for **TFB-TBOA** ($0.4 \pm 0.1 \mu$ M), ***p*-MeO-azo-TBOA** in *trans* ($2.5 \pm 0.4 \mu$ M), *cis* ($9.1 \pm 1.5 \mu$ M) and ***p*-HexO-azo-TBOA** in *trans* ($0.7 \pm 0.1 \mu$ M) and *cis* ($0.6 \pm 0.1 \mu$ M), experiments performed in duplicate. **C:** Binding affinity of compounds to Glt_{Tk} , determined using Isothermal Titration Calorimetry (ITC), including the standard error.

Reversibility and temporal control are important features of bio-active molecules with photo-controlled activity, since they enable the control over time and place (tissue or group of cells) where the inhibitor is active. To test whether the 3.6-fold difference in IC_{50} values between *trans* and *cis* isomers of ***p*-MeO-azo-TBOA** is sufficient to reversibly control the transport in time, we attempted to photoswitch this inhibitor between the higher and lower potency states during the uptake assay. As shown in **Figure 6A**, the experiment was started with the *cis* isomer of ***p*-MeO-azo-TBOA** (weaker inhibitor) and fast uptake was observed. Upon irradiation with white light, the inhibitor was switched to the *trans* isomer (stronger inhibitor) and uptake was attenuated. Subsequent irradiation with UV light again resulted in switching to the weaker inhibitor and an increase in uptake rate was observed. The second irradiation with white light to the *trans* isomer, attenuated the uptake again. The same experiment was performed starting with the *trans* isomer (**Figure 6B**), showing that irradiating with UV light increases uptake rate and with white light decreases uptake rate, in a reversible manner. As controls, aspartate transport was measured with in the presence of 1 vol% DMSO, while continuously irradiating with UV light or with visible light (Figure S87). No changes in transport rate were observed, demonstrating that the proteoliposomes are not affected by light and further supporting the reversibility and temporal control of ***p*-MeO-azo-TBOA** over transport.

Besides the ‘strong inhibitor *trans*’ and ‘weak inhibitor *cis*’ states, different *cis-trans* ratios between the thermal *cis-trans* ratio and the PSS ratio can be obtained by dosing the duration and intensity of irradiation. To demonstrate this concept, several *cis-trans* ratios of ***p*-MeO-azo-TBOA** were acquired by tuning the duration of irradiation and for all mixtures their effect on the transport rate was measured (**Figure 6C**), showing a linear dependence of the transport rate on the percentage of *cis* isomer achieved by irradiation.

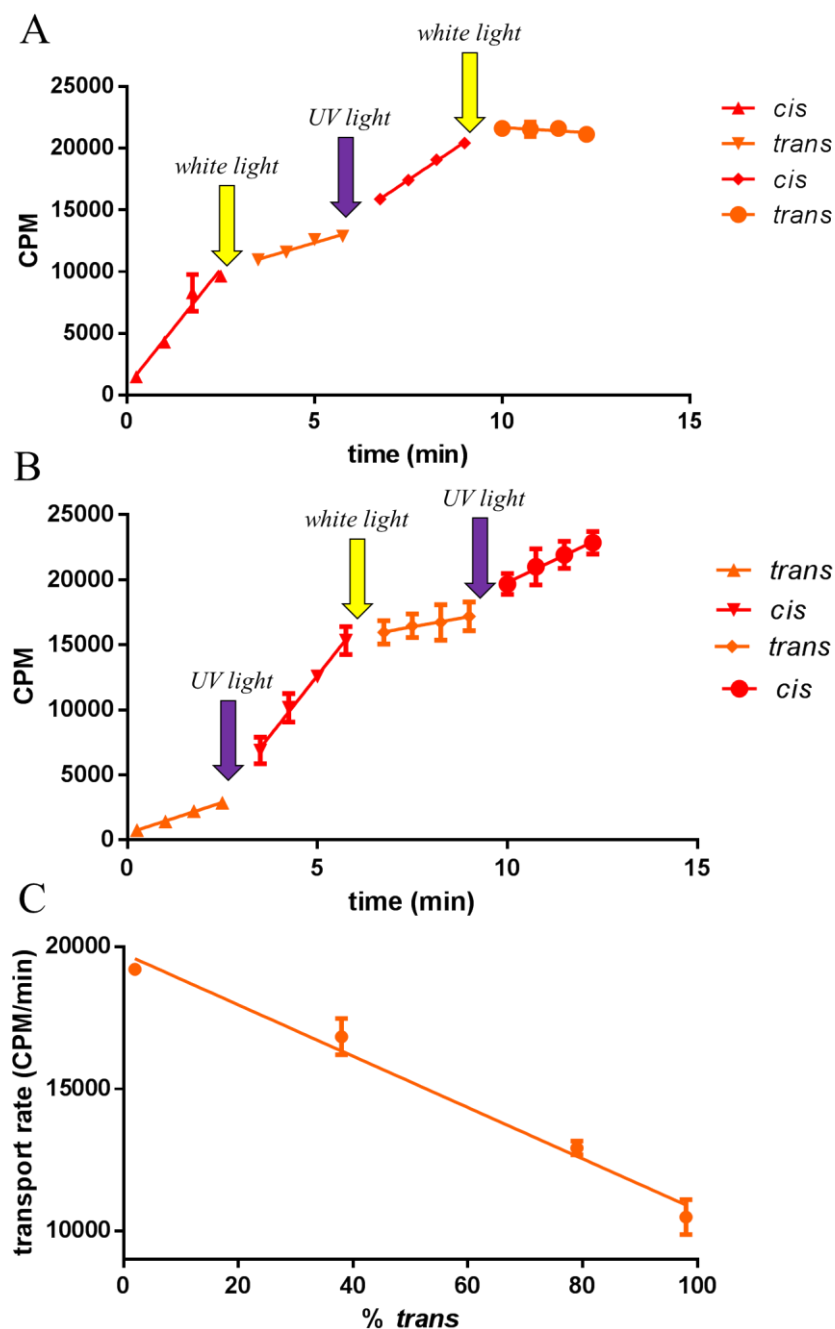


Figure 6: Photo-control over the transport rate by switching *p*-MeO-azo-TBOA. **A:** Irradiation reversibly controls the transport, starting with *cis*-*p*-MeO-azo-TBOA, irradiated with white light (45 s) after 2.5 min, UV light (45 s) after 5.75 min and white light (45 s) after 9 min, **B:** Irradiation reversibly controls the transport, starting with *trans*-*p*-MeO-azo-TBOA, irradiated with UV light (45 s) after 2.5 min, white light (45 s) after 5.75 min and UV light (45 s) after 9 min., **C:** Transport rate of [14 C]aspartate as a function of % *trans*-*p*-MeO-azo-TBOA at 50 μ M. All experiments were done in duplicate.

3. Conclusions

We present the design, synthesis and biological evaluation of inhibitors of the SLC1 transporter Glt_{TK} with photo-controlled activity. Based on the known inhibitor **TFB-TBOA**, seven **azo-TBOAs** were synthesized using a key stereoselective enzymatic step. Of the seven **azo-TBOAs**, those with alkyloxy substituents on the *para*-position showed excellent PSS and long half-lives of the *cis* isomer. The largest difference in inhibitory activity was observed for ***p*-MeO-azo-TBOA**; the *trans* isomer is 3.6 fold more active compared to the *cis* isomer.

Notably, ***p*-HexO-azo-TBOA** shows an excellent PSS but no difference in activity between *cis* and *trans*. This means that switching from *trans* to *cis* or from *cis* to *trans* has no effect on the biological activity, even despite the large structural change. In fact, ***p*-MeO-azo-TBOA** and ***p*-HexO-azo-TBOA** have nearly identical photochemical properties. Therefore, these compounds give insight into the relation between structure and binding to Glt_{TK}, providing important structural guidance in the rational design of new photo-controlled glutamate transporter inhibitors.

We demonstrate the reversible and temporal control over glutamate transport using photo-controlled inhibitors and light. Besides switching ‘on’ and ‘off’, also intermediate transport rates between those in the presence of full *cis* and full *trans* isomers can be achieved by dosing the light, demonstrating the concept of photodosimetry. Employing glutamate transporter inhibitors with photo-controlled activity can potentially provide a better understanding of the role of glutamate transporters in healthy tissues and disease pathology.

Supporting Information

Supporting Information is available from the Wiley Online Library or from the author.

Acknowledgements

This research was financially supported by the Netherlands Organization for Scientific Research (NWO-CW), ECHO grant 711.017.012 to W.S. and D.J.S. and KIEM grants 731.013.110 and 731.015.108 to G.J.P., the China Scholarship Council (scholarship to H.F) and the Ministry of Education, Culture and Science (Gravitation program 024.001.035) to B.L.F.

Received: ((will be filled in by the editorial staff))

Revised: ((will be filled in by the editorial staff))

Published online: ((will be filled in by the editorial staff))

References

- [1] D. J. Slotboom, W. Konings, J. S. Lolkema, *Microbol. Mol. Biol. Rev.* **1999**, 63, 293.
- [2] N. C. Danbolt, *Prog. Neurobiol.* **2001**, 65, 1.
- [3] J. T. Brosnan, M. E. Brosnan, *Amino Acids* **2013**, 45, 413.
- [4] M. C. Walker, W. A. Van der Donk, *J. Ind. Microbiol. Biotechnol.* **2017**, 43, 419.
- [5] Y. Zhou, N. C. Danbolt, *J. Neural. Transm.* **2014**, 121, 799.
- [6] R. J. Bridges, C. S. Esslinger, *Pharmacol. Ther.* **2005**, 107, 271.
- [7] A. Lau, M. Tymianski, *Eur. J. Physiol.* **2010**, 460, 525.
- [8] D. Yernool, O. Boudker, Y. Jin, E. Gouaux, *Nature* **2004**, 421, 811.
- [9] O. Boudker, R. M. Ryan, D. Yernool, K. Shimamoto, E. Gouaux, *Nature* **2007**, 445, 387.
- [10] N. Reyes, C. Ginter, O. Boudker, *Nature* **2009**, 462, 880.
- [11] G. Verdon, O. Boudker, *Nat. Struct. Mol. Biol.* **2013**, 19, 355.
- [12] S. Jensen, A. Guskov, S. Rempel, I. Hänelt, D. J. Slotboom, *Nat. Struct. Mol. Biol.* **2013**, 20, 1224.
- [13] N. Reyes, S. Oh, O. Boudker, *Nat. Struct. Mol. Biol.* **2013**, 20, 634.
- [14] G. Verdon, S. Oh, R. N. Serio, O. Boudker, *Elife* **2014**, 3, e02283.
- [15] N. Akyuz, E. R. Georgieva, Z. Zhou, S. Stolzenberg, M. A. Cuendet, G. Khelashvili, R. B. Altman, D. S. Terry, J. H. Freed, H. Weinstein, O. Boudker, S. C. Blanchard, *Nature* **2014**, 518, 68.
- [16] A. Guskov, S. Jensen, I. Faustino, S. J. Marrink, D. J. Slotboom, *Nat. Commun.* **2016**, 7, 13420.
- [17] B. I. Kanner, *Nat. Struct. Mol. Biol.* **2013**, 20, 1142.
- [18] J. C. Canul-tec, R. Assal, E. Cirri, P. Legrand, S. Brier, J. Chamot-rooke, N. Reyes, *Nature* **2017**, 544, 446.

- [19] B. I. Kanner, S. Schuldiner, *CRC Crit. Rev. Biochem.* **1987**, 22, 1.
- [20] L. Bozzo, J. Chatton, *Brain Res.* **2009**, 16, 27.
- [21] S. Tsukada, M. Iino, Y. Takayasu, K. Shimamoto, S. Ozawa, *Neuropharmacology* **2005**, 48, 479.
- [22] B. Lebrun, M. Sakaitani, K. Shimamoto, Y. Yasuda-kamatani, T. Nakajima, *J. Biol. Chem.* **1997**, 272, 20336.
- [23] K. Shimamoto, B. Lebrun, Y. Yasuda-kamatani, M. Sakaitani, Y. Shigeri, Y. Noboru, T. Nakajima, *Mol. Pharmacol.* **1998**, 53, 195.
- [24] Y. Xie, A. W. Chan, A. McGirr, S. Xue, X. D. Xiao, H. Zeng, T. H. Murphy, *J. Neurosci.* **2016**, 36, 1261.
- [25] B. Cheng, D. Shchepakina, M. P. Kavanaugh, D. Trauner, *ACS Chem. Neurosci.* **2017**, 9, 1668.
- [26] W. A. Velema, W. Szymanski, B. L. Feringa, *J. Am. Chem. Soc.* **2014**, 136, 2178.
- [27] M. M. Lerch, M. J. Hansen, G. M. Van Dam, W. Szymanski, B. L. Feringa, *Angew. Chem. Int.* **2016**, 55, 10978.
- [28] J. Broichhagen, J. A. Frank, D. Trauner, *Acc. Chem. Res.* **2015**, 48, 1947.
- [29] A. A. Beharry, G. A. Woolley, *Chem. Soc. Rev.* **2011**, 40, 4422.
- [30] O. Sadoski, A. A. Beharry, F. Zhang, G. A. Woolley, *Angew. Chem. Int. Ed.* **2009**, 48, 1484.
- [31] C. Brown, S. K. Rastogi, S. L. Barrett, H. E. Anderson, E. Twichell, S. Gralinski, A. McDonald, W. J. Brittain, *J. Photochem. Photobiol.* **2017**, 336, 140.
- [32] W. A. Velema, J. P. van der Berg, M. J. Hansen, W. Szymanski, A. J. M. Driessen, B. L. Feringa, *Nat. Chem.* **2013**, 5, 924.
- [33] M. Wegener, M. J. Hansen, A. J. M. Driessen, W. Szymanski, B. L. Feringa, *J. Am. Chem. Soc.* **2017**, 139, 17979.
- [34] W. Szymanski, M. E. Ourailidou, W. A. Velema, F. J. Dekker, B. L. Feringa, *Chem.*

- Eur. J.* **2015**, *21*, 16517.
- [35] M. Borowiak, W. Nahaboo, M. Reynders, K. Nekolla, P. Jalinot, J. Hasserodt, M. Rehberg, M. Delattre, S. Zahler, A. Vollmar, D. Trauner, O. Thorn-seshold, *Cell* **2015**, *162*, 403.
- [36] A. J. Engdahl, E. A. Torres, S. E. Lock, T. B. Engdahl, P. S. Mertz, C. N. Streu, *Org. Lett.* **2015**, *4*, 4546.
- [37] J. E. Sheldon, M. M. Dcona, C. E. Lyons, J. C. Hackett, M. C. T. Hartman, *Org. Biomol. Chem.* **2016**, *14*, 40.
- [38] S. K. Rastogi, Z. Zhao, S. L. Barrett, S. D. Shelton, M. Zafferani, H. E. Anderson, M. O. Blumenthal, L. R. Jones, L. Wang, X. Li, C. N. Streu, L. Du, W. J. Brittain, *Eur. J. Med. Chem.* **2018**, *143*, 1.
- [39] R. Ferreira, J. R. Nilsson, C. Solano, J. Andréasson, M. Grøtli, *Sci. Rep.* **2015**, *5*, 9769.
- [40] D. Lachmann, C. Studte, B. Männel, H. Hübner, P. Gmeiner, B. König, *Chem. a Eur. J.* **2017**, *23*, 13423.
- [41] S. Pittolo, X. Gómez-santacana, K. Eckelt, X. Rovira, J. Dalton, C. Goudet, J. Pin, A. Llobet, J. Giraldo, A. Llebaria, P. Gorostiza, *Nat. Chem. Biol.* **2014**, *10*, 813.
- [42] E. C. Carroll, S. Berlin, J. Levitz, M. A. Kienzler, Z. Yuan, D. Madsen, D. S. Larsen, E. Y. Isacoff, *PNAS* **2015**, E776.
- [43] J. Broichhagen, A. Damijonaitis, J. Levitz, K. R. Sokol, P. Leippe, D. Konrad, E. Y. Isacoff, D. Trauner, *ACS Cent. Sci.* **2015**, *1*, 383.
- [44] J. A. Frank, M. Moroni, R. Moshourab, M. Sumser, G. R. Lewin, D. Trauner, *Nat. Commun.* **2015**, *6*, 7118.
- [45] J. A. R. Dalton, I. Lans, X. Rovira, F. Malhaire, X. Gómez-santacana, S. Pittolo, P. Gorostiza, A. Llebaria, C. Goudet, J. Pin, J. Giraldo, *Curr. Neuropharmacol.* **2016**, *14*, 441.
- [46] X. Rovira, A. Trapero, S. Pittolo, C. Zussy, A. Faucherre, C. Jopling, J. Giraldo, J. Pin,

- P. Gorostiza, C. Goudet, A. Llebaria, *Cell Chem. Biol.* **2016**, 23, 929.
- [47] M. V Westphal, M. A. Schafroth, R. C. Sarott, M. A. Imhof, C. P. Bold, P. Leippe, A. Dhopeswarkar, J. M. Grandner, V. Katritch, K. Mackie, D. Trauner, E. M. Carreira, J. A. Frank, *J. Am. Chem. Soc.* **2017**, 139, 18206.
- [48] X. Gomez-Santacana, S. Pittolo, X. Rovira, M. Lopez, C. Zussy, J. A. R. Dalton, A. Faucherre, C. Jopling, J.-P. Pain, F. Ciruela, C. Goudet, J. Giraldo, P. Gorostiza, A. Llebaria, *ACS Cent. Sci.* **2017**, 3, 81.
- [49] P. C. Donthamsetti, N. Winter, M. Schönberger, J. Levitz, C. Stanley, J. A. Javitch, E. Y. Isacoff, D. Trauner, *J. Am. Chem. Soc.* **2017**, 139, 18522.
- [50] K. Shimamoto, *Beta-Benzylxyaspartate Derivates with Amino Group on Benzene Ring*, **2003**, WO 03/000698 A1.
- [51] M. Schoenberger, A. Damijonaitis, Z. Zhang, D. Nagel, D. Trauner, *ACS Chem. Neurosci.* **2014**, 5, 514.
- [52] W. Szymanski, B. Wu, C. Poloni, D. B. Janssen, B. L. Feringa, *Angew. Chem. Int. Ed.* **2013**, 52, 2068.
- [53] H. Raj, W. Szymanski, J. de Villiers, H. J. Rozeboom, V. P. Veetil, C. R. Reis, M. De Villiers, F. J. Dekker, S. de Wildeman, W. J. Quax, A.-M. W. H. Thunnissen, B. L. Feringa, D. B. Janssen, G. J. Poelarends, *Nat. Chem.* **2012**, 4, 478.
- [54] H. Raj, W. Szymanski, J. de Villiers, V. P. Veetil, W. J. Quax, K. Shimamoto, D. B. Janssen, B. L. Feringa, G. J. Poelarends, *Chem. Eur. J.* **2013**, 19, 11148.
- [55] H. Fu, S. H. H. Younes, M. Saifuddin, P. G. Tepper, J. Zhang, E. Keller, A. Heeres, W. Szymanski, G. J. Poelarends, *Org. Biomol. Chem.* **2017**, 15, 2341.
- [56] R. A. Copeland, *Nat. Rev. Drug Discov.* **2016**, 15, 87.

Copyright WILEY-VCH Verlag GmbH & Co. KGaA, 69469 Weinheim, Germany, 2016.

The table of contents entry should be 50–60 words long, and the first phrase should be bold.

The design, synthesis and evaluation of the photochemical and biological properties of light-controlled glutamate transporter inhibitors is presented. Application of these compounds enables remote, reversible and spatiotemporally resolved regulation of activity of an important class of transporter proteins.

Keywords

Keywords: Glutamate transport, photopharmacology, azobenzene, photo-controlled inhibitor

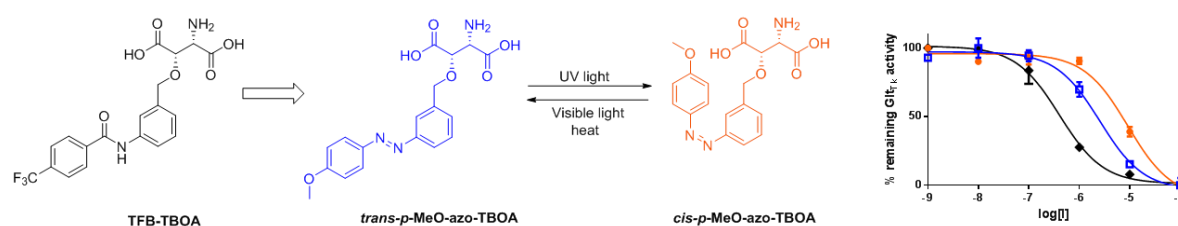
Authors

Mark W. H. Hoorens#, Haigen Fu#, Ria H. Duurkens, Gianluca Trinco, Valentina Arkhipova,

Ben L. Feringa, Gerrit J. Poelarends, Dirk J. Slotboom, Wiktor Szymanski*

Title

Glutamate Transporter Inhibitors with Photo-controlled Activity



Supporting Information

Title Glutamate Transporter Inhibitors with Photo-controlled Activity

*Mark W. H. Hoorens[#], Haigen Fu[#], Ria H. Duurkens, Gianluca Trinco, Valentina Arkhipova, Ben L. Feringa, Gerrit J. Poelarends, Dirk J. Slotboom, Wiktor Szymanski**

[#] These authors contributed equally to this work

M. W. H. Hoorens, Dr. W. Szymanski

Department of Radiology, University of Groningen, University Medical Center Groningen,
Hanzeplein 1, 9713 GZ, Groningen, The Netherlands

E-mail: w.szymanski@umcg.nl

M. W. H. Hoorens, Prof. B. L. Feringa, Dr. W. Szymanski

Centre for Systems Chemistry, Stratingh Institute for Chemistry, Faculty of Science and
Engineering, University of Groningen, Nijenborgh 7, 9747 AG Groningen, The Netherlands

H. Fu, Prof. G. J. Poelarends

Department of Chemical and Pharmaceutical Biology, Groningen Research Institute of
Pharmacy, University of Groningen, Antonius Deusinglaan 1, 9713 AV, Groningen, The
Netherlands

R. H. Duurkens, G. Trinco, Dr. V. Arkhipova, Prof. D. J. Slotboom

Department of Biochemistry, Groningen Biomolecular Sciences and Biotechnology Institute,
Nijenborgh 4, 9747 AG Groningen, The Netherlands

1 Chemical Synthesis

1.1 General remarks

1.2 Experimental procedures

1.2.1 Synthesis of azobenzene-based O-alkylating agents 4a-g

1.2.2 Synthesis of chiral building block 17

1.2.3 Synthesis of *L-trans-R*-azo-TBOAs 1a-g

1.3 NMR spectra

2 Photochemical data

3 Biological evaluation

3.1 DNA manipulation, protein purification and concentration determination.

3.2 Uptake assay

3.3 Isothermal Titration Calorimetry

4. Statistical analysis

5. References

1.1 General remarks

All chemicals for synthesis were obtained from commercial sources and used as received unless stated otherwise. Solvents were reagent grade. Thin-layer chromatography (TLC) was performed using commercial Kieselgel 60, F254 silica gel plates, and components were visualized with KMnO_4 or phosphomolybdic acid reagent. Flash chromatography was performed on silica gel (Silicycle Siliaflash P60, 230-400 mesh). Drying of solutions was performed with MgSO_4 and solvents were removed with a rotary evaporator. Chemical shifts for ^1H NMR measurements were determined in CDCl_3 relative to the tetramethylsilane internal standard (TMS, $\delta = 0.00$). Chemical shifts for ^{13}C NMR measurements were determined relative to the residual solvent peaks (CHCl_3 , $\delta = 77.0$; DMSO-d_6 , $\delta = 40.0$). The following abbreviations are used to indicate signal multiplicity: s, singlet; d, doublet; t, triplet; q, quartet; m, multiplet; br s, broad signal; app, apparent. High resolution mass spectra (electrospray ionisation) spectra were obtained on a Thermo scientific LTQ Orbitrap XL. Melting points were recorded using a Buchi melting point B-545 apparatus.

1.2 Experimental procedures

Synthetic route for target compounds: general overview.

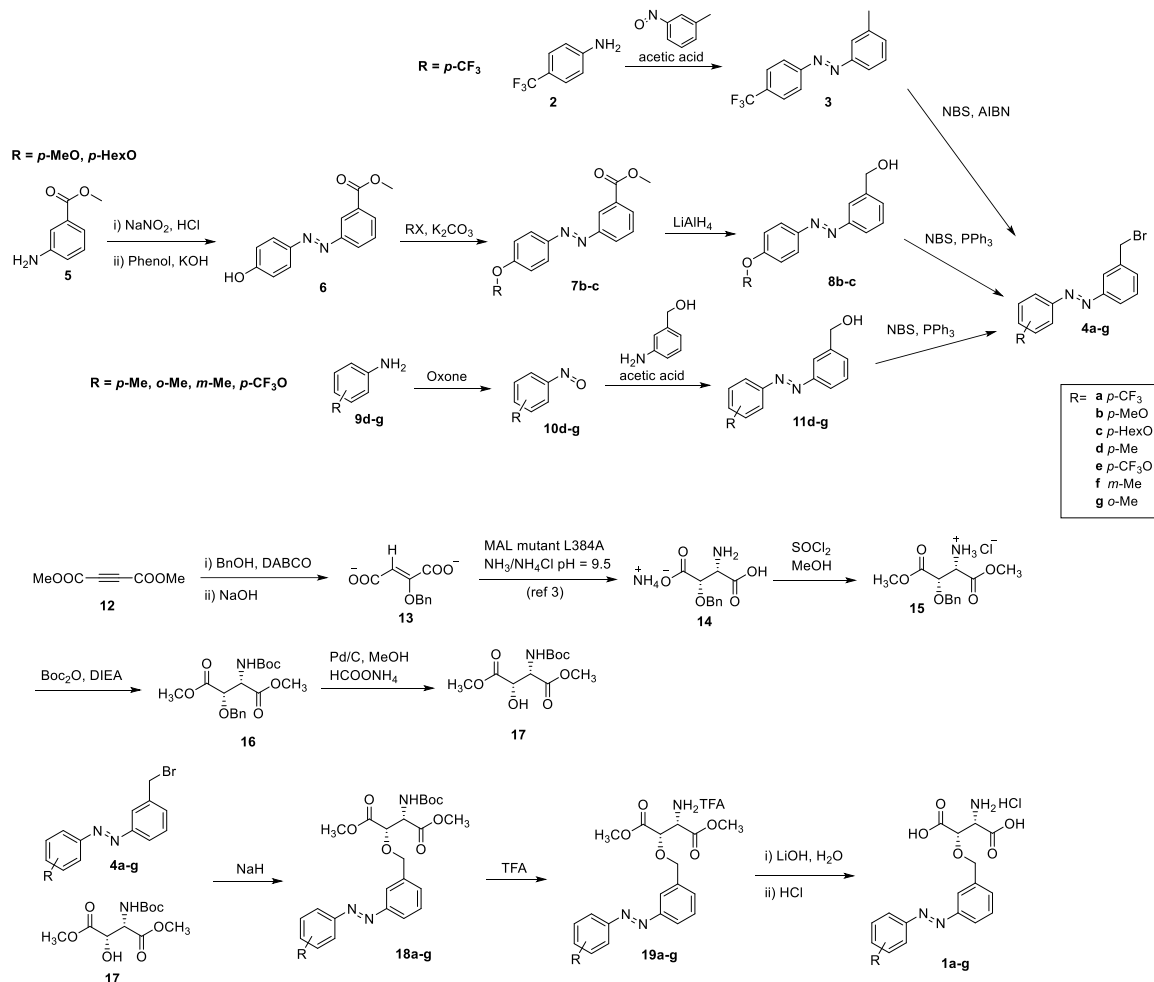


Figure S1: Synthesis of azo-TBOAs

1.2.1 Synthesis of azobenzene-based *O*-alkylating agents 4a-g

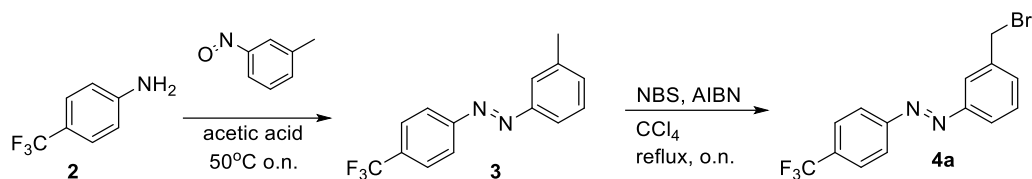


Figure S2: Synthesis of alkylating agent **4a**.

1-(*m*-tolyl)-2-(4-(trifluoromethyl)phenyl)diazene (**3**)

A solution of 3-nitrosotoluene (2.56 mmol, 310 mg) and 4-trifluoromethyl-aniline **2** (3.33 mmol, 537 mg) in acetic acid (8 mL) was heated at 50 °C overnight. The reaction mixture was diluted with diethyl ether (100 mL) and washed with 1 N aq. HCl (80 mL), sat. aq. NaHCO₃ (2 x 80 mL) and brine (80 mL). The organic phase was dried (MgSO₄) and the solvent was evaporated. The product was purified by flash chromatography (Silicagel, 40-63 μm, pentane) to give red solid (240 mg, 36%). R_f = 0.30 (pentane); Mp. 54-55 °C; ¹H NMR (400 MHz, CDCl₃): δ 2.47 (s, 3H, CH₃), 7.34 (d, *J* = 7.6 Hz, 1H, ArH), 7.43 (t, *J* = 8.0 Hz, 1H, ArH), 7.74-7.83 (m, 4H, ArH), 8.00 (d, *J* = 8.0 Hz, 2H, ArH); ¹³C NMR (100 MHz, CDCl₃): δ 21.3, 120.8, 122.9, 123.3, 126.2, 126.3, 129.0, 132.1 (q, ²*J*_{C,F} = 32.3 Hz), 132.6, 139.1, 152.5, 154.5; ¹⁹F NMR (376 MHz, CDCl₃): -62.5 (s); HRMS (ESI+) calc. for [M+H]⁺ (C₁₄H₁₂F₃N₂): 265.0947, found: 265.0942.

1-(3-(bromomethyl)phenyl)-2-(4-(trifluoromethyl)phenyl)diazene (**4a**)

A solution of compound **3** (0.90 mmol, 240 mg), *N*-bromosuccinimide (1.24 mmol, 220 mg) and AIBN (0.21 mmol, 35 mg) in carbon tetrachloride (9 mL) was heated at reflux for 20 h. Another portion of AIBN (35 mg) was added, and the reaction was heated at reflux for additional 20 h. The product was purified by flash chromatography (Silicagel, 40-63 μm,

pentane – pentane/Et₂O, 95:5, v/v) and recrystallization from methanol to give red needles (190 mg, 62% yield). R_f = 0.23 (pentane); Mp. 76-78 °C; ¹H NMR (400 MHz, CDCl₃): δ 4.59 (s, 2H, CH₂Br), 7.50-7.60 (m, 2H, ArH), 7.79 (d, *J* = 7.6 Hz, 2H, ArH), 7.90 (d, *J* = 7.6 Hz, 1H, ArH), 7.98 (s, 1H, ArH), 8.01 (d, *J* = 8.0 Hz, 2H, ArH); ¹³C NMR (100 MHz, CDCl₃): δ 32.6, 123.1, 123.1, 123.6, 126.3, 126.3, 129.7, 132.2, 132.4 (q, ²*J*_{C,F} = 32.6 Hz), 139.1, 152.6, 154.2; ¹⁹F NMR (376 MHz, CDCl₃): -62.6 (s); HRMS (ESI+) calc. for [M+H]⁺ (C₁₄H₁₁BrF₃N₂): 345.0032, found: 345.0033.

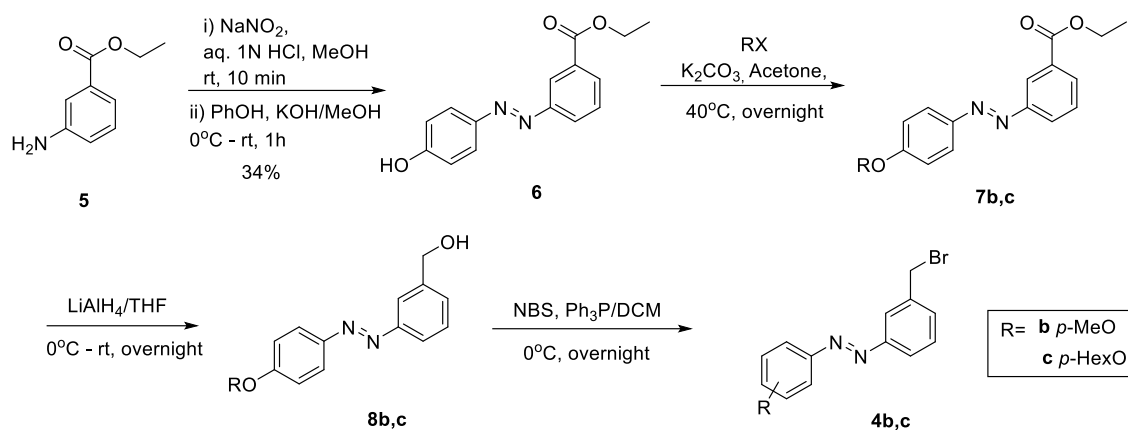


Figure S3: Synthesis of alkylating agents **1b,c**

Ethyl (*E*)-3-((4-hydroxyphenyl)diazenyl)benzoate (**6**)

Ethyl 3-aminobenzoate **5** (3.0 mL, 2.7 g, 17 mmol) was dissolved in aq. 1 N HCl (50 mL) and NaNO₂ (1.60 g, 23 mmol) was added. The reaction mixture was stirred in an ice-bath for 10 min. MeOH (25 mL) was added to the reaction mixture and a solution of PhOH (1.93 g, 14.6 mmol) and KOH (2.14 g, 38.1 mmol) in MeOH (20 mL) was added dropwise. The reaction mixture was stirred at room temperature for 1h. After completion, aq. 1 N HCl (50 mL) and EtOAc (50 mL) were added to the reaction mixture and the aqueous layer was extracted with EtOAc (3 x 50 mL). The combined organic layers were concentrated *in vacuo*, Et₂O was

added (100 mL) and the precipitated product was filtered off and washed with pentane. The product was obtained as an orange solid (1.58 g, 5.8 mmol, 34% yield). Mp: 141-146 °C, ^1H NMR (400 MHz, CDCl_3) δ 1.44 (t, $J = 7.1$ Hz, 3H, CH_3), 4.38 – 4.48 (m, 2H, CH_2), 5.65 (s, 1H, ArOH), 6.98 (d, $J = 6.9$ Hz, 2H, ArH), 7.58 (t, $J = 7.8$ Hz, 1H, ArH), 7.91 (d, $J = 6.9$ Hz, 2H, ArH), 8.05 (d, $J = 7.9$ Hz, 1H, ArH), 8.12 (d, $J = 7.7$ Hz, 1H, ArH), 8.52 (s, 1H, ArH). ^{13}C NMR (101 MHz, CDCl_3) δ 14.3, 61.4, 115.9, 123.9, 125.2, 126.4, 129.1, 131.1, 147.0, 152.7, 158.7, 166.4. HRMS (ESI+) calc. for. $[\text{M}+\text{H}^+]$ ($\text{C}_{15}\text{H}_{15}\text{N}_2\text{O}_3$) 271.1077, found: 271.1074.

Ethyl (*E*)-3-((4-methoxyphenyl)diazenyl)benzoate (7b)

Compound **6** (0.70 g, 2.6 mmol) was dissolved in acetone (20 mL) and MeI (3.0 mL, 1.3 g, 9.3 mmol) and K_2CO_3 (3.7 g, 26.8 mmol) were added. The reaction mixture was stirred at 40 °C overnight. After completion, Et_2O (50 mL) and water (50 mL) were added and the organic layer was separated, dried with MgSO_4 and concentrated *in vacuo*. The product was purified by flash chromatography (Silicagel 40 – 63 nm, 0-10% EtOAc in pentane). The product was obtained as an orange solid (0.62 g, 2.2 mmol, 85% yield). Mp: 40 - 42 °C, ^1H NMR (400 MHz, CDCl_3) δ 1.42 (d, $J = 14.3$ Hz, 3H, CH_3), 3.85 (s, 3H, OCH_3), 4.42 (q, $J = 7.1$ Hz, 2H, CH_2), 6.99 (d, $J = 9.0$ Hz, 2H, ArH), 7.54 (t, $J = 7.8$ Hz, 1H, ArH), 7.94 (d, $J = 9.0$ Hz, 2H, ArH), 8.11 (d, $J = 7.9$ Hz, 1H, ArH), 8.53 (s, 1H, ArH). ^{13}C NMR (101 MHz, CDCl_3) δ 14.4, 55.5, 61.2, 76.8, 77.1, 77.4, 114.2, 123.9, 125.0, 126.3, 129.0, 131.0, 131.6, 146.8, 152.7, 162.4, 166.1. HRMS (ESI+) calc. for. $[\text{M}+\text{H}^+]$ ($\text{C}_{16}\text{H}_{16}\text{N}_2\text{O}_3$) 285.1234, found: 285.1232.

(*E*)-3-((4-methoxyphenyl)diazenyl)phenyl)methanol (8b)

Compound **7b** (0.50 g, 1.8 mmol) was dissolved in dry THF (5 mL) and the reaction mixture was cooled in an ice-bath. LiAlH_4 (1.8 mL of 1M solution in THF) was added and the reaction mixture was stirred overnight at room temperature. After completion, MeOH (5 mL),

EtOAc (50 mL), and sodium tartrate (5 g in 100 mL H₂O) were added and the resulting mixture was stirred for 1 h. The layers were separated and the aqueous layer was extracted with EtOAc (3 x 20 mL). The combined organic layers were washed with water and brine, dried with MgSO₄ and concentrated *in vacuo*. The product was purified by flash chromatography (Silicagel 40 – 63 nm, pentane, 0 - 50% Et₂O in pentane) and precipitated with pentane. The product was obtained as an orange solid (0.27 g, 1.1 mmol, 61% yield). Mp: 54 - 55 °C, ¹H NMR (400 MHz, CDCl₃) δ 3.86 (s, 3H, OCH₃), 4.74 (s, 2H, CH₂OH), 6.99 (d, *J* = 8.7 Hz, 2H, ArH), 7.37 – 7.50 (m, 2H, ArH), 7.75 – 7.86 (m, 2H, ArH), 7.90 (d, *J* = 8.6 Hz, 2H, ArH). ¹³C NMR (101 MHz, CDCl₃) δ 55.6, 64.9, 114.2, 120.3, 122.3, 124.8, 128.7, 129.2, 142.0, 146.9, 152.9, 162.1. HRMS (ESI+) calc. for. [M+H⁺] (C₁₄H₁₅N₂O₂) 243.1128, found: 243.1125.

(E)-1-(3-(bromomethyl)phenyl)-2-(4-methoxyphenyl)diazene (4b)

Compound **8b** (0.23 g, 0.94 mmol) was dissolved in DCM (10 mL) and NBS (0.25 g, 1.4 mmol) and triphenylphosphine (0.34 g, 1.3 mmol) were added. The reaction was stirred overnight at room temperature. After completion, the reaction mixture was concentrated *in vacuo*. The product was purified by flash chromatography (Silicagel 40 – 63 nm, pentane, 0 - 5% Et₂O). The product was obtained as an orange solid (0.20 g, 0.65 mmol, 69% yield). ¹H NMR (400 MHz, CDCl₃) δ 3.88 (s, 3H, OCH₃), 4.57 (s, 2H, CH₂Br), 7.01 (d, *J* = 9.0 Hz, 2H, ArH), 7.47 (d, *J* = 6.0 Hz, 2H, ArH), 7.81 (dd, *J* = 6.2, 2.8 Hz, 1H, ArH), 7.87 – 7.96 (m, 3H, ArH). Mp: 56 - 60 °C. ¹³C NMR (101 MHz, CDCl₃) δ 33.0, 55.6, 114.3, 122.6, 123.1, 124.9, 129.5, 130.8, 138.8, 146.9, 153.0, 162.3. HRMS (ESI+) calc. for. [M+H⁺] (C₁₄H₁₄BrN₂O₂) 305.0282, found: 305.0283.

Ethyl (E)-3-((4-methoxyphenyl)diazenyl)benzoate (7c)

Compound **6** (0.70 g, 2.6 mmol) was dissolved in acetone (20 mL) and 1-bromohexane (3.0 mL, 1.3 g, 9.3 mmol) and K₂CO₃ (3.7 g, 26.8 mmol) were added. The reaction mixture was stirred at 40 °C overnight. After completion, Et₂O (50 mL) and water (50 mL) were added and the organic layer was separated, dried with MgSO₄ and concentrated *in vacuo*. The product was purified by flash chromatography (Silicagel 40 – 63 nm, pentane; 0-10% EtOAc in pentane). The product was obtained as an orange solid (0.62 g, 2.2 mmol, 85% yield). Mp: 40 - 42 °C, ¹H NMR (400 MHz, CDCl₃) δ 1.42 (d, *J* = 14.3 Hz, 3H, CH₃), 3.85 (s, 3H, OCH₃), 4.42 (q, *J* = 7.1 Hz, 2H, CH₂), 6.99 (d, *J* = 9.0 Hz, 2H, ArH), 7.54 (t, *J* = 7.8 Hz, 1H, ArH), 7.94 (d, *J* = 9.0 Hz, 2H, ArH), 8.11 (d, *J* = 7.9 Hz, 1H, ArH), 8.53 (s, 1H, ArH). ¹³C NMR (101 MHz, CDCl₃) δ 14.4, 55.5, 61.2, 76.8, 77.1, 77.4, 114.2, 123.9, 125.0, 126.3, 129.0, 131.0, 131.6, 146.8, 152.7, 162.4, 166.1. HRMS (ESI+) calc. for. [M+H⁺] (C₁₆H₁₆N₂O₃) 285.1234, found: 285.1232.

(E)-(3-((4-hexyloxyphenyl)diazenyl)phenyl)methanol (8c)

Compound **7c** (0.61 g, 1.7 mmol) was dissolved in dry THF (5 mL) and the reaction mixture was cooled in an ice-bath. LiAlH₄ (1.8 mL of 1M solution in THF) was added and the reaction mixture was stirred overnight at room temperature. After completion MeOH (5 mL), EtOAc (50 mL), sodium tartrate (5 g in 100 mL) were added to reaction mixture and stirred for 1 hour. The layers were separated and the aqueous layer was extracted with EtOAc (3 x 20 mL). The combined organic layers were washed with water and brine, dried with MgSO₄ and concentrated *in vacuo*. The product was purified by flash chromatography (Silicagel 40 – 63 nm, pentane, 0 - 50% Et₂O in pentane) and precipitated with pentane. The product was obtained as an orange solid (0.46 g, 1.5 mmol, 88% yield). Mp: 43 - 46 °C, ¹H NMR (400 MHz, CDCl₃) δ 0.88 – 0.97 (m, 3H, CH₃), 1.28 – 1.41 (m, 4H, CH₂, CH₂), 1.41 – 1.53 (m, 2H, CH₂), 1.77 – 1.88 (m, 2H, CH₂), 4.03 (t, *J* = 6.6 Hz, 2H, CH₂), 4.77 (s, 2H, CH₂OH), 6.99 (d, *J* = 9.0 Hz, 2H, ArH), 7.41 – 7.52 (m, 2H, ArH), 7.80 (d, *J* = 7.7 Hz, 1H, ArH), 7.86 (s, 1H,

ArH), 7.90 (d, $J = 9.0$ Hz, 2H, ArH). ^{13}C NMR (101 MHz, CDCl_3) δ 14.0, 22.6, 25.7, 29.1, 31.6, 65.0, 68.4, 114.7, 120.3, 122.3, 124.8, 128.6, 129.2, 141.9, 146.8, 153.0, 161.8. HRMS (ESI+) calc. for. $[\text{M}+\text{H}^+]$ ($\text{C}_{19}\text{H}_{25}\text{N}_2\text{O}_2$) 313.1911, found: 313.1908.

(E)-1-(3-(bromomethyl)phenyl)-2-(4-hexyloxyphenyl)diazene (4c)

Compound **8c** (0.36 g, 1.2 mmol) was dissolved in DCM (10 mL) and NBS (0.24 g, 1.4 mmol) and triphenylphosphine (0.39 g, 1.5 mmol) were added. The reaction was stirred overnight at room temperature. After completion, the reaction mixture was concentrated *in vacuo*. The product was purified by flash chromatography (Silicagel 40 – 63 nm, pentane, 0-5% Et_2O). The product was obtained as an orange solid (0.32 g, 0.86 mmol, 72% yield). Mp: 51 - 53 °C, ^1H NMR (400 MHz, CDCl_3) δ 0.92 (t, $J = 6.8$ Hz, 3H, CH_3), 1.29 – 1.41 (m, 4H, CH_2 , CH_2), 1.43 – 1.54 (m, 2H, CH_2), 1.81 (p, $J = 6.7$ Hz, 2H, CH_2), 4.03 (t, $J = 6.5$ Hz, 2H, CH_2), 4.56 (s, 2H, CH_2Br), 7.00 (d, $J = 8.8$ Hz, 2H, ArH), 7.46 (d, $J = 6.0$ Hz, 2H, ArH), 7.80 (s, 1H, ArH), 7.91 (m, 3H, ArH). ^{13}C NMR (101 MHz, CDCl_3) δ 14.1, 22.6, 25.7, 29.2, 31.6, 33.0, 68.4, 114.7, 122.6, 123.0, 124.9, 129.5, 130.7, 138.8, 146.7, 153.0, 161.9. HRMS (ESI+) calc. for. $[\text{M}+\text{H}^+]$ ($\text{C}_{19}\text{H}_{24}\text{BrN}_2\text{O}_2$) 375.1067, found: 375.1067.

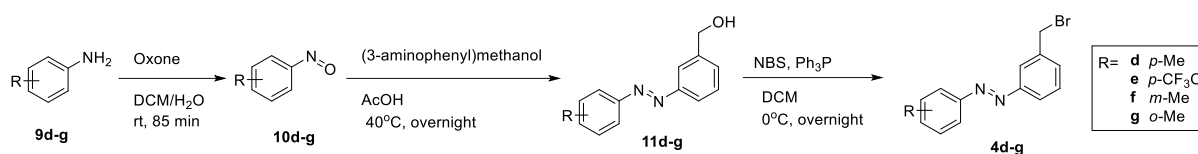


Figure S4: Synthesis of alkylating agents **1d-g**

(E)-(3-(*p*-tolyl diazenyl)phenyl)methanol (11d**)**

Para-toluidine **9d** (1.0 g, 9.3 mmol) was dissolved in DCM (20 mL) and water (100 mL) and Oxone (5.2 g, 19 mmol) was added. The reaction mixture was stirred at room temperature for 85 min. After completion, DCM (20 mL) was added and the aqueous layer was extracted with DCM (3 x 20 mL). The combined organic layers were washed with sat. aq. NaHCO₃, 1 N HCl and brine and concentrated *in vacuo*. The crude product was flushed over a silica gel column (Silicagel 40 – 63 nm, pentane). Without further purification, the crude product (0.18 g, 1.4 mmol) was dissolved in acetic acid (5 mL) and (3-aminophenyl)methanol (0.3 g, 2.4 mmol) was added. The reaction mixture was stirred at 40 °C overnight. After completion EtOAc (15 mL) and sat aq. NaHCO₃ (10 mL) were added and the reaction mixture was stirred overnight. EtOAc (50 mL) and water (50 mL) were added and the aqueous layer was extracted with EtOAc (3 x 20 mL). The combined organic layers were washed with sat. aq. NaHCO₃, 1 N HCl and brine, dried with MgSO₄ and concentrated *in vacuo*. The product was purified by flash chromatography (Silicagel 40 – 63 nm, pentane; 0 – 50% Et₂O). The product was obtained as an orange solid (0.17 g, 0.8 mmol, 51% yield over two steps). Mp: 66 - 68 °C, ¹H NMR (400 MHz, CDCl₃) δ 2.40 (s, 4H, CH₃, OH), 4.71 (s, 2H, CH₂OH), 7.28 (d, *J* = 8.1 Hz, 2H, ArH), 7.43 (m, 2H, ArH), 7.67 – 7.94 (m, 4H, ArH). ¹³C NMR (101 MHz, CDCl₃) δ 21.5,

64.8, 120.5, 122.4, 122.9, 129.1, 129.2, 129.8, 141.7, 142.0, 150.7, 152.8. HRMS (ESI+) calc. for. $[M+H^+]$ ($C_{14}H_{15}N_2O$) 227.1180, found: 227.1176.

(E)-1-(3-(bromomethyl)phenyl)-2-(p-tolyl)diazene (4d)

Compound **11d** (0.15 g, 0.66 mmol) was dissolved in DCM (10 mL) and NBS (0.18 g, 1.0 mmol) and triphenylphosphine (0.25 g, 0.95 mmol) were added. The reaction was stirred at room temperature overnight. After completion, the reaction mixture was concentrated *in vacuo*. The product was purified by flash chromatography (Silicagel 40 – 63 nm, pentane; 0 – 5% Et₂O). The product was obtained as an orange solid (0.12 g, 0.42 mmol, 63% yield). Mp: 68 – 69 °C, ¹H NMR (400 MHz, CDCl₃) δ 2.42 (s, 3H, CH₃), 4.55 (s, 2H, CH₂Br), 7.30 (d, *J* = 8.2 Hz, 2H, ArH), 7.46 (d, *J* = 5.2 Hz, 2H, ArH), 7.83 (d, *J* = 8.2 Hz, 3H, ArH), 7.91 (s, 1H, ArH). ¹³C NMR (101 MHz, CDCl₃) δ 21.6, 32.9, 122.8, 123.0, 123.2, 129.5, 129.8, 131.1, 138.8, 141.9, 150.7, 152.9. HRMS (ESI+) calc. for. $[M+H^+]$ ($C_{14}H_{14}BrN_2$) 289.0335, found: 289.0335.

E)-(3-((4-(trifluoromethoxy)phenyl)diazenyl)phenyl)methanol (11e)

4-(trifluoromethoxy)aniline **9e** (2.00 g, 11.3 mmol) was dissolved in DCM (20 mL) and water (100 mL) and Oxone (8.0 g, 26 mmol) was added. The reaction mixture was stirred at room temperature for 1 h. After completion, DCM (20 mL) was added and the aqueous layer was extracted with DCM (3 x 20 mL). The combined organic layers were washed with sat. aq. NaHCO₃, 1 N HCl and brine and concentrated in *vacuo*. The crude product was flushed over a silica gel column (Silicagel 40 – 63 nm, pentane). Without further purification, the crude product (0.73 g, 2.5 mmol) was dissolved in acetic acid (20 mL) and (3-aminophenyl)methanol (1.5 g, 5.1 mmol) was added. The reaction mixture was stirred at 40 °C overnight. After completion EtOAc (15 mL) and sat aq. NaHCO₃ (10 mL) were added and the

reaction mixture was stirred overnight. EtOAc (50 mL) and water (50 mL) were added and the aqueous layer was extracted with EtOAc (3 x 20 mL). The combined organic layers were washed with sat. aq. NaHCO₃, 1 N HCl and brine, dried with MgSO₄ and concentrated *in vacuo*. The product was purified by flash chromatography (Silicagel 40 – 63 nm, pentane; 0 – 30% Et₂O). The product was obtained as orange solid (0.73 g, 2.5 mmol, 22% yield). Mp: 47 - 48 °C, ¹H NMR (400 MHz, CDCl₃) δ 4.79 (s, 2H, CH₂OH), 7.34 (d, *J* = 8.8 Hz, 2H, ArH), 7.50 (d, *J* = 6.8 Hz, 2H, ArH), 7.83 (d, *J* = 7.0 Hz, 1H, ArH), 7.90 (s, 1H, ArH), 7.95 (d, *J* = 8.7 Hz, 2H, ArH). ¹³C NMR (101 MHz, CDCl₃) δ 152.6, 150.9, 150.6, 142.1, 129.7, 129.3, 124.4, 122.7, 121.3, 120.7, 64.8. ¹⁹F NMR (376 MHz, CDCl₃) δ -57.7. HRMS (ESI+) calc. for. [M+H⁺] (C₁₄H₁₂F₃N₂O₂) 297.0844, found: 297.0844.

(E)-1-(3-(bromomethyl)phenyl)-2-(4-(trifluoromethoxy)phenyl)diazene (4e)

Compound **11e** (0.3 g, 1 mmol) was dissolved in DCM (10 mL) and NBS (0.29 g, 1.6 mmol) and triphenylphosphine (0.33 g, 1.3 mmol) were added. The reaction was stirred at room temperature overnight. After completion, the reaction mixture was concentrated *in vacuo*. The product was purified by flash chromatography (Silicagel 40 – 63 nm, pentane; 0 – 5% Et₂O). The product was obtained as an orange solid (0.31 g, 0.85 mmol, 83% yield). Mp: 64 - 67 °C, ¹H NMR (400 MHz, CDCl₃) δ 4.58 (s, 2H, CH₂Br), 7.36 (d, *J* = 8.2 Hz, 2H, ArH), 7.52 (d, *J* = 7.0 Hz, 2H, ArH), 7.86 (d, *J* = 6.8 Hz, 1H, ArH), 7.92 – 8.01 (m, 3H, ArH). ¹³C NMR (101 MHz, CDCl₃) δ 32.7, 121.3, 123.0, 123.4, 124.4, 129.6, 131.7, 139.0, 150.6, 151.1, 152.6. ¹⁹F NMR (376 MHz, CDCl₃) δ -57.7. HRMS (ESI+) calc. for. [M+H⁺] (C₁₄H₁₁BrF₃N₂O⁺) Exact Mass: 359.0002, found: 359.0001.

(E)-(3-(*m*-tolylidiazenyl)phenyl)methanol (11f)

Meta-toluidine **9f** (1.0 g, 9.3 mmol) was dissolved in DCM (20 mL) and water (100 mL) and Oxone (5.2 g, 19 mmol) was added. The reaction mixture was stirred at room temperature for 90 min. After completion, DCM (20 mL) was added and the aqueous layer was extracted with DCM (3 x 20 mL). The combined organic layers were washed with sat. aq. NaHCO₃, 1 N HCl and brine and concentrated *in vacuo*. The crude product was flushed over a silica gel column (Silicagel 40 – 63 nm, pentane). Without further purification, the crude product (0.18 g, 1.4 mmol) was dissolved in acetic acid (5 mL) and (3-aminophenyl)methanol (0.30 g, 2.4 mmol) was added. The reaction mixture was stirred at 40°C overnight. After completion EtOAc (15 mL) and sat aq. NaHCO₃ (10 mL) were added and the reaction mixture was stirred overnight. EtOAc (50 mL) and water (50 mL) were added and the aqueous layer was extracted with EtOAc (3 x 20 mL). The combined organic layers were washed with sat. aq. NaHCO₃, 1 N HCl and brine, dried with MgSO₄ and concentrated *in vacuo*. The product was purified by flash chromatography (Silicagel 40 – 63 nm, pentane; 0 – 50% Et₂O). The product was obtained as orange oil (0.17 g, 0.8 mmol, 51% yield over two steps). ¹H NMR (400 MHz, CDCl₃) δ 2.41 (s, 3H, CH₃), 2.77 (s, 1H, OH), 4.69 (s, 2H, CH₂OH), 7.25 (d, *J* = 7.8 Hz, 1H, ArH), 7.33 – 7.46 (m, 3H, ArH), 7.69 (d, *J* = 6.4 Hz, 2H, ArH), 7.79 (d, *J* = 7.5 Hz, 1H, ArH), 7.83 (s, 1H, ArH). ¹³C NMR (101 MHz, CDCl₃) δ 21.4, 64.7, 120.5, 120.6, 122.5, 123.0, 128.9, 129.2, 129.3, 131.9, 139.0, 142.1, 152.7, 152.8. HRMS (ESI+) calc. for. [M+H⁺] (C₁₄H₁₅N₂O) 227.1180, found: 227.1179.

(E)-1-(3-(bromomethyl)phenyl)-2-(*m*-tolyl)diazene (4f)

Compound **11f** (0.15 g, 0.66 mmol) was dissolved in DCM (10 mL) and NBS (0.18 g, 1.0 mmol) and triphenylphosphine (0.25 g, 0.95 mmol) were added. The reaction was stirred at

room temperature overnight. After completion, the reaction mixture was concentrated *in vacuo*. The product was purified by flash chromatography (Silicagel 40 – 63 nm, pentane; 0 – 5% Et₂O). The product was obtained as an orange oil (0.12 g, 0.42 mmol, 63% yield) ¹H NMR (400 MHz, CDCl₃) δ 2.49 (s, 3H, CH₃), 4.59 (s, 2H, CH₂Br), 7.33 (d, *J* = 7.7 Hz, 1H, ArH), 7.45 (t, *J* = 8.0 Hz, 1H, ArH), 7.52 (m, 2H, ArH), 7.80 (m, 2H, ArH), 7.91 (m, 1H, ArH), 7.99 (s, 1H, ArH) ¹³C NMR (101 MHz, CDCl₃) δ 21.5, 32.9, 120.7, 122.9, 123.3, 129.0, 129.6, 131.4, 132.1, 139.0, 152.6, 152.9. HRMS (ESI+) calc. for. [M+H⁺] (C₁₄H₁₅BrN₂) 289.0335, found: 289.0335.

(*E*)-(3-(*o*-tolyldiazenyl)phenyl)methanol (11g)

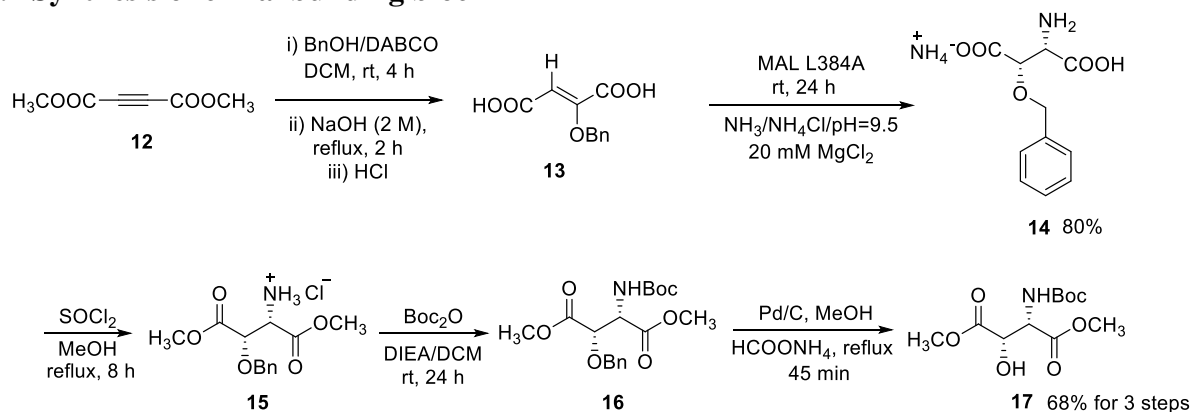
Ortho-toluidine **9g** (1.0 ml, 1.0 g, 9.3 mmol) was dissolved in DCM (20 mL) and water (100 mL) and Oxone (5.2 g, 19 mmol) was added. The reaction mixture was stirred at room temperature for 20 min. After completion, DCM (20 mL) was added and the aqueous layer was extracted with DCM (3 x 20 mL). The combined organic layers were washed with sat. aq. NaHCO₃, 1 N HCl and brine and concentrated *in vacuo*. The crude product was flushed over a silica gel column (Silicagel 40 – 63 nm, pentane). Without further purification, the crude product (0.20 g, 1.7 mmol) was dissolved in acetic acid (5 mL) and (3-aminophenyl)methanol (0.3 g, 2.4 mmol) was added. The reaction mixture was stirred at 40°C overnight. After completion EtOAc (15 mL) and sat aq. NaHCO₃ (10 mL) were added and the reaction mixture was stirred overnight. EtOAc (50 mL) and water (50 mL) were added and the aqueous layer was extracted with EtOAc (3 x 20 mL). The combined organic layers were washed with sat. aq. NaHCO₃, 1 N HCl and brine, dried with MgSO₄ and concentrated *in vacuo*. The product was purified by flash chromatography (Silicagel 40 – 63 nm, pentane, pentane; 0 – 50% Et₂O). The product was obtained as orange oil (0.17 g, 0.8 mmol, 6% yield

over two steps). ^1H NMR (400 MHz, CDCl_3) δ 2.70 (s, 3H, CH_3), 4.72 (s, 2H, CH_2Br), 7.24 (t, $J = 7.0$ Hz, 1H, ArH), 7.33 (m, 2H, ArH), 7.38 – 7.48 (m, 2H, ArH), 7.60 (d, $J = 8.0$ Hz, 1H, ArH), 7.81 (d, $J = 7.5$ Hz, 1H), 7.86 (s, 1H). ^{13}C NMR (101 MHz, CDCl_3) δ 17.6, 64.8, 115.5, 121.1, 122.3, 129.2, 129.2, 131.0, 131.3, 138.1, 142.0, 150.7, 153.1. HRMS (ESI+) calc. for. $[\text{M}+\text{H}^+]$ ($\text{C}_{14}\text{H}_{15}\text{N}_2\text{O}$): 227.1180, found: 227.1176.

(*E*)-1-(3-(bromomethyl)phenyl)-2-(*o*-tolyl)diazene (4g)

Compound **11g** (0.15 g, 0.66 mmol) was dissolved in DCM (10 mL) and NBS (0.16 g, 0.9 mmol) and triphenylphosphine (0.24 g, 0.92 mmol) were added. The reaction was stirred at room temperature overnight. After completion, the reaction mixture was concentrated *in vacuo*. The product was purified by flash chromatography (Silicagel 40 – 63 nm, pentane; 0 – 5% Et_2O). The product was obtained as an orange solid (0.11 g, 0.38 mmol, 57% yield). Mp: 46 – 48 °C, ^1H NMR (400 MHz, CDCl_3) δ 2.73 (s, 3H, CH_3), 4.59 (s, 2H, CH_2Br), 7.28 (d, $J = 8.1$ Hz, 1H, ArH), 7.32 – 7.40 (m, 2H, ArH), 7.50 (m, 2H, ArH), 7.63 (d, $J = 8.3$ Hz, 1H, ArH), 7.82 – 7.89 (m, 1H, ArH), 7.93 (s, 1H). ^{13}C NMR (101 MHz, CDCl_3) δ 17.5, 32.9, 115.4, 123.1, 123.3, 126.4, 129.5, 131.2, 131.3, 138.3, 138.8, 150.6, 153.2. HRMS (ESI+) calc. for. $[\text{M}+\text{H}^+]$ ($\text{C}_{14}\text{H}_{14}\text{BrN}_2$) 289.0335, found: 289.0335.

1.2.2 Synthesis of chiral building block 17

**Figure S5:** Synthesis of alkylating agent 17**trans-2-benzyloxy fumaric acid (13)**

To a stirred solution of dimethyl acetylenedicarboxylate (**12**, 14.2 g, 100 mmol) in DCM (250 mL), DABCO (1.1 g, 10 mmol) and benzyl alcohol (10.8 g, 100 mmol) were added and the reaction mixture was stirred at room temperature. After completion of the reaction (TLC monitoring), the solvent was removed under vacuum to provide crude products as a dark oil, which contained *trans* and *cis* isomers (*trans/cis* = 6/4). The crude product was dissolved in ethanol (300 mL) and subjected to basic hydrolysis using 2 M NaOH (300 mL) at reflux for 2 h. After complete hydrolysis, the reaction mixture was cooled to room temperature and extracted using EtOAc (2 x 300 mL). The aqueous layer was acidified with HCl (con.) until pH = 1 (ice-bath) and extracted with EtOAc (3 x 300 mL). The combined organic layers were washed with brine (2 x 500 mL), dried over anhydrous Na₂SO₄ and evaporated to provide a dark yellow solid. Recrystallization was performed using hexane/Et₂O (v/v = 1/3) to provide pure *trans*-2-benzyloxy-fumaric acid **13** (8.5 g, 38 mmol yield 38% over 2 steps). ¹H NMR (500 MHz, DMSO-*d*₆) δ 5.10 (s, 2H, CH₂), 6.08 (s, 1H, CH), 7.43 – 7.32 (m, 5H, ArH). The ¹H NMR spectra are in agreement with published data.¹

(L-threo)-3-benzyloxyaspartate (14, L-TBOA)

To a slowly stirred solution of *trans*-2-benzyloxy-fumaric acid **13** (2.4 g, 11 mmol) in 220 mL of buffer (5 M NH₃/NH₄Cl, 20 mM MgCl₂, pH = 9.5) was added MAL L384A¹ (0.01 mol%, 5 mL, 12.3 mg/mL), and the reaction mixture was incubated for 24 hours at room temperature. After completion of the enzymatic reaction (¹H NMR monitoring, >98% conversion), the reaction mixture was warmed up to 60 °C for 10 min until the enzyme precipitated, followed by filtration through cotton to remove the white precipitates. Most of the water in the reaction mixture was evaporated under vacuum, then the resulting concentrated mixture was acidified with HCl (conc.) to pH = 1 (ice-bath). The acidified solution was loaded onto a column packed with cation-exchange resin (1000 g of Dowex 50W X8, 50-100 mesh), which was pre-treated with 2 M aqueous ammonia (4 column volumes), 1 M HCl (2 column volumes) and distilled water (4 column volumes). The column was washed with water (2 column volumes) and the product was eluted with 2 M aqueous ammonia (2 column volumes). The ninhydrin-positive fractions were collected and lyophilized to yield the product L-TBOA (**14**) as ammonium salt (white powder, 2.3 g, 8.8 mmol, 80% yield). ¹H NMR (500 MHz, D₂O) δ 3.99 (d, *J* = 2.3 Hz, 1H, CH), 4.32 (d, *J* = 2.3 Hz, 1H, CH), 4.47 (d, *J* = 11.6 Hz, 1H, BnH), 4.71 (d, *J* = 11.6 Hz, 1H, BnH), 7.43 – 7.34 (m, 5H, ArH). The ¹H NMR spectra are in agreement with published data.¹

(L-threo)-dimethyl 2-amino-3-(benzyloxy)succinate hydrochloride (15)

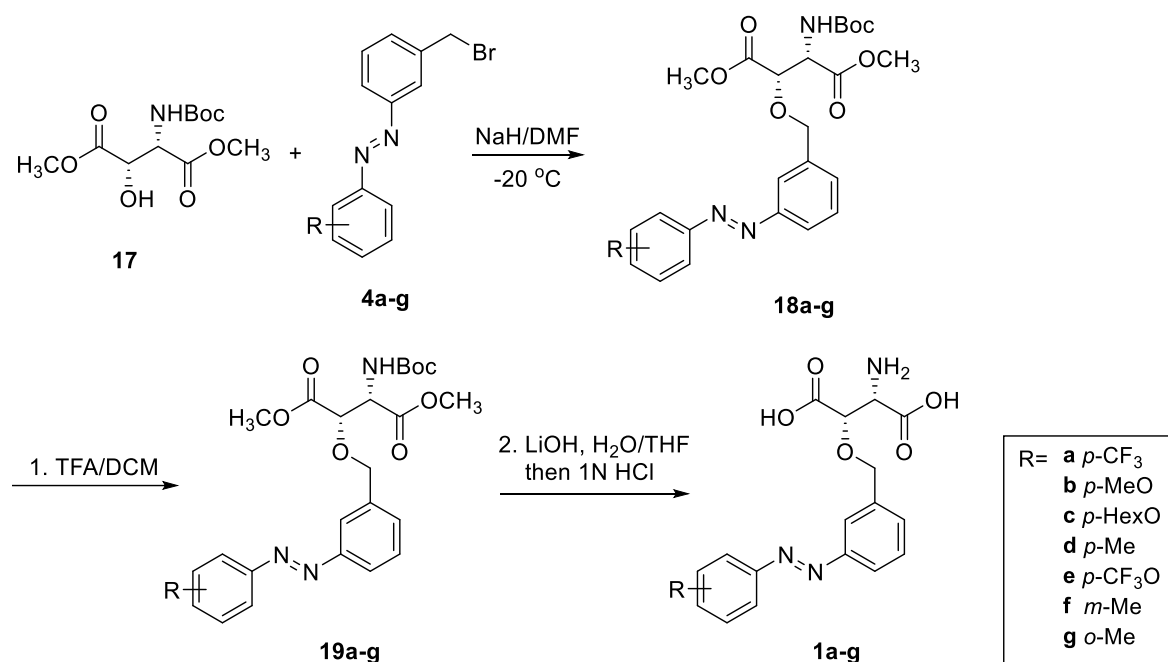
To a stirred suspension of L-TBOA (**14**, 1.6 g, 6.2 mmol) in dry MeOH (30 mL) at was added SOCl₂ (4.5 mL, 62 mmol) dropwise (in an ice-bath). After 20 minutes, the cooling system was removed and the reaction mixture was heated to reflux for 8 h. After completion of the reaction (TLC monitoring), the reaction mixture was cooled to room temperature, and solvent was removed to provide crude product **15** as a white solid (1.8 g, 95%). No purification was needed, the crude product **15** was directly used for the next step.

(L-threo)-dimethyl 2-(benzyloxy)-3-[(tert-butoxycarbonyl)amino]succinate (16)

To a stirred solution of **15** (1.8 g, 5.9 mmol) in dry DCM (50 mL) was added DIEA (1.5 mL, 9.1 mmol) and Boc₂O (1.6 g, 7.4 mmol) under cooling in an ice-bath. After 10 minutes, the cooling was removed and the reaction mixture was stirred at room temperature for further 24 h. After completion of the reaction, the reaction mixture was diluted with DCM (50 mL), and washed with 0.5 M HCl (50 mL), saturated NaHCO₃ solution (100 mL) and brine (100 mL). The organic layer was dried over Na₂SO₄ and concentrated under vacuum to give crude product **16** as a clear oil (2.0 g, 5.3 mmol, 90% yield). No purification was needed, product **16** was directly used for the next step. ¹H NMR (500 MHz, DMSO-*d*₆) δ 1.36 (s, 9H, Boc-**H**₉), 3.60 (s, 3H, OCH₃), 3.67 (s, 3H, OCH₃), 4.42 (d, *J* = 11.9 Hz, 1H, Bn**H**), 4.47 (d, *J* = 4.3 Hz, 1H, **CH**), 4.62 (dd, *J* = 9.5, 4.3 Hz, 1H, **CH**), 4.67 (d, *J* = 11.9 Hz, 1H, Bn**H**), 7.05 (d, *J* = 9.5 Hz, 1H, **NH**), 7.28 – 7.36 (m, 5H, Ar**H**). The ¹H NMR spectra are in agreement with published data.²

(L-threo)-dimethyl 2-[(tert-butoxycarbonyl)amino]-3-hydroxy succinate (17)

To a stirred solution of **16** (2.0 g, 5.4 mmol) in dry MeOH (50 mL) was added Pd/C (10%, 1.8 g) and HCOONH₄ (2.5 g). The mixture was heated to reflux for 45 min. After completion of the reaction (TLC monitoring), the reaction mixture was filtered through Celite and evaporated under vacuum to provide crude product **17**. Purification was conducted *via* flash chromatography (EtOAc : petroleum ether, 1:4, v/v) to provide compound **17** as clear oil (1.2 g, 4.3 mmol, 80% yield). ¹H NMR (500 MHz, CDCl₃) δ 1.42 (s, 9H, Boc-**H**₉), 3.22 (d, *J* = 5.7 Hz, 1H, **OH**), 3.80 (s, 3H, OCH₃), 3.82 (s, 3H, OCH₃), 4.69 (dd, *J* = 5.8, 2.0 Hz, 1H, **CH**), 4.78 (dd, *J* = 9.3, 2.0 Hz, 1H, **CH**), 5.29 (d, *J* = 9.5 Hz, 1H, **NH**). ¹³C NMR (126 MHz, CDCl₃) δ 28.2, 52.9, 53.2, 56.1, 71.1, 80.4, 155.3, 169.8, 172.4. HRMS (ESI⁺): calc. for [M+Na]⁺ (C₁₁H₁₉NO₇Na) 300.1054, found 300.1053.

1.2.3 Synthesis of final compounds **1a-g****Figure S6:** Synthesis of azo-TBOAs **1a-g****(L-threo)-trans-dimethyl 2-((tert-butoxycarbonyl)amino)-3-(3-((4-(trifluoromethyl)-phenyl)diazenyl)benzyloxy) succinate (**18a**)**

Compound **17** (80 mg, 0.29 mmol) and **4a** (200 mg, 0.56 mmol) were dissolved in DMF (2 mL) under -20 °C and stirred over 10 min. NaH (60% in mineral oil, 11.6 mg, 0.29 mmol) was added, and the reaction mixture was stirred at -20 °C for 2 h. Afterwards, it was warmed to 0 °C (ice bath) and the stirring continued for another 2 h. The reaction mixture was quenched with cold water and then extracted with EtOAc (3 x 20 mL). The collected organic phases were washed with brine (3 x 50 mL), and dried with Na₂SO₄. The volatiles were evaporated and the product was purified by flash chromatography (EtOAc : petroleum ether, 9:91, v/v) to provide pure **18a** as yellow oil (72 mg, 46% yield). ¹H NMR (500 MHz, CDCl₃) δ 1.43 (s, 9H, Boc-**H**₉), 3.66 (s, 3H, OCH₃), 3.80 (s, 3H, OCH₃), 4.49 (d, *J* = 12.0 Hz, 1H, Bn**H**), 4.56 (d, *J* = 2.4 Hz, 1H, CH), 4.86 (dd, *J* = 10.0, 2.4 Hz, 1H, CH), 4.94 (d, *J* = 12.0 Hz,

1H, BnH), 5.37 (d, $J = 10.0$ Hz, 1H, NH), 7.43 (d, $J = 7.6$ Hz, 1H, ArH), 7.52 (t, $J = 7.7$ Hz, 1H, ArH), 7.79 (d, $J = 8.3$ Hz, 2H, ArH), 7.84 (s, 1H, ArH), 7.90 (d, $J = 7.9$ Hz, 1H, ArH), 8.00 (d, $J = 8.2$ Hz, 2H, ArH). ^{13}C NMR (126 MHz, CDCl_3) δ 28.3, 52.7, 52.9, 56.2, 72.4, 77.4, 80.5, 122.6, 123.2, 123.3, 124.0 (q, $J = 272.2$ Hz), 126.5 (q, $J = 3.8$ Hz), 129.5, 131.4, 132.5 (q, $J = 31.5$ Hz), 138.2, 152.6, 154.4, 155.6, 169.7, 169.8. HRMS (ESI+) calc for $[\text{M}+\text{Na}]^+$ ($\text{C}_{25}\text{H}_{28}\text{N}_3\text{O}_7\text{Na}$) 562.1772, found 562.1770.

(L-threo)-trans-3-(3-((4-(trifluoromethyl)phenyl)diazenyl)benzyloxy)aspartate (1a)

(L-trans-p-CF₃-azo-TBOA)

To a solution of **18a** (65 mg, 0.12 mmol) in dry DCM (2 mL), cooled in an ice-bath, trifluoroacetic acid (0.8 mL) was added dropwise. After 10 min, the ice-bath was removed and the reaction mixture was stirred at room temperature for 1.5 h until all the starting materials were consumed (TLC monitor). Volatiles were removed *in vacuo* to provide product **19a** which was used in the next step without further purification. Compound **19a** was dissolved in THF (1 mL) and water (1 mL) and LiOH (17 mg, 0.72 mmol) was added. The reaction mixture was stirred at room temperature for 2 h. Volatiles were removed *in vacuo* and, residue was washed with EtOAc (1 mL) and acidified with 1 M HCl until yellow precipitates appeared. The precipitate was filtered off, washed with cold water and dried under vacuum overnight to provide the final product **1a** as yellow solid (25 mg, 50% yield over two steps). ^1H NMR (400 MHz, $\text{DMSO}-d_6$) δ 3.71 (d, $J = 7.5$ Hz, 1H, CH), 4.16 (d, $J = 7.5$ Hz, 1H, CH), 4.58 (d, $J = 11.5$ Hz, 1H, BnH), 4.88 (d, $J = 11.5$ Hz, 1H, BnH), 7.58 (t, $J = 7.7$ Hz, 1H, ArH), 7.67 (d, $J = 7.5$ Hz, 1H, ArH), 7.85 (d, $J = 7.9$ Hz, 1H, ArH), 8.97 – 8.00 (m, 3H, ArH), 8.07 (d, $J = 8.4$ Hz, 2H, ArH); ^{13}C NMR (101 MHz, $\text{DMSO}-d_6$) δ 53.8, 71.5, 76.1, 121.6, 122.6, 123.1, 126.7 (q, $J = 5.0$ Hz), 129.2, 130.9, 131.7, 139.9, 151.7, 154.1,

168.3, 171.1. One Carbon is missing due to CF₃. ¹⁹F NMR (376 MHz, DMSO-*d*₆) δ -56.7 (s). HRMS (ESI+) calc for [M+H]⁺: (C₁₈H₁₇F₃N₃O₅) 412.1115, found 412.1114.

(*L*-threo)-trans-dimethyl 2-((*tert*-butoxycarbonyl)amino)-3-(3-((4-(methoxy)-phenyl)diazenyl)benzyloxy) succinate (18b**)**

Compound **17** (90 mg, 0.32 mmol) and **4b** (195 mg, 0.64 mmol) were dissolved in DMF (2 mL) under -20 °C and stirred over 10 min. NaH (60% in mineral oil, 12.8 mg, 0.32 mmol) was added, and the reaction mixture was stirred at -20 °C for 2 h. Afterwards, it was warmed to 0 °C (ice bath) and the stirring continued for another 2 h. The reaction mixture was quenched with cold water and then extracted with EtOAc (3 x 20 mL). The collected organic phases were washed with brine (3 x 50 mL), and dried with Na₂SO₄. The volatiles were evaporated and the product was purified by flash chromatography (EtOAc : petroleum ether, 18:82, v/v) to provide pure **18b** as yellow oil (53 mg, 33% yield). ¹H NMR (500 MHz, CDCl₃) δ 1.43 (s, 9H, Boc-**H**₉), 3.64 (s, 3H, O**CH**₃), 3.79 (s, 3H, O**CH**₃), 3.90 (s, 3H, O**CH**₃), 4.47 (d, *J* = 12.1 Hz, 1H, Bn**H**), 4.54 (d, *J* = 2.4 Hz, 1H, **CH**), 4.83 (dd, *J* = 10.0, 2.0 Hz, 1H, **CH**), 4.93 (d, *J* = 12.1 Hz, 1H, Bn**H**), 5.38 (d, *J* = 9.9 Hz, 1H, **NH**), 7.02 (d, *J* = 8.8 Hz, 2H, Ar**H**), 7.34 (d, *J* = 7.5 Hz, 1H, Ar**H**), 7.45 – 7.48 (m, 1H, Ar**H**), 7.75 (s, 1H, Ar**H**), 7.81 – 7.84 (m, 1H, Ar**H**), 7.91 – 7.94 (m, 2H, Ar**H**); ¹³C NMR (126 MHz, CDCl₃) δ 28.34, 52.6, 52.9, 55.8, 56.2, 65.2, 72.5, 77.1, 114.4, 120.4, 122.2, 122.7, 125.0, 128.9, 129.3, 130.1, 137.9, 147.0, 153.0, 162.4, 169.8. HRMS (ESI+) calc. for [M+H]⁺ (C₂₅H₃₂N₃O₈) 502.2184, found 502.2187.

(L-threo)-trans-3-(3-((4-(methoxy)phenyl)diazenyl)benzyloxy)aspartate (1b)**(L-trans-p-MeO-azo-TBOA)**

To a solution of **18b** (53 mg, 0.11 mmol) in dry DCM (2 mL), cooled in an ice-bath, trifluoroacetic acid (0.8 mL) was added dropwise. After 10 min, the ice-bath was removed and the reaction mixture was stirred at room temperature for 1.5 h until all the starting materials were consumed (TLC monitor). Volatiles were removed *in vacuo* to provide product **19b** which was used in the next step without further purification. Compound **19b** was dissolved in THF (1 mL) and water (1 mL) and LiOH (16 mg, 0.66 mmol) was added. The reaction mixture was stirred at room temperature for 2 h. Volatiles were removed *in vacuo* and, residue was washed with EtOAc (1 mL) and acidified with 1 M HCl until yellow precipitates appeared. The precipitate was filtered off, washed with cold water and dried under vacuum overnight to provide the final product **1b** as yellow solid (25 mg, 61% yield over two steps). ¹H NMR (400 MHz, DMSO-*d*₆) δ 3.86 – 3.89 (m, 4H, CH and OCH₃), 4.17 (dd, *J* = 9.7, 1.4 Hz, 1H, CH), 4.59 (d, *J* = 10.9 Hz, 1H, BnH), 4.94 (d, *J* = 10.9 Hz, 1H, BnH), 7.13 – 7.16 (m, 2H, ArH), 7.53 (t, *J* = 7.7 Hz, 1H, ArH), 7.60 (d, *J* = 7.6 Hz, 1H, ArH), 7.76 (d, *J* = 7.9 Hz, 1H, ArH), 7.90 – 7.93 (m, 3H, ArH); ¹³C NMR (101 MHz, DMSO-*d*₆) δ 53.2, 55.7, 72.4, 75.1, 114.7, 121.2, 122.2, 124.6, 129.1, 130.5, 139.3, 146.2, 152.0, 162.1, 168.5, 170.7. HRMS (ESI+) calc. for [M+H]⁺ (C₁₈H₂₀N₃O₆) 374.1347, found 374.1350.

(L-threo)-trans-dimethyl 2-((tert-butoxycarbonyl)amino)-3-(3-((4-(hexyloxy)phenyl)diazenyl)benzyloxy) succinate (18c)

Compound **17** (90 mg, 0.32 mmol) and **4a** (244 mg, 0.64 mmol) were dissolved in DMF (2 mL) under -20 °C and stirred over 10 min. NaH (60% in mineral oil, 12.8 mg, 0.32 mmol)

was added, and the reaction mixture was stirred at -20 °C for 2 h. Afterwards, it was warmed to 0 °C (ice bath) and the stirring continued for another 2 h. The reaction mixture was quenched with cold water and then extracted with EtOAc (3 x 20 mL). The collected organic phases were washed with brine (3 x 50 mL), and dried with Na₂SO₄. The volatiles were evaporated and the product was purified by flash chromatography (EtOAc : petroleum ether, 10:90, v/v) to provide pure **18c** as yellow oil (58 mg, 32% yield). ¹H NMR (500 MHz, CDCl₃) δ 0.92 (t, *J* = 6.7 Hz, 3H, CH₃), 1.34 – 1.37 (m, 4H, CH₂, CH₂), 1.43 (s, 9H, Boc-H₉), 1.46 – 1.50 (m, 2H, CH₂), 1.79 – 1.85 (m, 2H, CH₂), 3.63 (s, 3H, OCH₃), 3.79 (s, 3H, OCH₃), 4.04 (t, *J* = 6.5 Hz, 2H, OCH₂), 4.47 (d, *J* = 12.2 Hz, 1H, BnH), 4.54 (d, *J* = 2.5 Hz, 1H, CH), 4.82 – 4.84 (m, 1H, CH), 4.92 (d, *J* = 12.2 Hz, 1H, BnH), 5.38 (d, *J* = 10.0 Hz, 1H, NH), 6.99 – 7.01 (m, 2H, ArH), 7.33 (d, *J* = 7.2 Hz, 1H, ArH), 7.47 (t, *J* = 7.7 Hz, 1H, ArH), 7.75 (s, 1H, ArH), 7.82 (d, *J* = 7.4 Hz, 1H, ArH), 7.89 – 7.91 (m, 2H, ArH); ¹³C NMR (126 MHz, CDCl₃) δ 14.2, 22.8, 25.8, 28.3, 29.3, 31.7, 52.6, 52.9, 56.2, 68.5, 72.5, 77.1, 80.4, 114.9, 122.1, 122.7, 124.9, 129.3, 130.1, 137.8, 146.9, 153.0, 155.6, 162.0, 169.8. One C is missing due to overlap (two COOCH₃). HRMS (ESI+) calc. for [M+H]⁺ (C₃₀H₄₂N₃O₈) 572.2966, found 572.2972.

(L-threo)-trans-3-(3-((4-(hexyloxy)phenyl)diazenyl)benzyloxy)aspartate (1c)

(L-trans-p-HexO-azo-TBOA)

To a solution of **18c** (58 mg, 0.10 mmol) in dry DCM (2 mL), cooled in an ice-bath, trifluoroacetic acid (0.8 mL) was added dropwise. After 10 min, the ice-bath was removed and the reaction mixture was stirred at room temperature for 1.5 h until all the starting materials were consumed (TLC monitor). Volatiles were removed *in vacuo* to provide intermediate **19c** which was used in the next step without further purification. Compound **19c** was dissolved in THF (1 mL) and water (1 mL) and LiOH (14.4 mg, 0.60 mmol) was added.

The reaction mixture was stirred at room temperature for 2 h. Volatiles were removed *in vacuo* and, residue was washed with EtOAc (1 mL) and acidified with 1 M HCl until yellow precipitates appeared. The precipitate was filtered off, washed with cold water and dried under vacuum overnight to provide the final product **1c** as yellow solid (23 mg, 52% yield over two steps). ¹H NMR (400 MHz, DMSO-*d*₆) δ 0.89 (t, *J* = 8.5 Hz, 3H, CH₃), 1.29 – 1.36 (m, 4H, CH₂, CH₂), 1.40 – 1.47 (m, 2H, CH₂), 1.75 (p, *J* = 6.7 Hz, 2H, CH₂), 3.86 (d, *J* = 9.6 Hz, 1H, CH), 4.08 (t, *J* = 6.5 Hz, 2H, OCH₂), 4.16 (d, *J* = 9.6 Hz, 1H, CH), 4.59 (d, *J* = 11.0 Hz, 1H, BnH), 4.94 (d, *J* = 10.9 Hz, 1H, BnH), 7.12 – 7.14 (m, 2H, ArH), 7.53 (t, *J* = 7.7 Hz, 1H, ArH), 7.59 (d, *J* = 7.3 Hz, 1H, ArH), 7.75 (d, *J* = 7.9 Hz, 1H, ArH), 7.88 – 7.93 (m, 3H, ArH); ¹³C NMR (101 MHz, DMSO-*d*₆) δ 14.0, 22.1, 25.2, 28.6, 31.0, 53.2, 68.1, 72.3, 75.1, 115.1, 121.1, 122.1, 124.6, 129.0, 130.4, 139.3, 146.1, 152.0, 161.5, 168.4, 170.6. HRMS (ESI+) calc. for [M+H]⁺ (C₂₃H₃₀N₃O₆) 444.2129, found 444.2134.

(L-threo)-trans-dimethyl 2-((tert-butoxycarbonyl)amino)-3-(3-((4-(methyl)-phenyl)diazenyl)benzyloxy) succinate (18d)

Compound **17** (77 mg, 0.28 mmol) and 4d (120 mg, 0.42 mmol) were dissolved in DMF (2 mL) under -20 °C and stirred over 10 min. NaH (60% in mineral oil, 11.2 mg, 0.28 mmol) was added, and the reaction mixture was stirred at -20 °C for 2 h. Afterwards, it was warmed to 0 °C (ice bath) and the stirring continued for another 2 h. The reaction mixture was quenched with cold water and then extracted with EtOAc (3 x 20 mL). The collected organic phases were washed with brine (3 x 50 mL), and dried with Na₂SO₄. The volatiles were evaporated and the product was purified by flash chromatography (EtOAc : petroleum ether, 10:90, v/v) to provide pure **18d** as yellow oil (42 mg, 31% yield). ¹H NMR (500 MHz, CDCl₃) δ 1.43 (s, 9H, Boc-H₉), 2.44 (s, 3H, CH₃), 3.64 (s, 3H, OCH₃), 3.79 (s, 3H, OCH₃), 4.48 (d, *J* = 12.1 Hz, 1H, BnH), 4.54 (d, *J* = 2.3 Hz, 1H, CH), 4.84 (dd, *J* = 10.0, 2.4 Hz, 1H,

CH), 4.93 (d, $J = 12.1$ Hz, 1H, **BnH**), 5.38 (d, $J = 9.9$ Hz, 1H, **NH**), 7.32 (d, $J = 8.0$ Hz, 2H, **ArH**), 7.36 (dt, $J = 7.4, 1.3$ Hz, 1H, **ArH**), 7.49 (t, $J = 7.7$ Hz, 1H, **ArH**), 7.77 (d, $J = 1.9$ Hz, 1H, **ArH**), 7.84 (dd, $J = 11.6, 8.7$ Hz, 3H, **ArH**); ^{13}C NMR (126 MHz, DMSO- d_6) δ 21.1, 28.0, 52.1, 52.4, 55.6, 71.5, 77.5, 78.8, 121.6, 121.8, 122.6, 129.3, 130.0, 130.4, 138.9, 141.9, 150.0, 151.9, 155.3, 169.5, 169.5. HRMS (ESI+) calc for $[\text{M}+\text{H}]^+$ ($\text{C}_{25}\text{H}_{32}\text{N}_3\text{O}_7$) 486.2235, found 486.2233.

***L-threo*)-trans-3-(3-((4-(methyl)phenyl)diazenyl)benzyloxy)aspartate (1d)**

(*L-trans-p*-Me-azo-TBOA)

To a solution of **18d** (42 mg, 0.087 mmol) in dry DCM (2 mL), cooled in an ice-bath, trifluoroacetic acid (0.8 mL) was added dropwise. After 10 min, the ice-bath was removed and the reaction mixture was stirred at room temperature for 1.5 h until all the starting materials were consumed (TLC monitor). Volatiles were removed *in vacuo* to provide product **19d** which was used in the next step without further purification. Compound **19d** was dissolved in THF (1 mL) and water (1 mL) and LiOH (12.5 mg, 0.52 mmol) was added. The reaction mixture was stirred at room temperature for 2 h. Volatiles were removed *in vacuo* and, residue was washed with EtOAc (1 mL) and acidified with 1 M HCl until yellow precipitates appeared. The precipitate was filtered off, washed with cold water and dried under vacuum overnight to provide the final product **1d** as yellow solid (22 mg, 71% yield over two steps). ^1H NMR (400 MHz, DMSO- d_6) δ 2.42 (s, 3H, **CH**₃), 3.87 (dd, $J = 9.7, 1.7$ Hz, 1H, **CH**), 4.17 (dd, $J = 9.6, 1.8$ Hz, 1H, **CH**), 4.60 (d, $J = 10.9$ Hz, 1H, **BnH**), 4.95 (d, $J = 11.0$ Hz, 1H, **BnH**), 7.42 (d, $J = 7.3$ Hz, 2H, **ArH**), 7.55 (td, $J = 7.7, 1.7$ Hz, 1H, **ArH**), 7.63 (d, $J = 6.7$ Hz, 1H, **ArH**), 7.76 – 7.86 (m, 3H, **ArH**), 7.96 (s, 1H, **ArH**); ^{13}C NMR (101 MHz, DMSO- d_6) δ 21.1, 53.2, 72.3, 75.0, 121.3, 122.3, 122.6, 129.1, 130.0, 130.9, 139.4, 141.8,

150.1, 151.9, 168.4, 170.6. HRMS (ESI+) calc for [M+H] (C₁₈H₂₀N₃O₅) 358.1398, found 358.1396.

(L-threo)-trans-dimethyl 2-((tert-butoxycarbonyl)amino)-3-(3-((4-(trifluoromethoxy)phenyl)diazenyl)benzyloxy) succinate (18e)

Compound **17** (80 mg, 0.29 mmol) and **4e** (130 mg, 0.36 mmol) were dissolved in DMF (2 mL) under -20 °C and stirred over 10 min. NaH (60% in mineral oil, 11.6 mg, 0.29 mmol) was added, and the reaction mixture was stirred at -20 °C for 2 h. Afterwards, it was warmed to 0 °C (ice bath) and the stirring continued for another 2 h. The reaction mixture was quenched with cold water and then extracted with EtOAc (3 x 20 mL). The collected organic phases were washed with brine (3 x 50 mL), and dried with Na₂SO₄. The volatiles were evaporated and the product was purified by flash chromatography (EtOAc : petroleum ether, 10:90, v/v) to provide pure **18e** as yellow oil (54 mg, 34% yield). ¹H NMR (500 MHz, CDCl₃) δ 1.42 (s, 9H, Boc-**H**₉), 3.65 (s, 3H, OCH₃), 3.79 (s, 3H, OCH₃), 4.48 (d, *J* = 12.0 Hz, 1H, Bn**H**), 4.55 (d, *J* = 2.3 Hz, 1H, **CH**), 4.85 (dd, *J* = 10.0, 2.4 Hz, 1H, **CH**), 4.93 (d, *J* = 12.0 Hz, 1H, Bn**H**), 5.38 (d, *J* = 10.0 Hz, 1H, **NH**), 7.36 (d, *J* = 8.8 Hz, 2H, Ar**H**), 7.40 (d, *J* = 7.6 Hz, 1H, Ar**H**), 7.50 (t, *J* = 7.7 Hz, 1H, Ar**H**), 7.80 (t, *J* = 1.8 Hz, 1H, Ar**H**), 7.86 (d, *J* = 7.9 Hz, 1H, Ar**H**), 7.96 (d, *J* = 8.8 Hz, 2H, Ar**H**); ¹³C NMR (126 MHz, CDCl₃) δ 28.3, 52.6, 52.9, 56.2, 72.4, 77.3, 80.4, 121.4, 122.4, 123.1, 124.5, 129.4, 131.0, 138.1, 150.7, 151.1 (d, *J* = 0.9 Hz), 152.6, 155.6, 169.7, 169.8. One C is missing due to overlap (CF₃). HRMS (ESI+) calc for [M+H]⁺ (C₂₅H₂₉N₃O₈F₃) 556.1901, found 556.1899.

(L-threo)-trans-3-(3-((4-(trifluoromethoxy)phenyl)diazenyl)benzyloxy)aspartate (1e)

(L-trans-p-CF₃O-azo-TBOA)

To a solution of **18e** (54 mg, 0.10 mmol) in dry DCM (2 mL), cooled in an ice-bath, trifluoroacetic acid (0.8 mL) was added dropwise. After 10 min, the ice-bath was removed and the reaction mixture was stirred at room temperature for 1.5 h until all the starting materials were consumed (TLC monitor). Volatiles were removed *in vacuo* to provide product **19e** which was used in the next step without further purification. Compound **19e** was dissolved in THF (1 mL) and water (1 mL) and LiOH (14.4 mg, 0.60 mmol) was added. The reaction mixture was stirred at room temperature for 2 h. Volatiles were removed *in vacuo* and, residue was washed with EtOAc (1 mL) and acidified with 1 M HCl until yellow precipitates appeared. The precipitate was filtered off, washed with cold water and dried under vacuum overnight to provide the final product **1e** as yellow solid (30 mg, 70% yield over two steps). ¹H NMR (400 MHz, DMSO-*d*₆) δ 3.88 (d, *J* = 9.7 Hz, 1H, CH), 4.17 (d, *J* = 9.6 Hz, 1H, CH), 4.61 (d, *J* = 11.0 Hz, 1H, BnH), 4.96 (d, *J* = 11.0 Hz, 1H, BnH), 7.56 – 7.62 (m, 3H, ArH), 7.67 (d, *J* = 7.1 Hz, 1H, ArH), 7.83 (d, *J* = 8.0 Hz, 1H, ArH), 8.00 – 8.04 (m, 3H, ArH); ¹³C NMR (101 MHz, DMSO-*d*₆) δ 53.2, 72.2, 75.0, 121.6, 121.9, 122.6, 124.5, 129.2, 131.5, 139.5, 150.1, 150.5, 151.8, 168.4, 170.6. One C is missing due to CF₃. ¹⁹F NMR (376 MHz, DMSO-*d*₆) δ -61.1 (s). HRMS (ESI+) calc for [M+H]⁺ (C₁₈H₁₇N₃O₆F₃) 428.1064, found 428.1064.

(L-threo)-trans-dimethyl 2-((tert-butoxycarbonyl)amino)-3-(3-((3-(methyl-phenyl)diazenyl)benzyloxy) succinate (18f)

Compound **17** (91 mg, 0.33 mmol) and **4f** (120 mg, 0.42 mmol) were dissolved in DMF (2 mL) under -20 °C and stirred over 10 min. NaH (60% in mineral oil, 13.2 mg, 0.33 mmol) was added, and the reaction mixture was stirred at -20 °C for 2 h. Afterwards, it was warmed to 0 °C (ice bath) and the stirring continued for another 2 h. The reaction mixture was

quenched with cold water and then extracted with EtOAc (3 x 20 mL). The collected organic phases were washed with brine (3 x 50 mL), and dried with Na₂SO₄. The volatiles were evaporated and the product was purified by flash chromatography (EtOAc : petroleum ether, 10:90, v/v) to provide pure **18f** as yellow oil (50 mg, 31% yield). ¹H NMR (500 MHz, CDCl₃) δ 1.43 (s, 9H, Boc-**H**₉), 2.46 (s, 3H, **CH**₃), 3.64 (s, 3H, O**CH**₃), 3.79 (s, 3H, O**CH**₃), 4.48 (d, J = 12.1 Hz, 1H, Bn**H**), 4.55 (d, J = 2.4 Hz, 1H, **CH**), 4.84 (dd, J = 10.0, 2.4 Hz, 1H, **CH**), 4.93 (d, J = 12.1 Hz, 1H, Bn**H**), 5.38 (d, J = 10.0 Hz, 1H, **NH**), 7.30 (d, J = 7.4 Hz, 1H, Ar**H**), 7.38 (dt, J = 7.6, 1.3 Hz, 1H, Ar**H**), 7.41 (t, J = 8.0 Hz, 1H, Ar**H**), 7.50 (t, J = 7.7 Hz, 1H, Ar**H**), 7.72 – 7.73 (m, 2H, Ar**H**), 7.79 (s, 1H, Ar**H**), 7.86 (dt, J = 8.0, 1.5 Hz, 1H, Ar**H**); ¹³C NMR (126 MHz, DMSO-*d*₆) δ 20.9, 28.0, 52.1, 52.4, 55.6, 71.5, 77.5, 78.8, 120.3, 121.6, 121.7, 121.8, 122.5, 122.5, 129.3, 130.6, 132.3, 138.9, 139.0, 152.0, 155.3, 169.5, 169.5. HRMS (ESI+) calc for [M+H]⁺ (C₂₅H₃₂N₃O₇) 486.2235, found 486.2234.

(L-threo)-trans-3-(3-((3-(methyl)phenyl)diazenyl)benzyloxy)aspartate (1f)

(L-trans-m-Me-azo-TBOA)

To a solution of **18f** (50 mg, 0.10 mmol) in dry DCM (2 mL), cooled in an ice-bath, trifluoroacetic acid (0.8 mL) was added dropwise. After 10 min, the ice-bath was removed and the reaction mixture was stirred at room temperature for 1.5 h until all the starting materials were consumed (TLC monitor). Volatiles were removed *in vacuo* to provide product **19f** which was used in the next step without further purification. Compound **19f** was dissolved in THF (1 mL) and water (1 mL) and LiOH (14.4 mg, 0.60 mmol) was added. The reaction mixture was stirred at room temperature for 2 h. Volatiles were removed *in vacuo* and, residue was washed with EtOAc (1 mL) and acidified with 1 M HCl until yellow precipitates appeared. The precipitate was filtered off, washed with cold water and dried under vacuum overnight to provide the final product **1f** as yellow solid (18 mg, 50% yield over two steps).

^1H NMR (400 MHz, DMSO- d_6) δ 2.43 (s, 3H, CH_3), 3.87 (d, $J = 9.7$ Hz, 1H, CH), 4.17 (d, $J = 9.7$ Hz, 1H, CH), 4.60 (d, $J = 11.0$ Hz, 1H, BnH), 4.95 (d, $J = 11.0$ Hz, 1H, BnH), 7.40 (d, $J = 7.7$ Hz, 1H, ArH), 7.47 – 7.52 (m, 1H, ArH), 7.56 (t, $J = 7.7$ Hz, 1H, ArH), 7.64 (d, $J = 7.5$ Hz, 1H, ArH), 7.70 – 7.72 (m, 2H, ArH), 7.80 (d, $J = 7.7$ Hz, 1H, ArH), 7.98 (s, 1H, ArH); ^{13}C NMR (101 MHz, DMSO- d_6) δ 20.9, 53.1, 72.3, 74.9, 120.2, 121.4, 122.4, 122.5, 129.1, 129.3, 131.0, 132.2, 139.0, 139.4, 151.9, 152.0, 168.4, 170.5. HRMS (ESI+) calc for $[\text{M}+\text{H}]^+$ ($\text{C}_{18}\text{H}_{20}\text{N}_3\text{O}_5$) 358.1398, found 358.1396.

(*L*-threo)-trans-dimethyl 2-((*tert*-butoxycarbonyl)amino)-3-(3-((2-(methyl)-phenyl)diazenyl)benzyloxy) succinate (18g**)**

Compound **17** (90 mg, 0.32 mmol) and **4f** (185 mg, 0.64 mmol) were dissolved in DMF (2 mL) under -20 °C and stirred over 10 min. NaH (60% in mineral oil, 12.8 mg, 0.32 mmol) was added, and the reaction mixture was stirred at -20 °C for 2 h. Afterwards, it was warmed to 0 °C (ice bath) and the stirring continued for another 2 h. The reaction mixture was quenched with cold water and then extracted with EtOAc (3 x 20 mL). The collected organic phases were washed with brine (3 x 50 mL), and dried with Na_2SO_4 . The volatiles were evaporated and the product was purified by flash chromatography (EtOAc : petroleum ether, 10:90, v/v) to provide pure **18g** as yellow oil (56 mg, 36% yield). ^1H NMR (500 MHz, CDCl_3) δ 1.42 (s, 9H, Boc- H_9), 2.73 (s, 3H, CH_3), 3.64 (s, 3H, OCH_3), 3.79 (s, 3H, OCH_3), 4.49 (d, $J = 12.1$ Hz, 1H, BnH), 4.55 (d, $J = 2.4$ Hz, 1H, CH), 4.84 (dd, $J = 9.9, 2.4$ Hz, 1H, CH), 4.93 (d, $J = 12.0$ Hz, 1H, BnH), 5.39 (d, $J = 9.9$ Hz, 1H, NH), 7.25 – 7.28 (m, 1H, ArH), 7.34 – 7.39 (m, 3H, ArH), 7.49 (t, $J = 7.7$ Hz, 1H, ArH), 7.62 (d, $J = 8.0$ Hz, 1H, ArH), 7.79 (d, $J = 1.9$ Hz, 1H, ArH), 7.86 (dd, $J = 8.0, 1.5$ Hz, 1H); ^{13}C NMR (126 MHz, DMSO- d_6) δ 17.1, 28.0, 52.1, 52.4, 55.6, 71.5, 77.5, 78.8, 115.1, 121.7, 122.1, 126.7, 129.2, 129.8, 130.4,

131.5, 137.7, 138.9, 149.9, 152.4, 155.3, 169.5, 169.5. HRMS (ESI+) calc for $[M+H]^+$ ($C_{25}H_{32}N_3O_7$) 486.2235, found 486.2234.

(L-threo)-trans-3-(3-((2-(methyl)phenyl)diazenyl)benzyloxy)aspartate (1g)

(L-trans-o-Me-azo-TBOA)

To a solution of **18g** (56 mg, 0.11 mmol) in dry DCM (2 mL), cooled in an ice-bath, trifluoroacetic acid (0.8 mL) was added dropwise. After 10 min, the ice-bath was removed and the reaction mixture was stirred at room temperature for 1.5 h until all the starting materials were consumed (TLC monitor). Volatiles were removed *in vacuo* to provide product **19g** which was used in the next step without further purification. Compound **19g** was dissolved in THF (1 mL) and water (1 mL) and LiOH (15.8 mg, 0.66 mmol) was added. The reaction mixture was stirred at room temperature for 2 h. Volatiles were removed *in vacuo* and, residue was washed with EtOAc (1 mL) and acidified with 1 M HCl until yellow precipitates appeared. The precipitate was filtered off, washed with cold water and dried under vacuum overnight to provide the final product **19** as yellow solid (27 mg, 69% yield over two steps). 1H NMR (400 MHz, DMSO- d_6) δ 2.69 (s, 3H, **CH**₃), 3.87 (dd, J = 9.6, 1.4 Hz, 1H, **CH**), 4.17 (dd, J = 9.6, 1.4 Hz, 1H, **CH**), 4.60 (d, J = 11.0 Hz, 1H, **BnH**), 4.96 (d, J = 11.0 Hz, 1H, **BnH**), 7.31 – 7.35 (m, 1H, **ArH**), 7.44 – 7.48 (m, 2H, **ArH**), 7.53 – 7.58 (m, 2H, **ArH**), 7.64 (d, J = 7.6 Hz, 1H, **ArH**), 7.79 (d, J = 7.8 Hz, 1H, **ArH**), 7.99 (s, 1H, **ArH**); ^{13}C NMR (101 MHz, DMSO- d_6) δ 17.2, 53.1, 72.3, 75.0, 115.1, 121.1, 122.9, 126.6, 129.1, 130.9, 131.4, 131.5, 137.7, 139.4, 145.0, 152.3, 168.4, 170.6. HRMS (ESI+) calc for $[M+H]^+$ ($C_{18}H_{20}N_3O_5$) 358.1397, found 358.1397.

1.3 NMR spectra

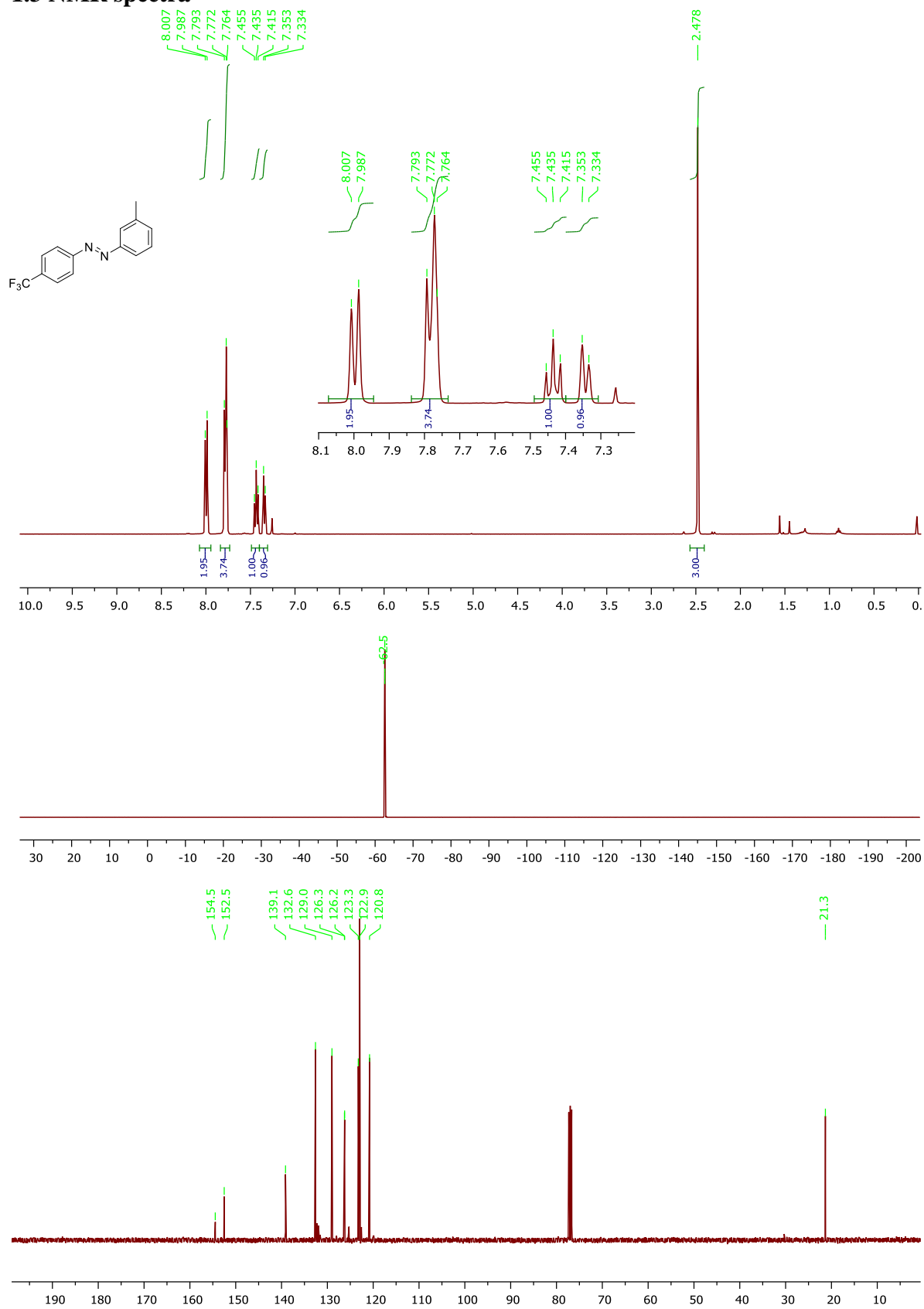


Figure S7: ^1H NMR spectrum and ^{13}C NMR spectrum of compound **3**

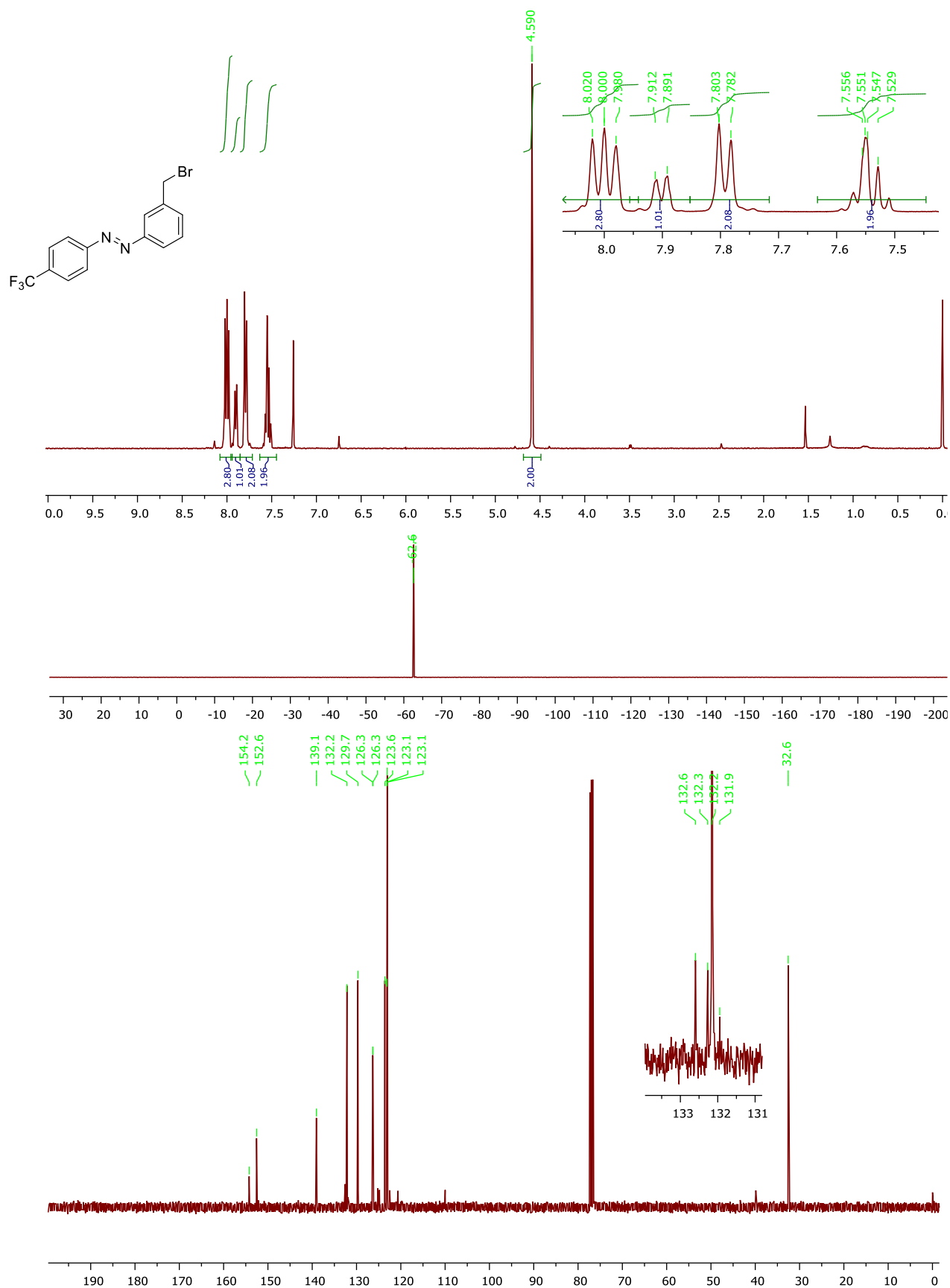


Figure S8: ¹H NMR spectrum and ¹³C NMR spectrum of compound **4a**

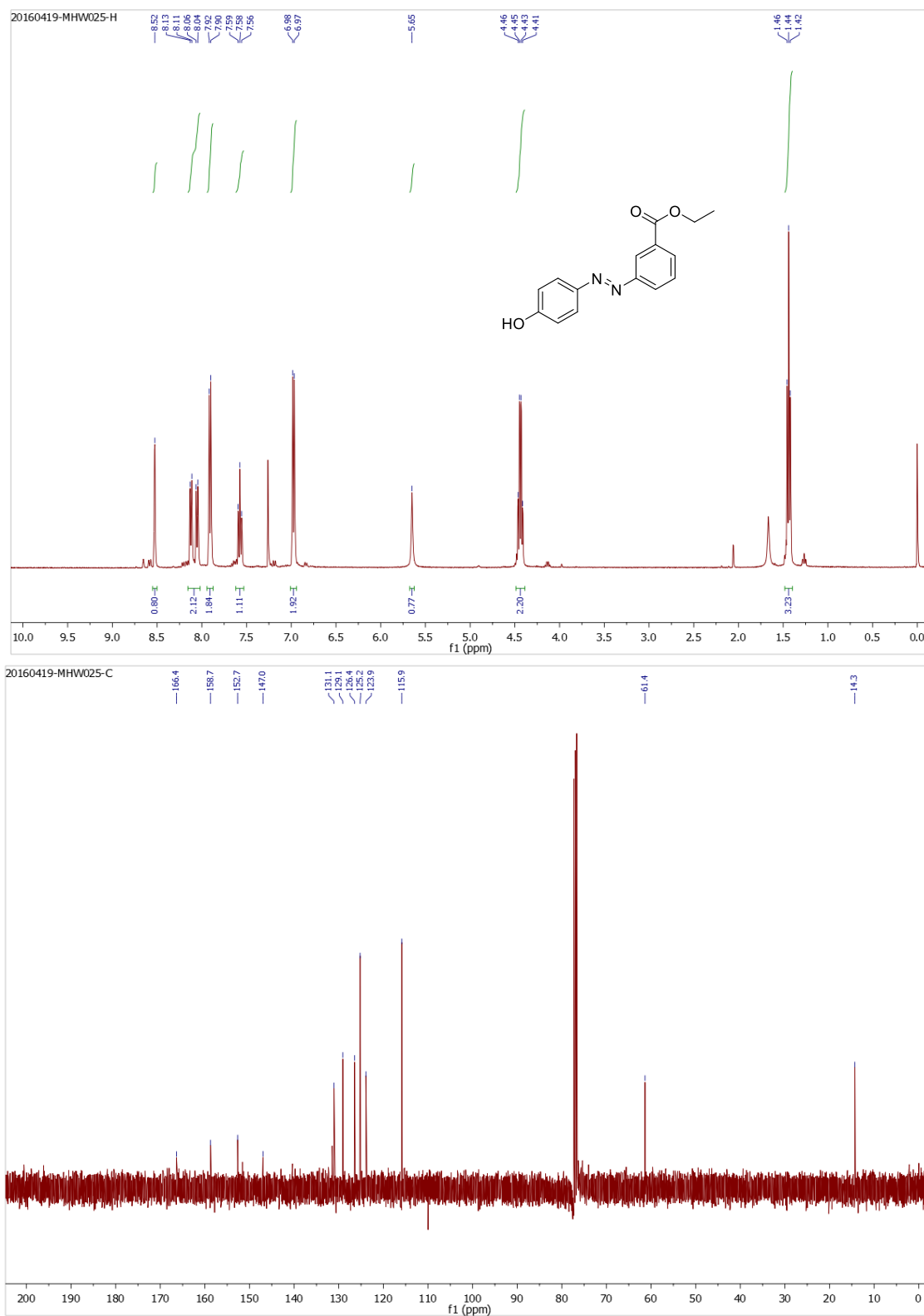


Figure S9: ¹H NMR spectrum and ¹³C NMR spectrum of compound 6

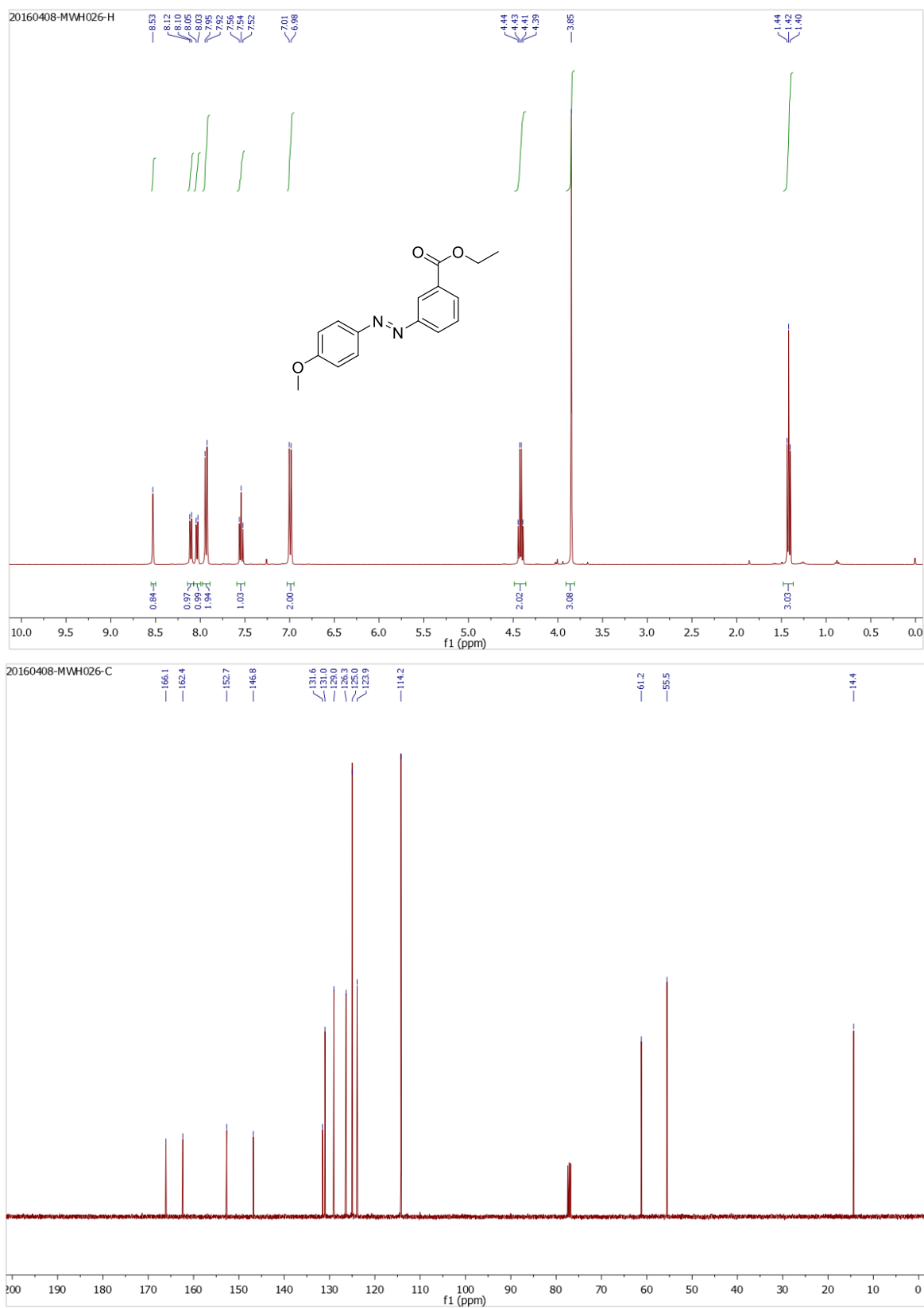


Figure S10: ¹H NMR spectrum and ¹³C NMR spectrum of compound **7b**

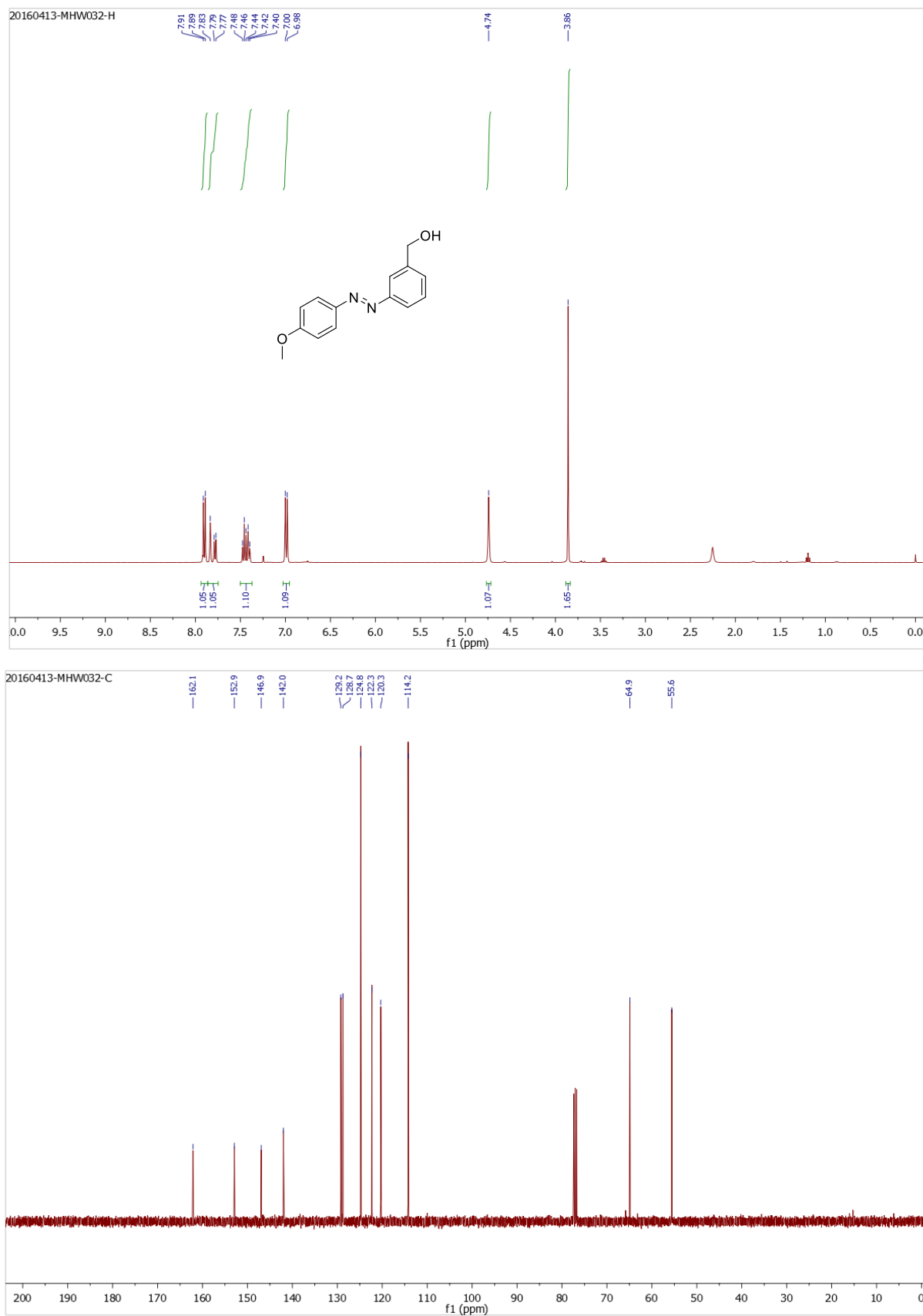


Figure S11: ^1H NMR spectrum and ^{13}C NMR spectrum of compound **8b**

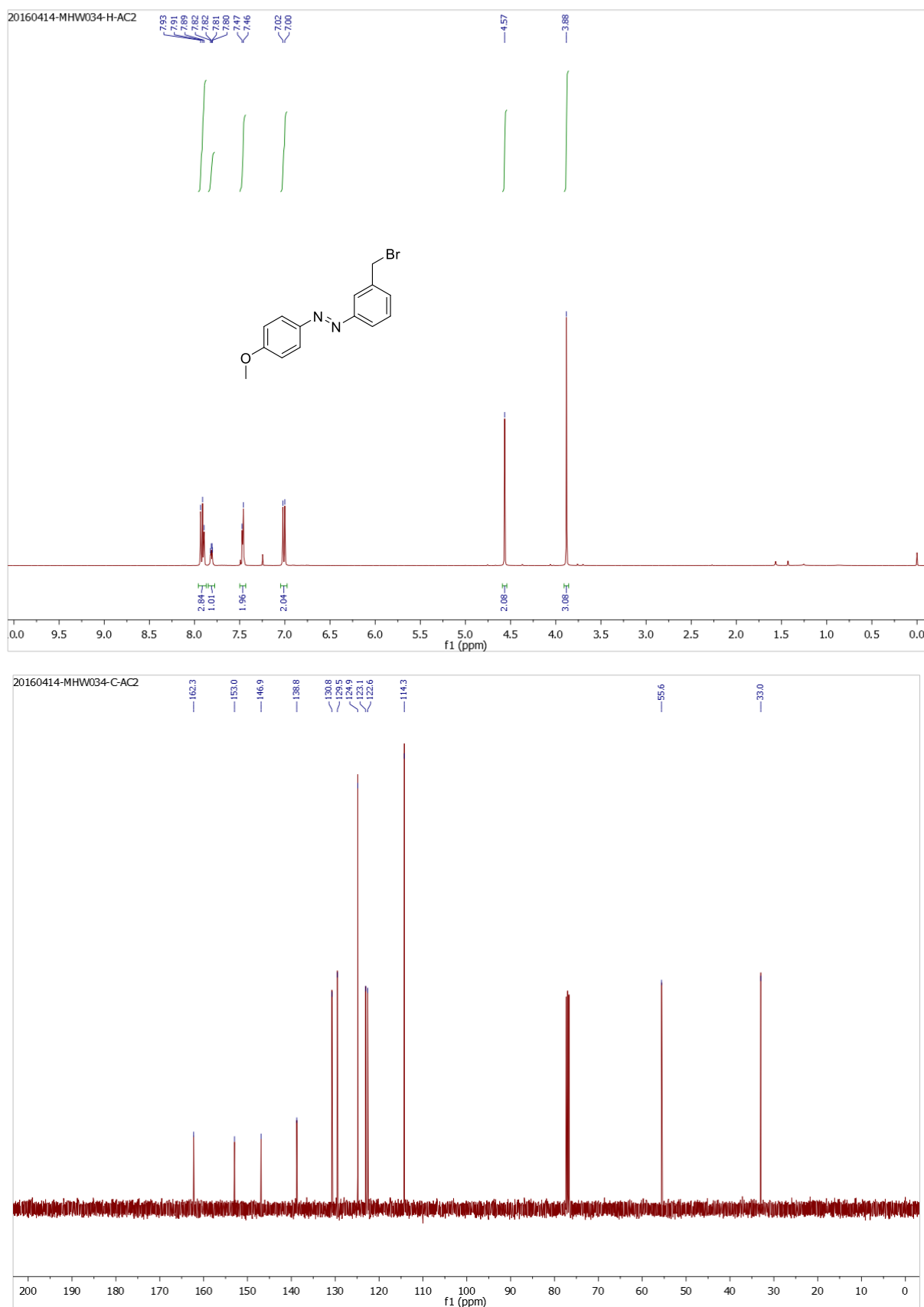


Figure S12: ¹H NMR spectrum and ¹³C NMR spectrum of compound **4b**

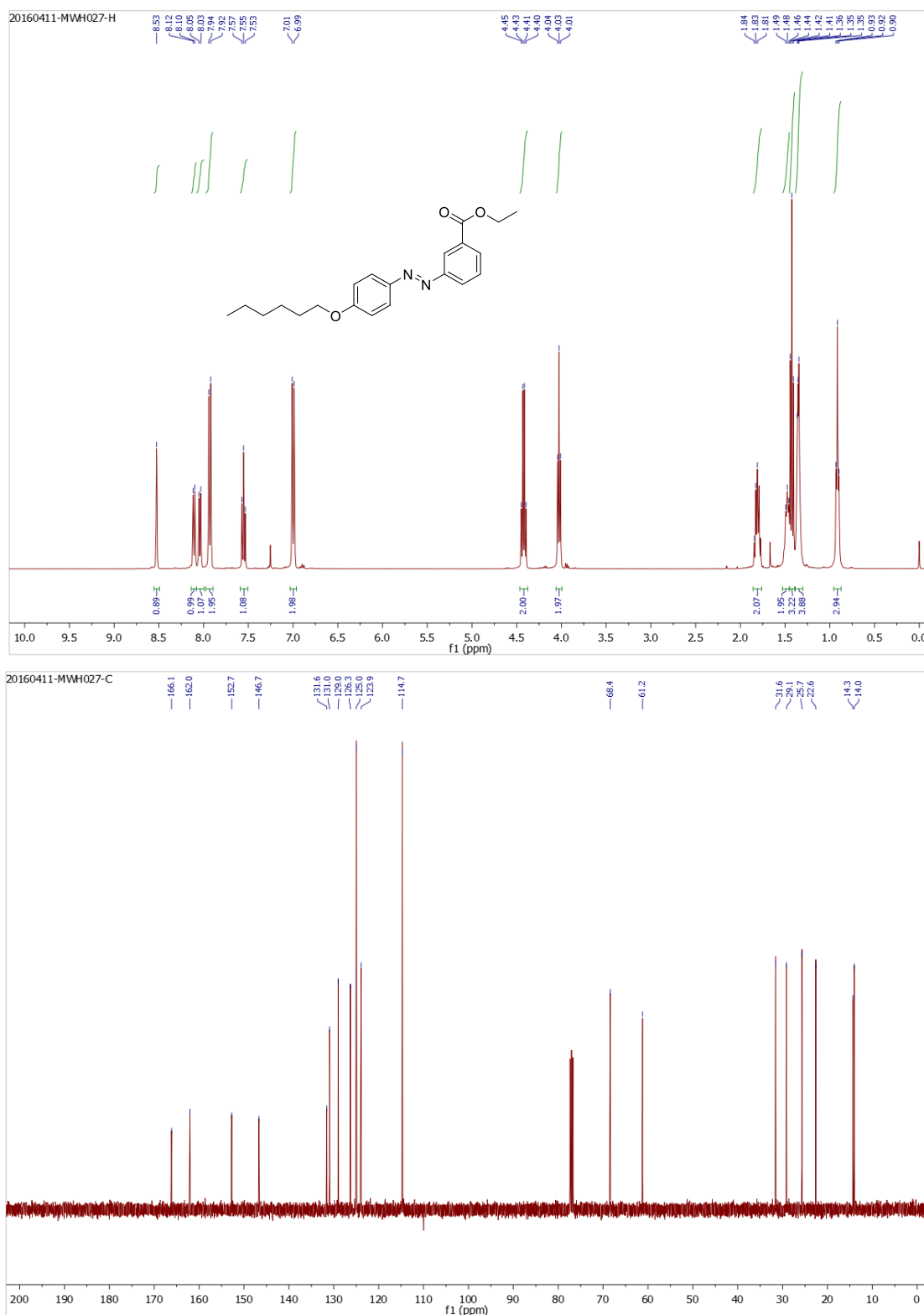


Figure S13: ¹H NMR spectrum and ¹³C NMR spectrum of compound **7c**

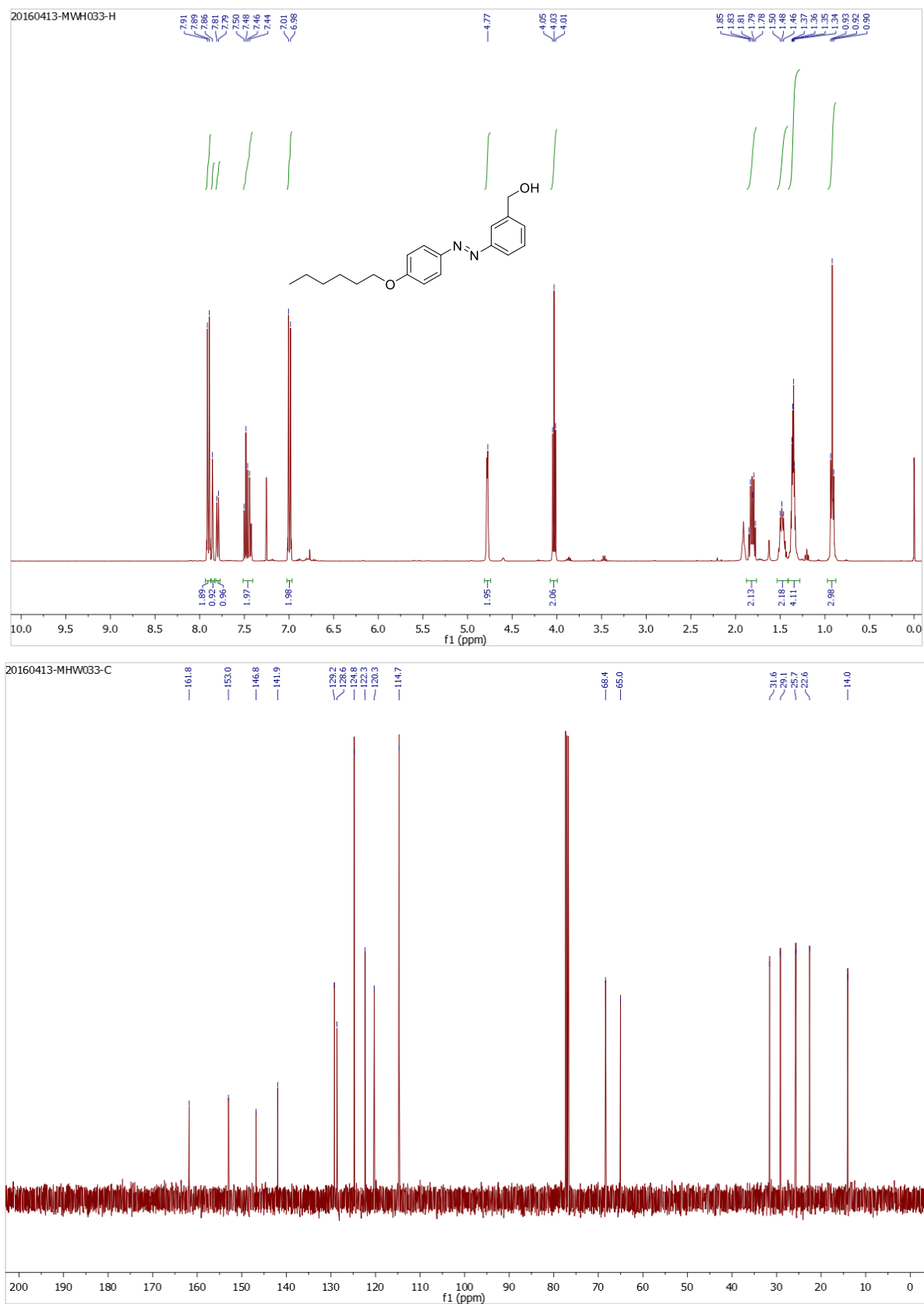


Figure S14: ^1H NMR spectrum and ^{13}C NMR spectrum of compound **8c**

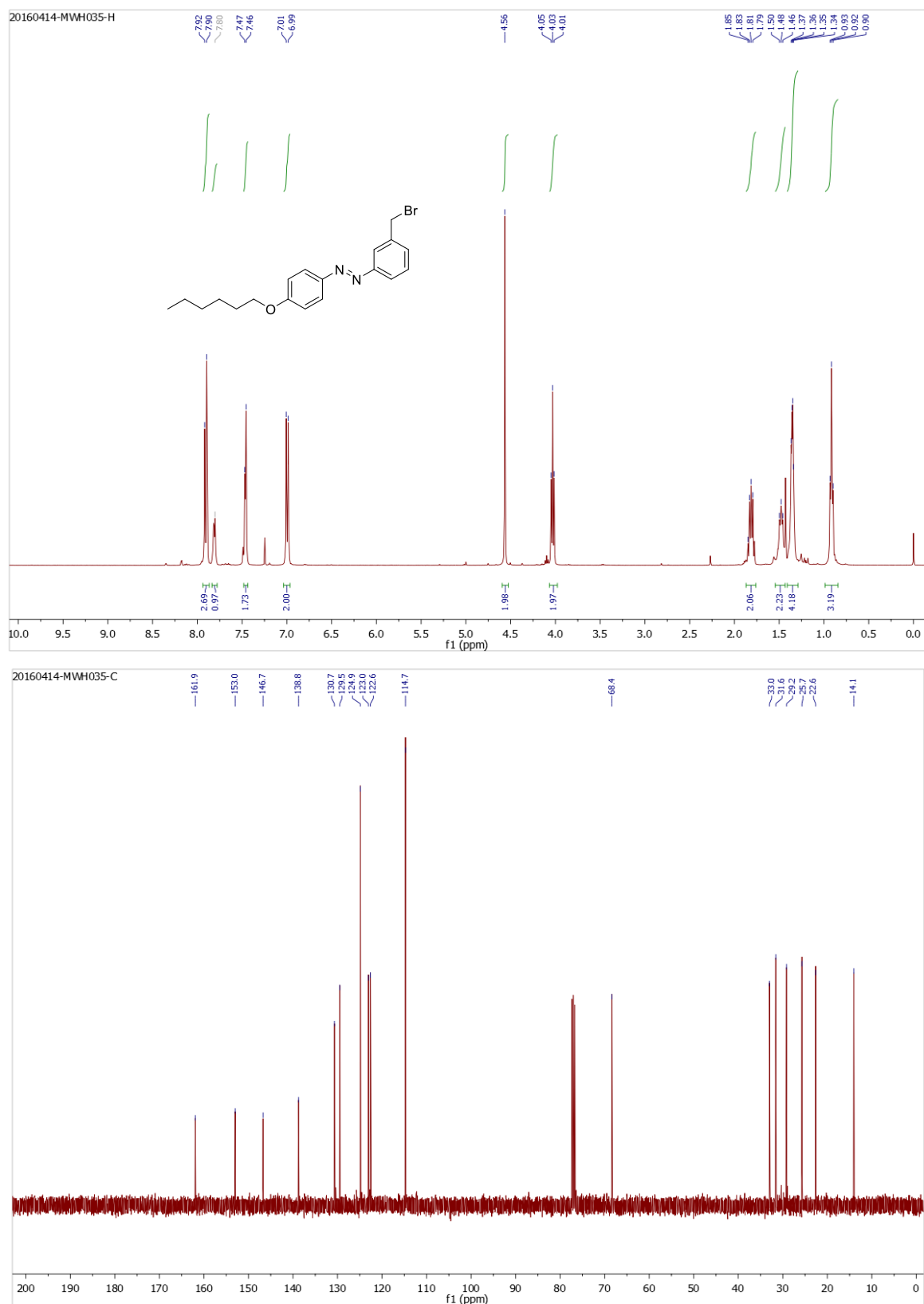


Figure S15: ¹H NMR spectrum and ¹³C NMR spectrum of compound **4c**

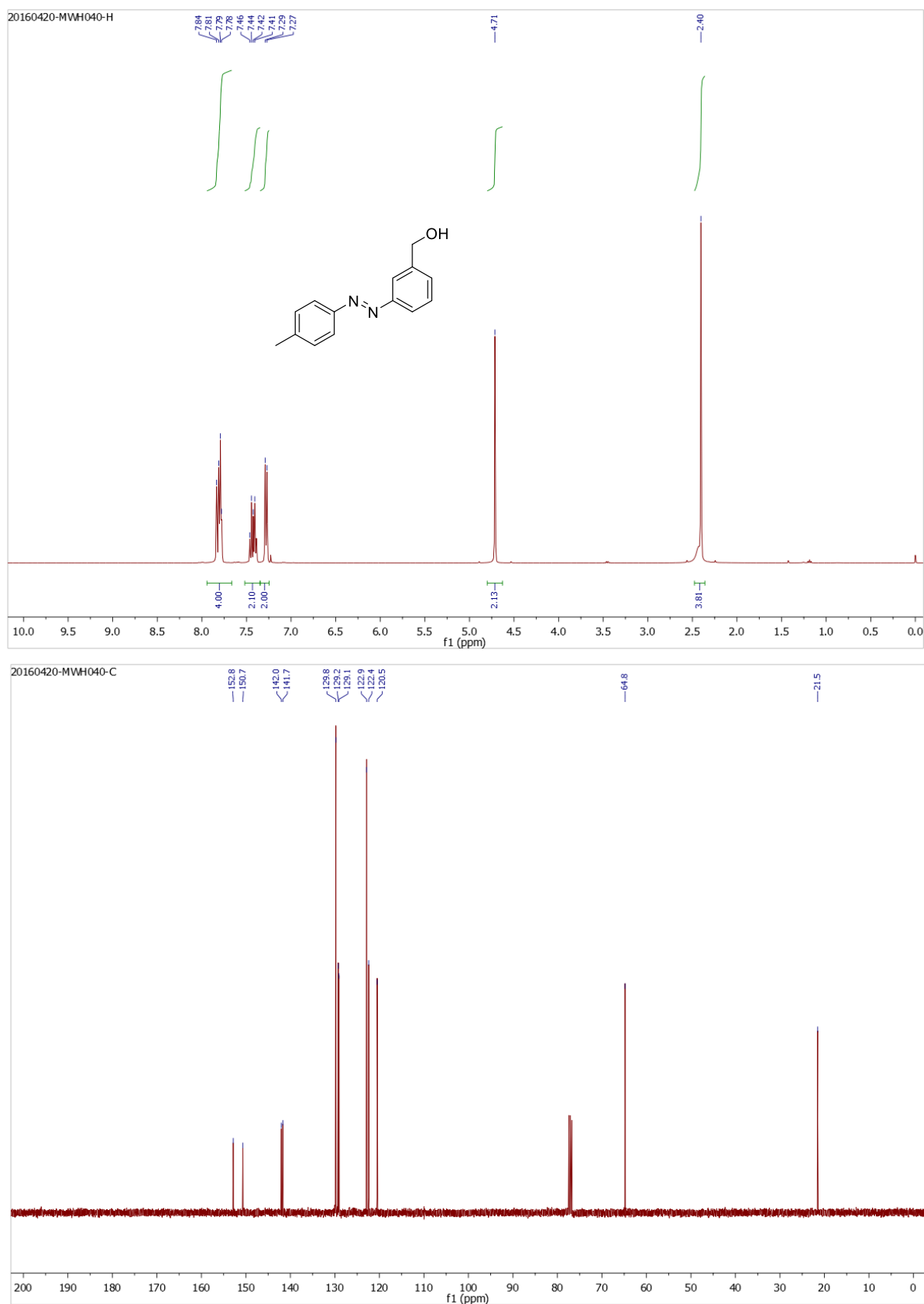


Figure S16: ^1H NMR spectrum and ^{13}C NMR spectrum of compound 11d

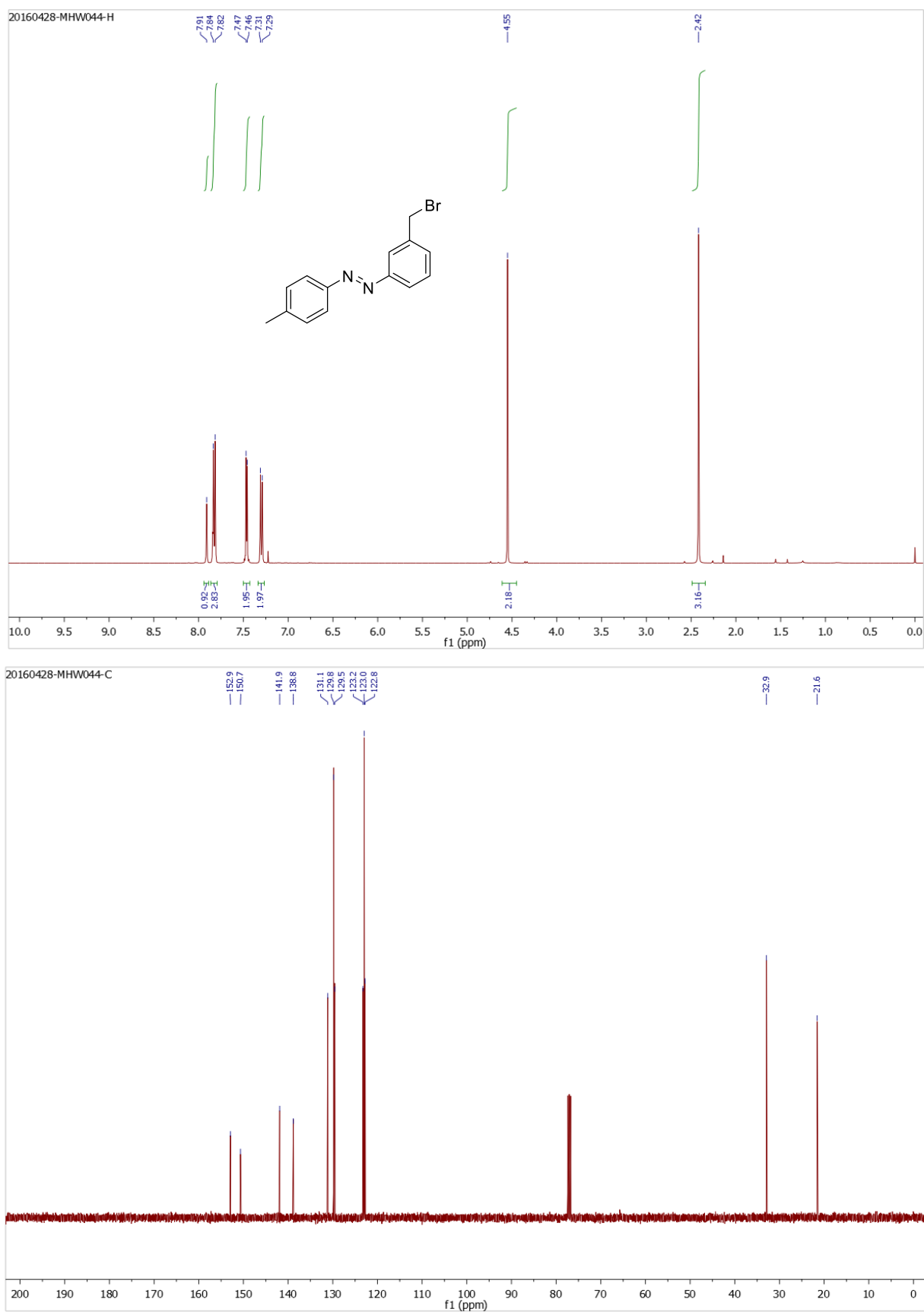


Figure S17: ^1H NMR spectrum and ^{13}C NMR spectrum of compound **4d**

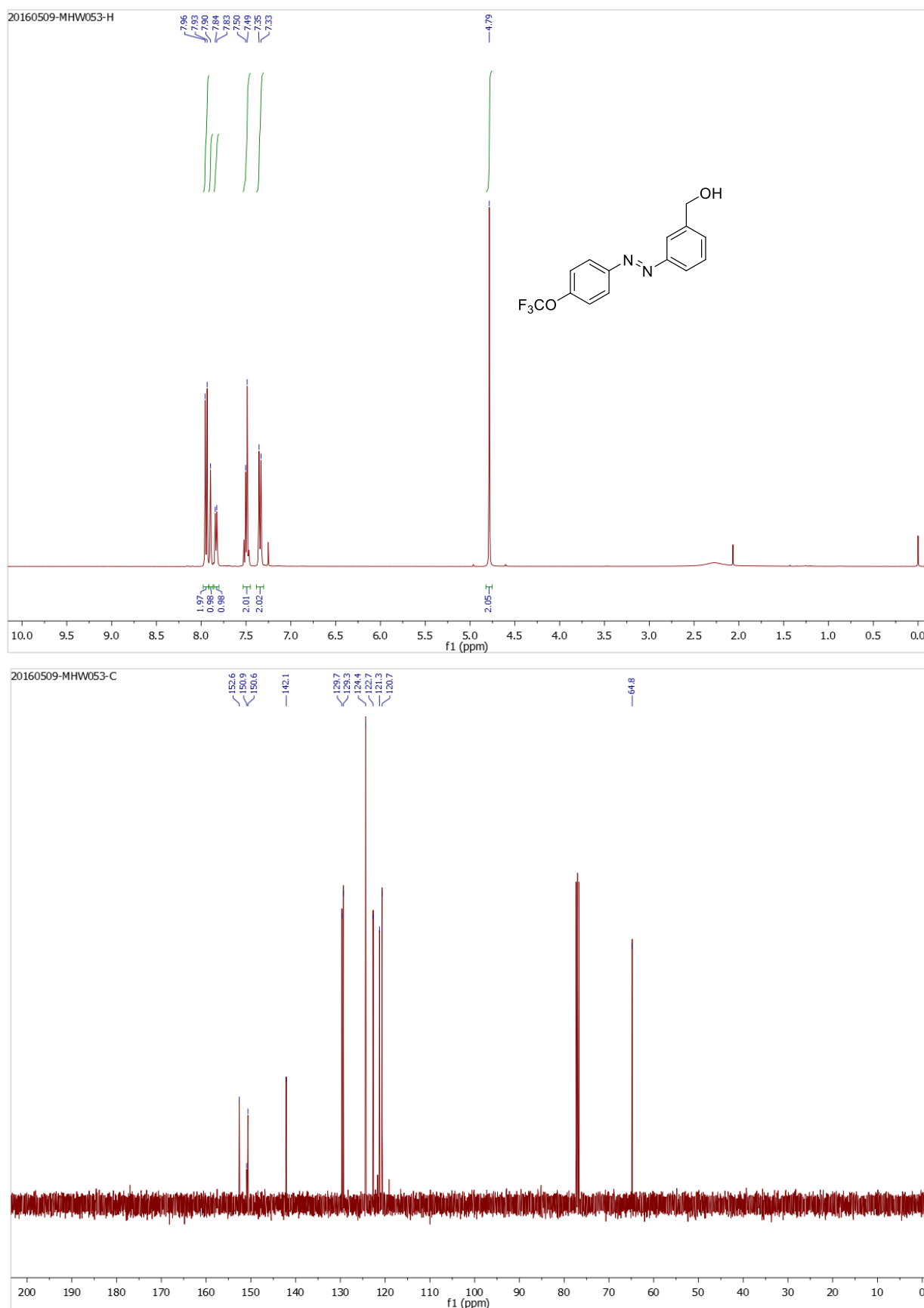


Figure S18: ^1H NMR spectrum and ^{13}C NMR spectrum of compound **11e**

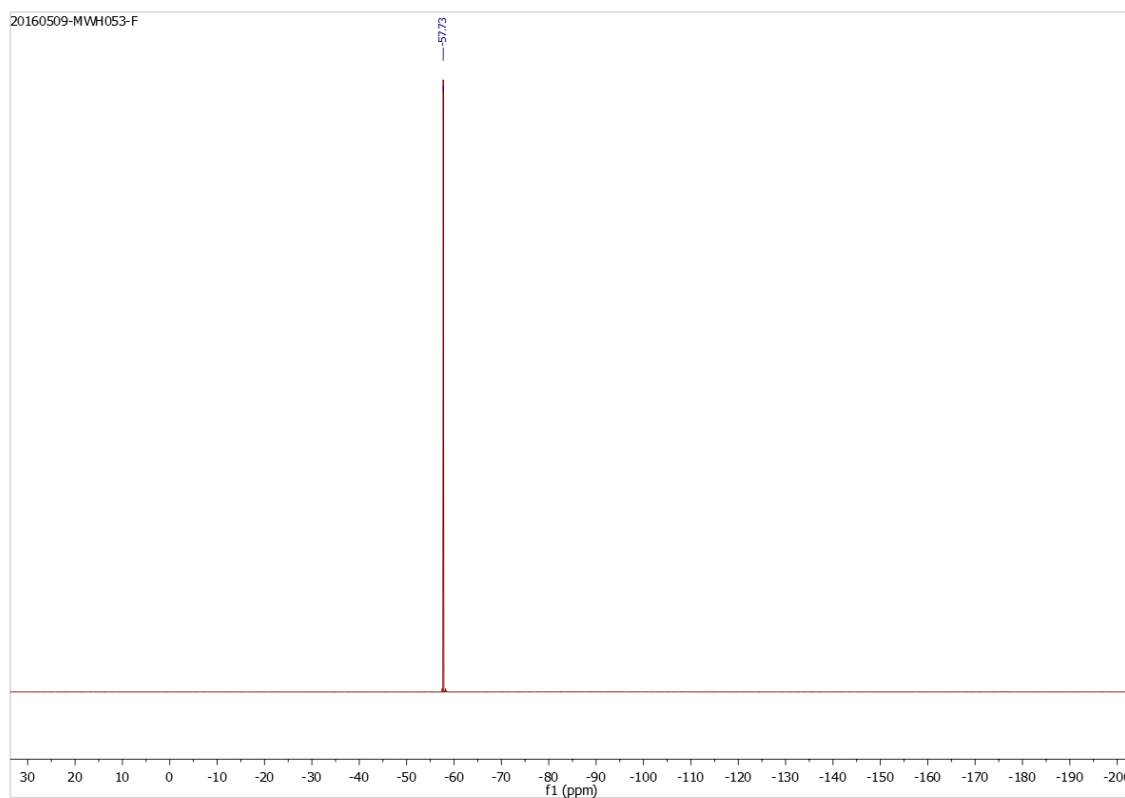


Figure S19: ^{19}F NMR spectrum of compound **11e**

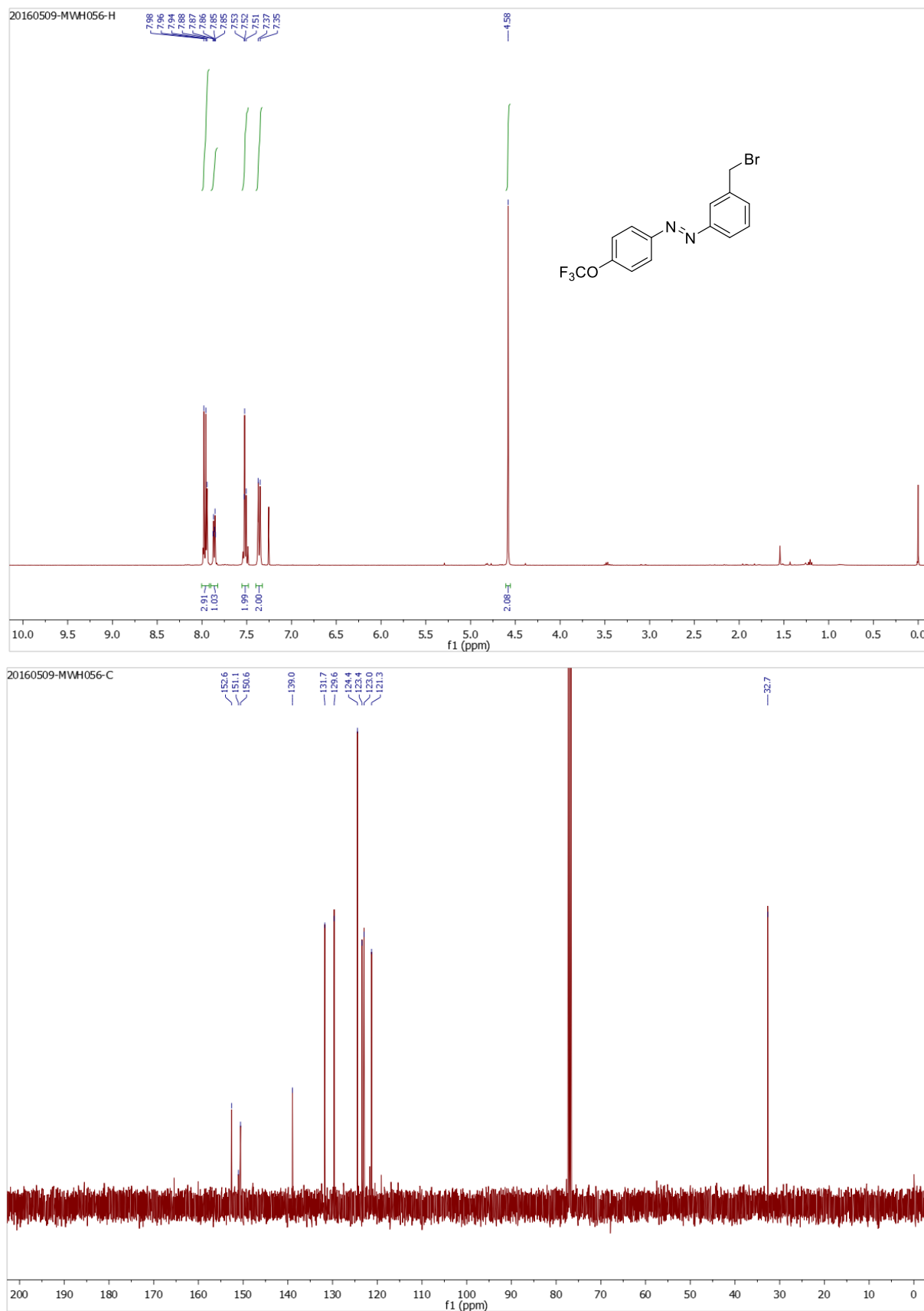


Figure S20: ¹H NMR spectrum and ¹³C NMR spectrum of compound **4e**

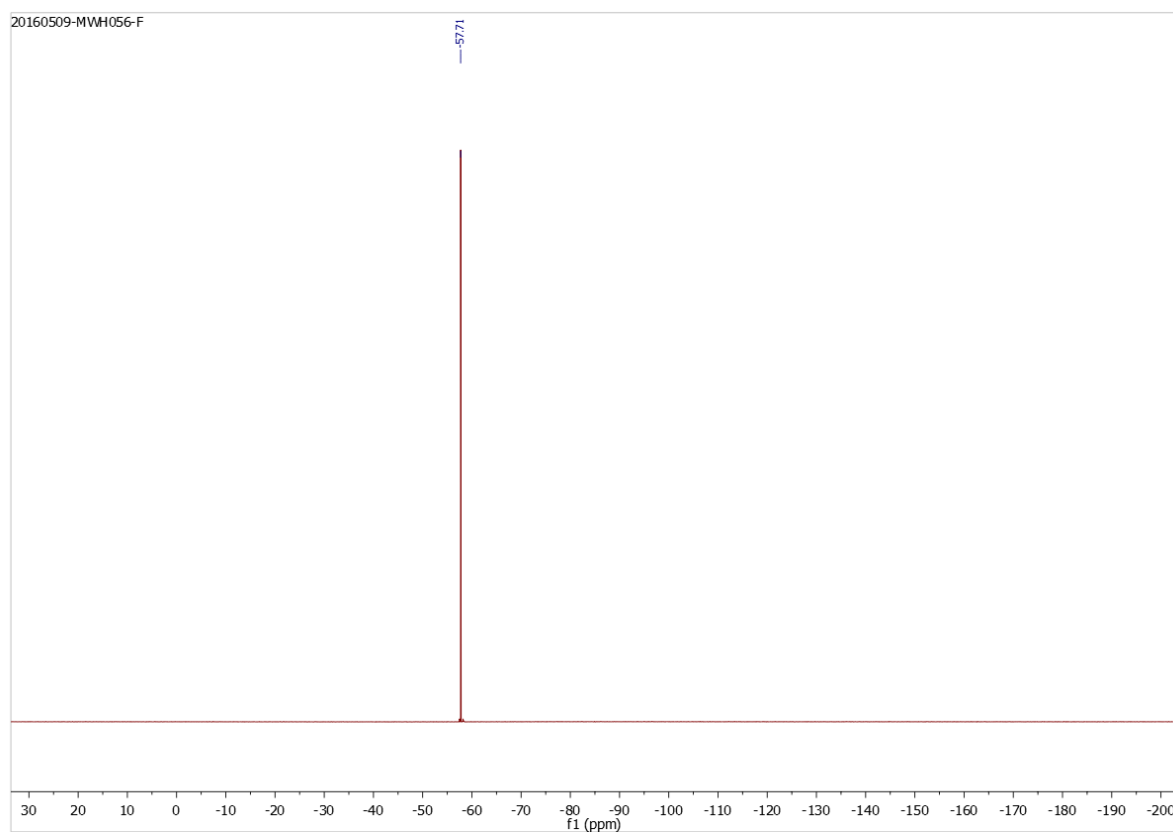


Figure S21: ^{19}F NMR spectrum of compound **4e**

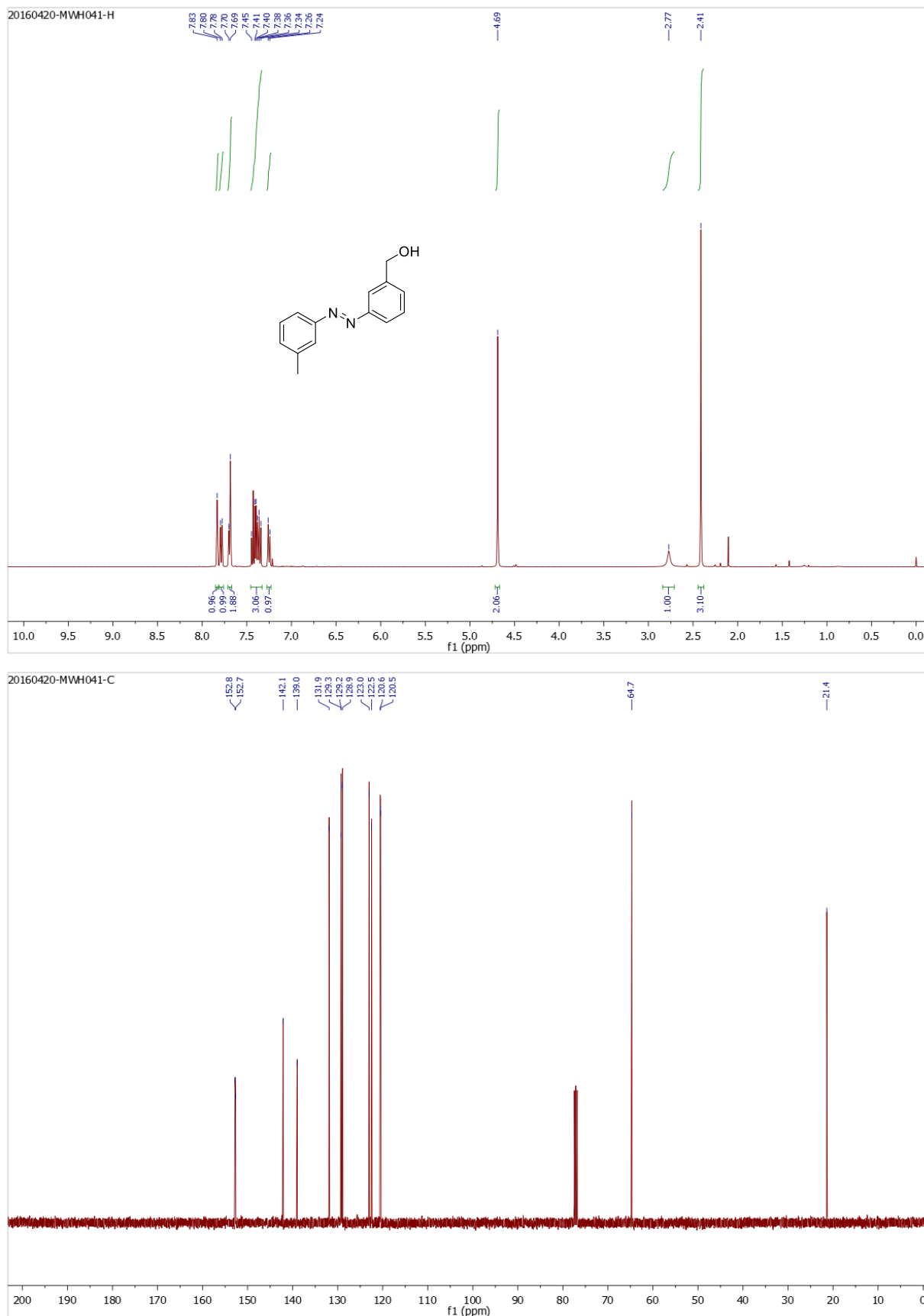


Figure S22: ^1H NMR spectrum and ^{13}C NMR spectrum of compound 11f

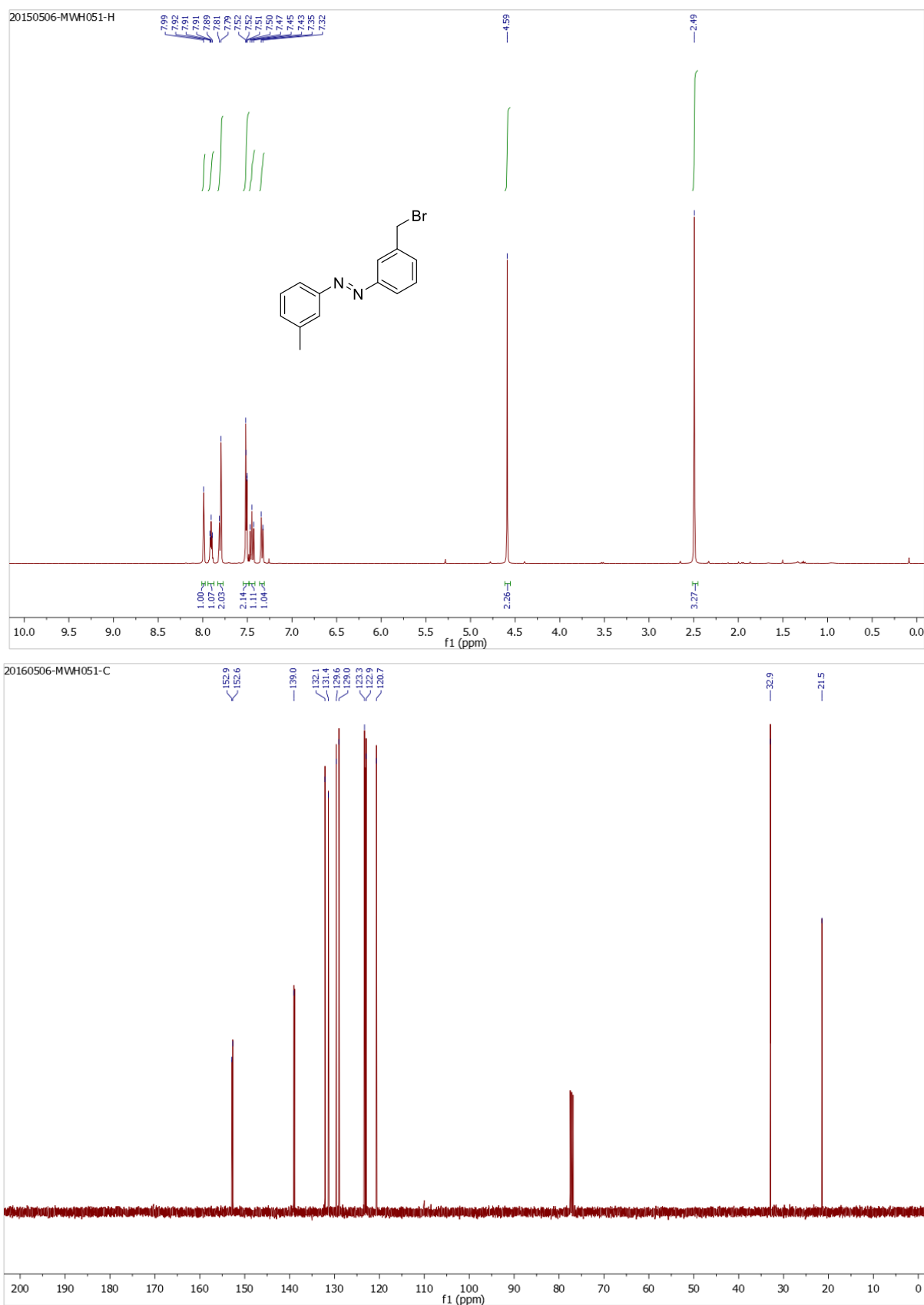


Figure S23: ^1H NMR spectrum and ^{13}C NMR spectrum of compound **4f**

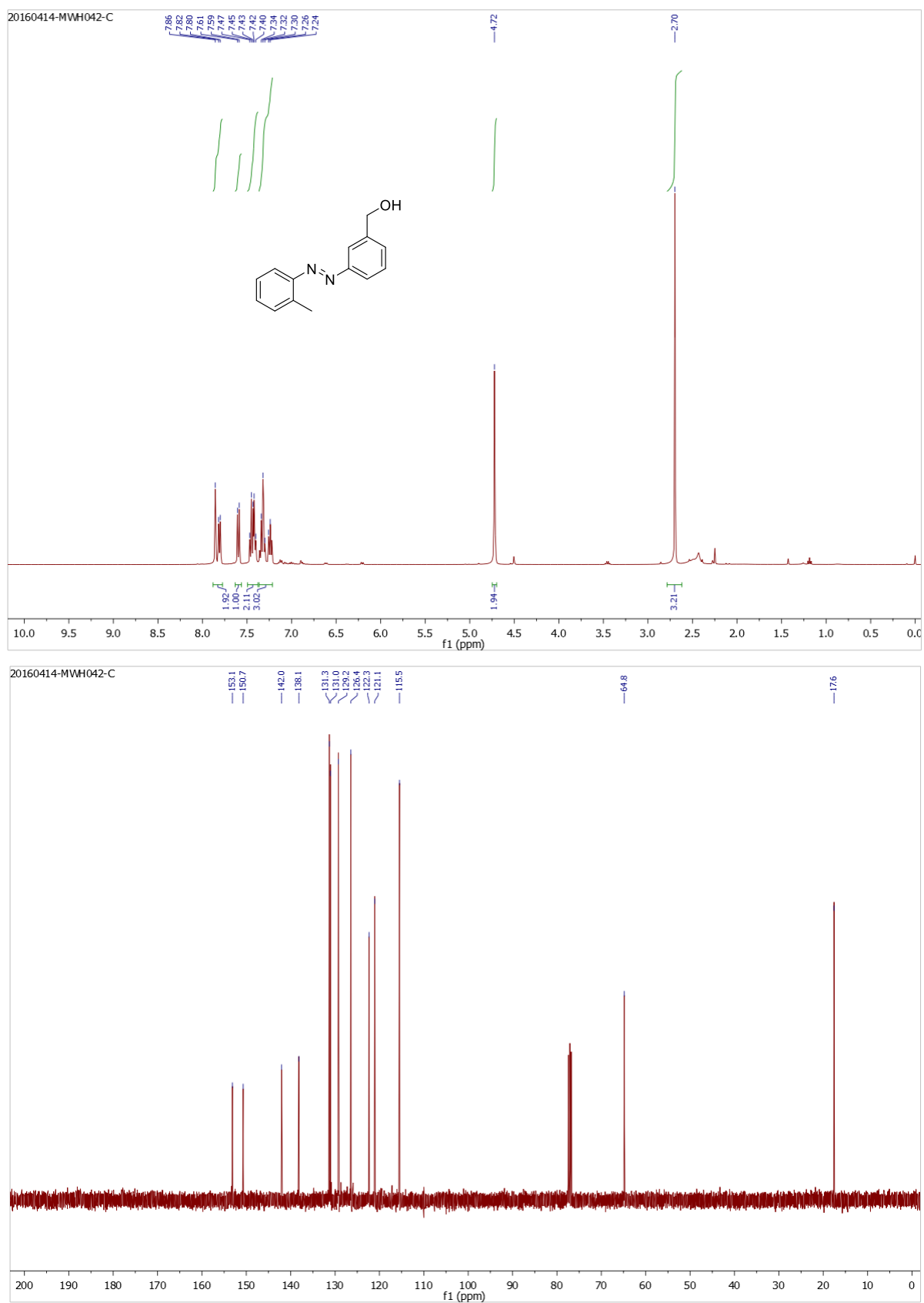


Figure S24: ^1H NMR spectrum and ^{13}C NMR spectrum of compound 11g

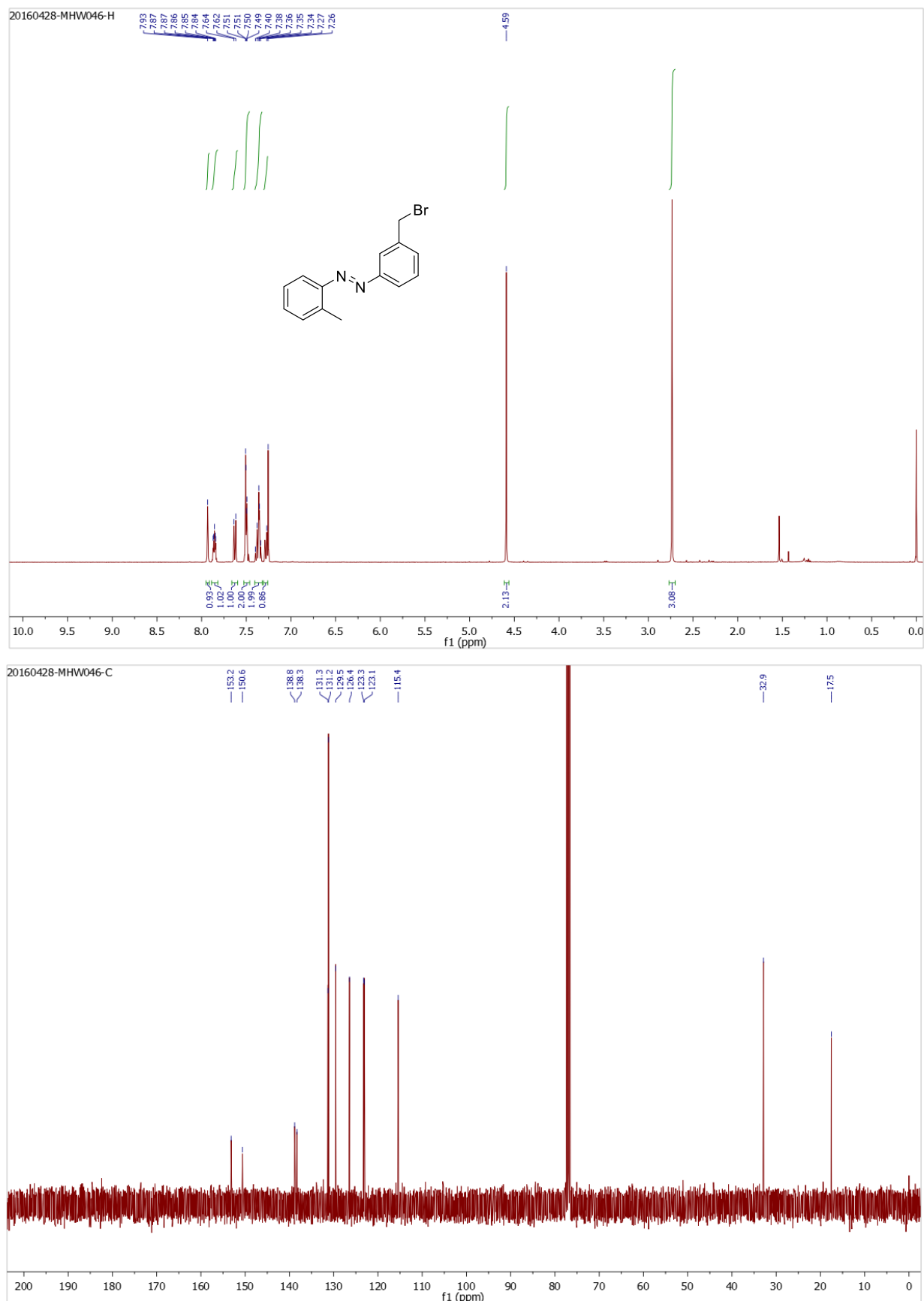
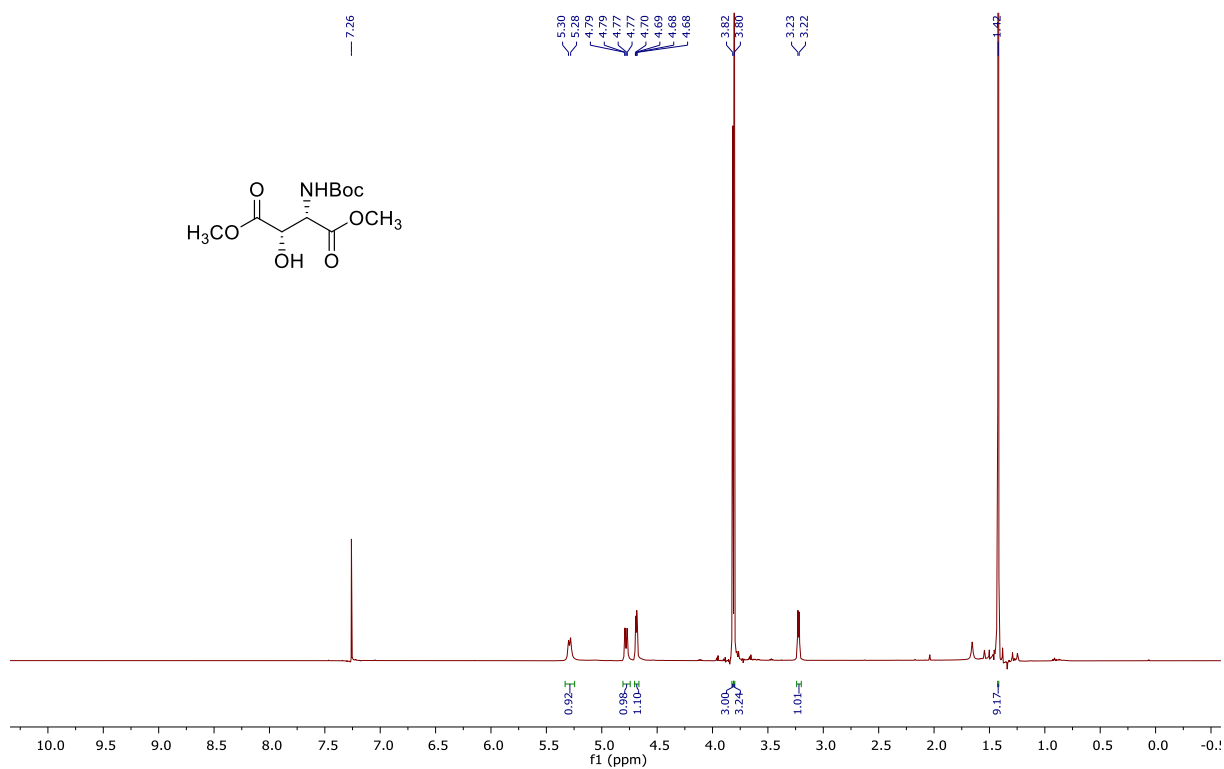


Figure S25: ¹H NMR spectrum and ¹³C NMR spectrum of compound **4g**

FH-10
PROTON CDCl₃



FH-10
C13 CDCl₃

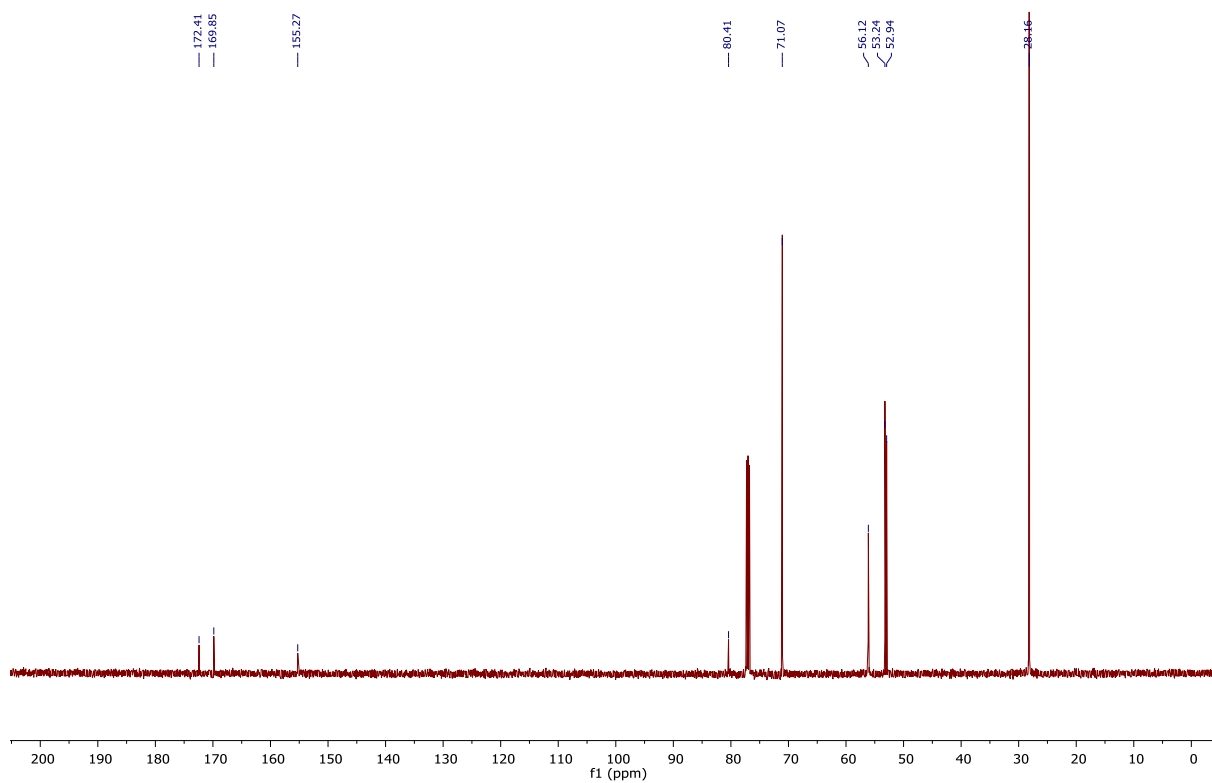


Figure S26: ¹H NMR spectrum and ¹³C NMR spectrum of compound 17

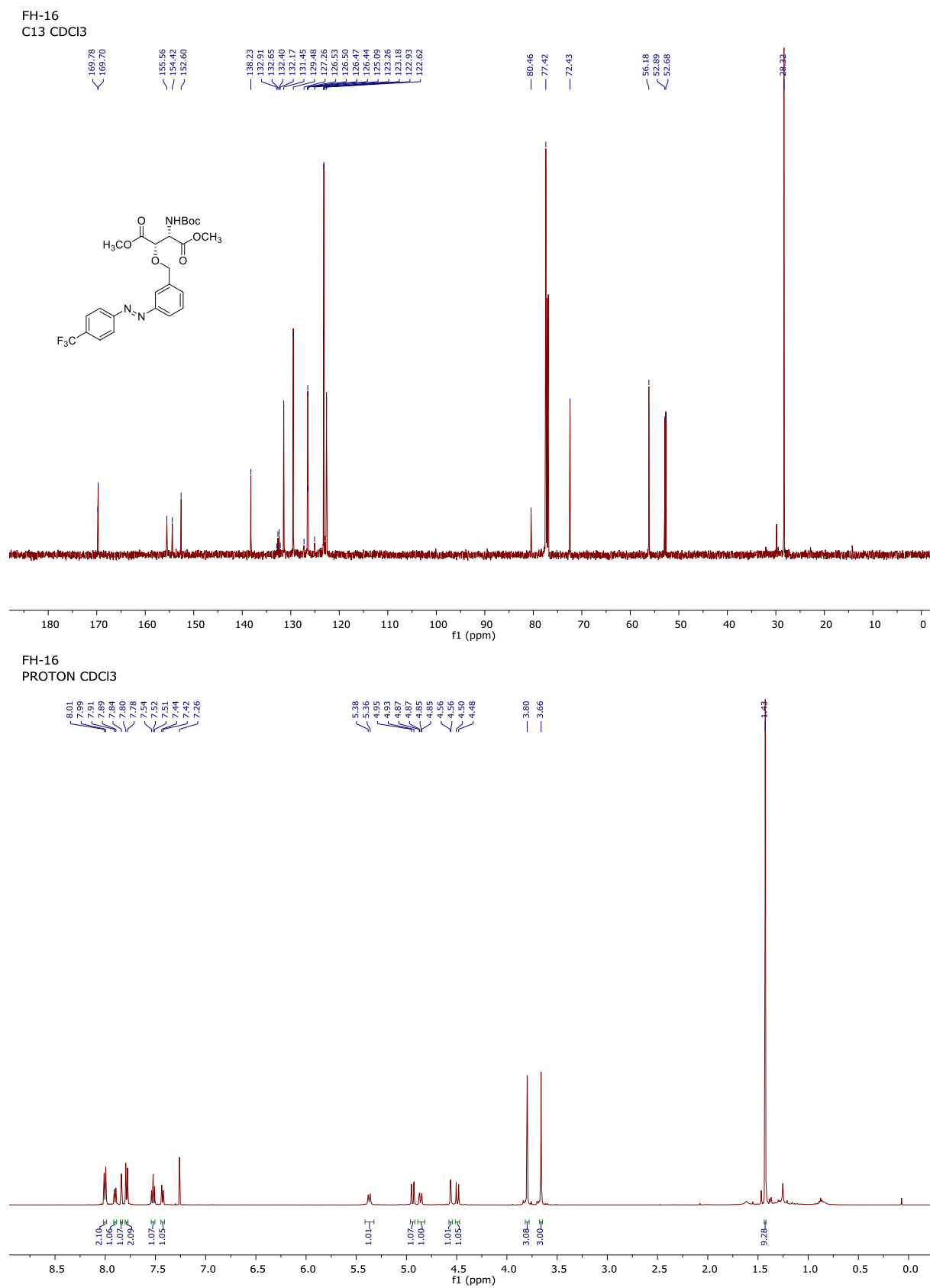


Figure S27: ^1H NMR spectrum and ^{13}C NMR spectrum of compound 18a

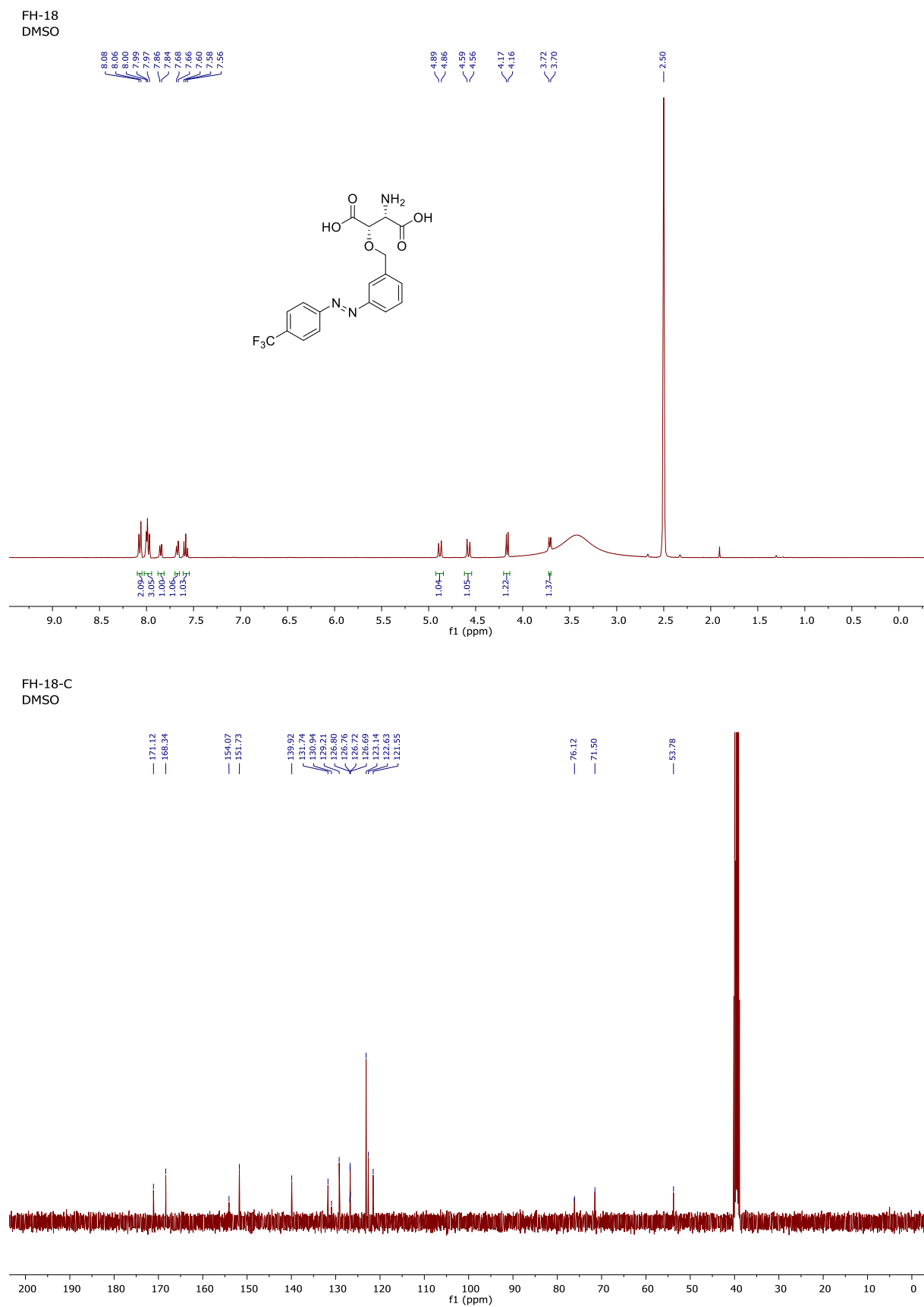


Figure S28: ¹H NMR spectrum and ¹³C NMR spectrum of compound **1a** (*p*-CF₃-azo-TBOA)

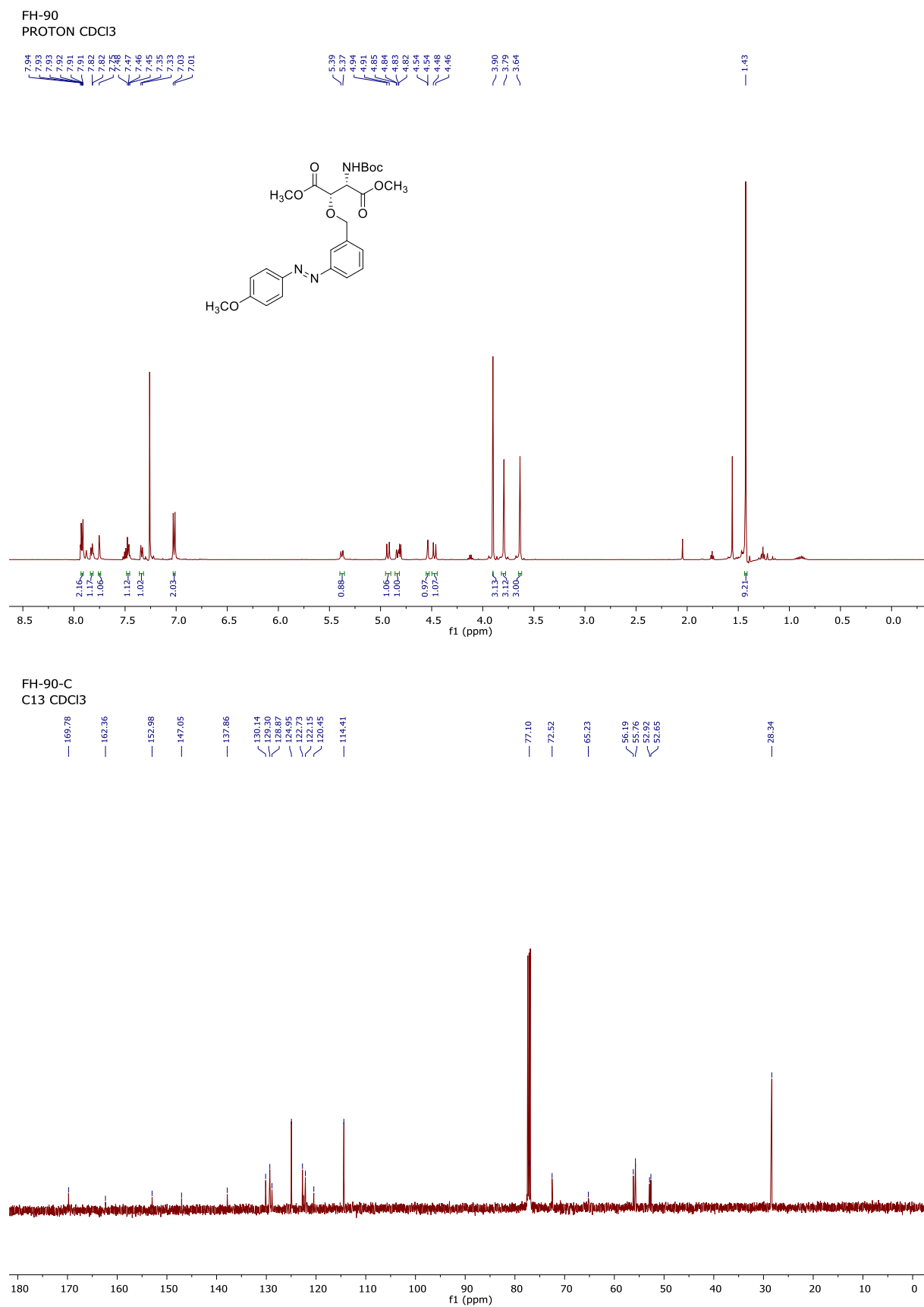
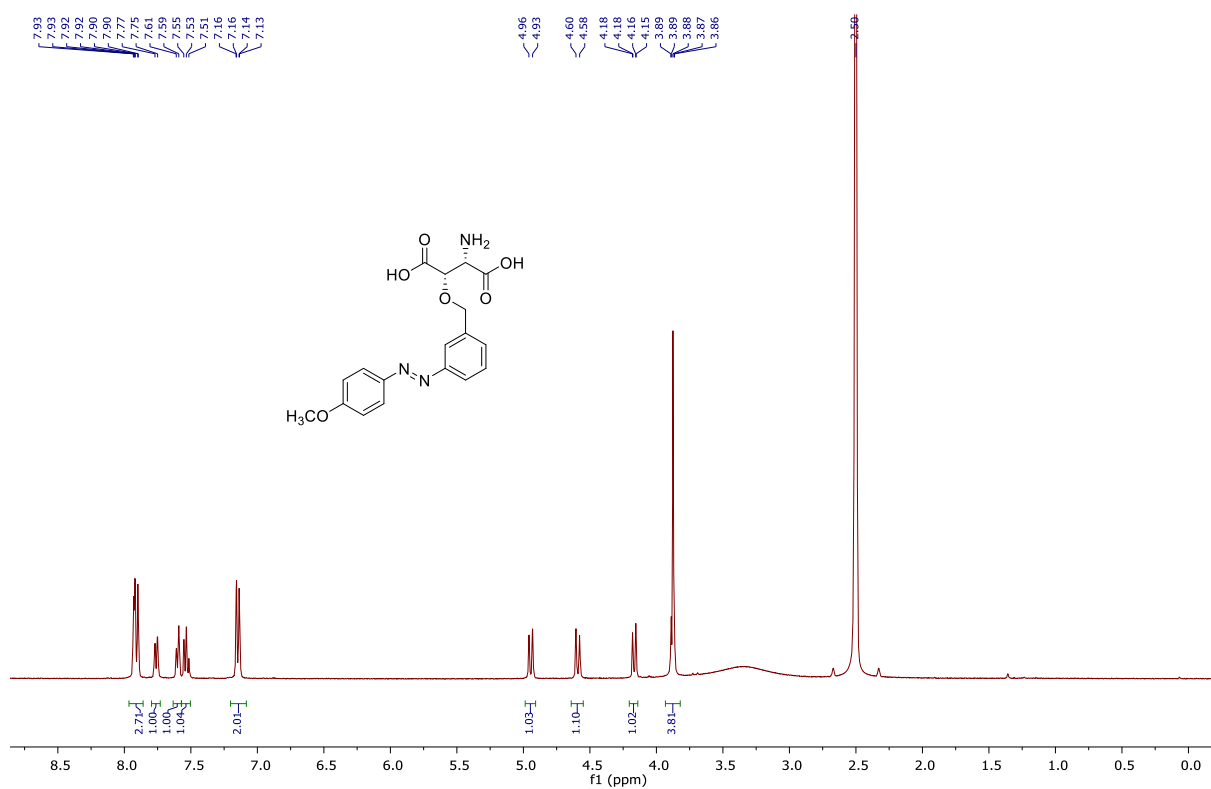


Figure S29: ¹H NMR spectrum and ¹³C NMR spectrum of compound 18b

20160502-FH092-thermo-H
DMSO



20160725-FH092-C
DMSO

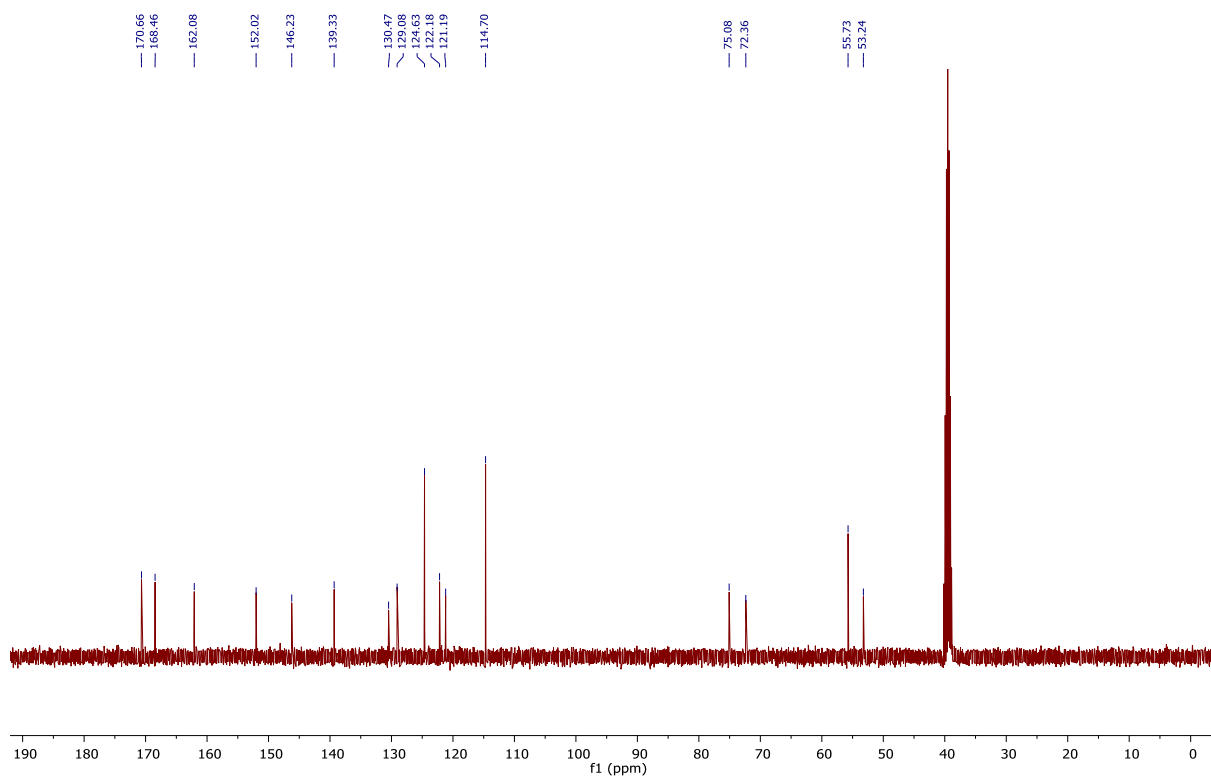


Figure S30: ¹H NMR spectrum and ¹³C NMR spectrum of compound **1b** (*p*-MeO-azo-TBOA)

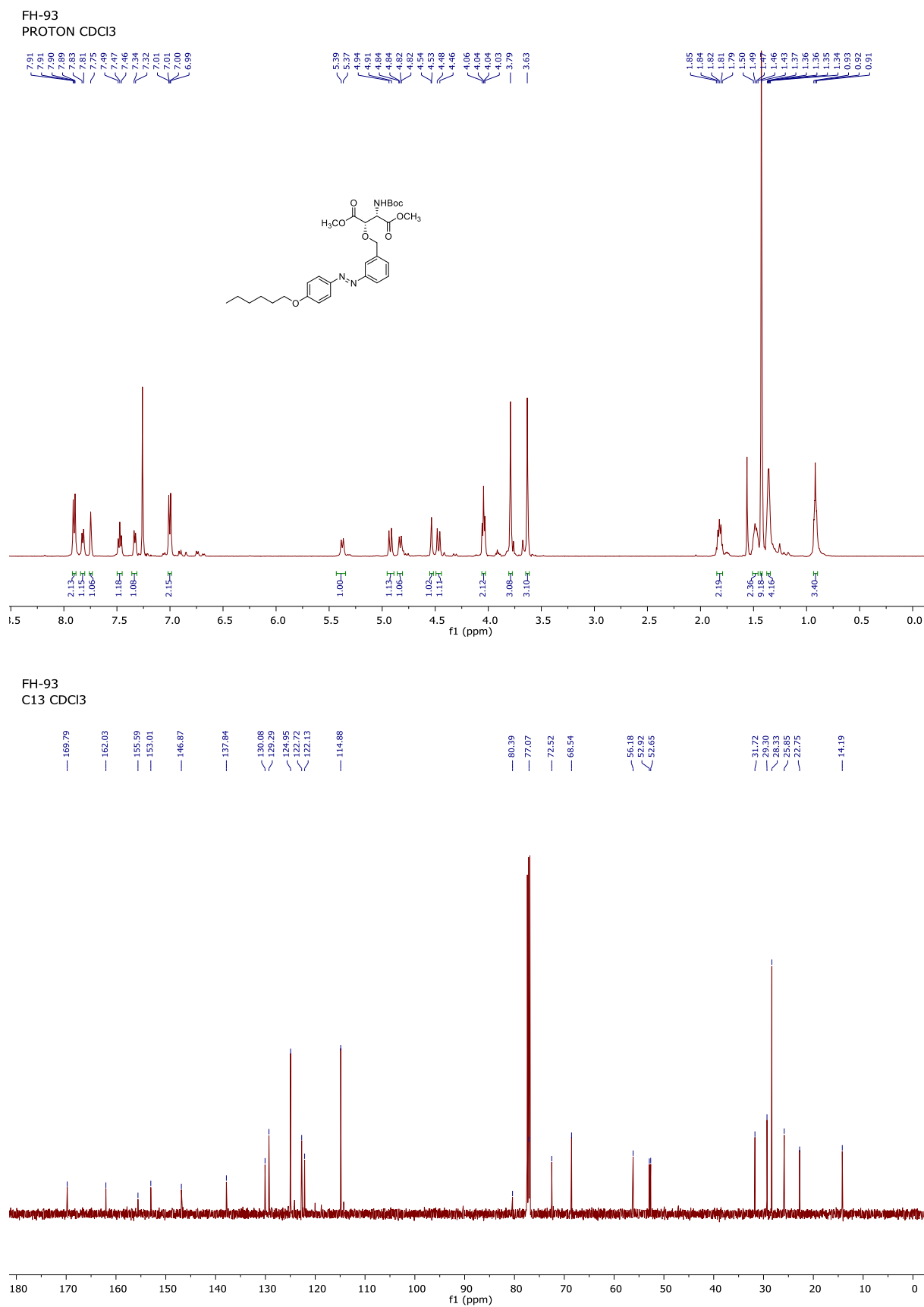


Figure S31: ¹H NMR spectrum and ¹³C NMR spectrum of compound 18c

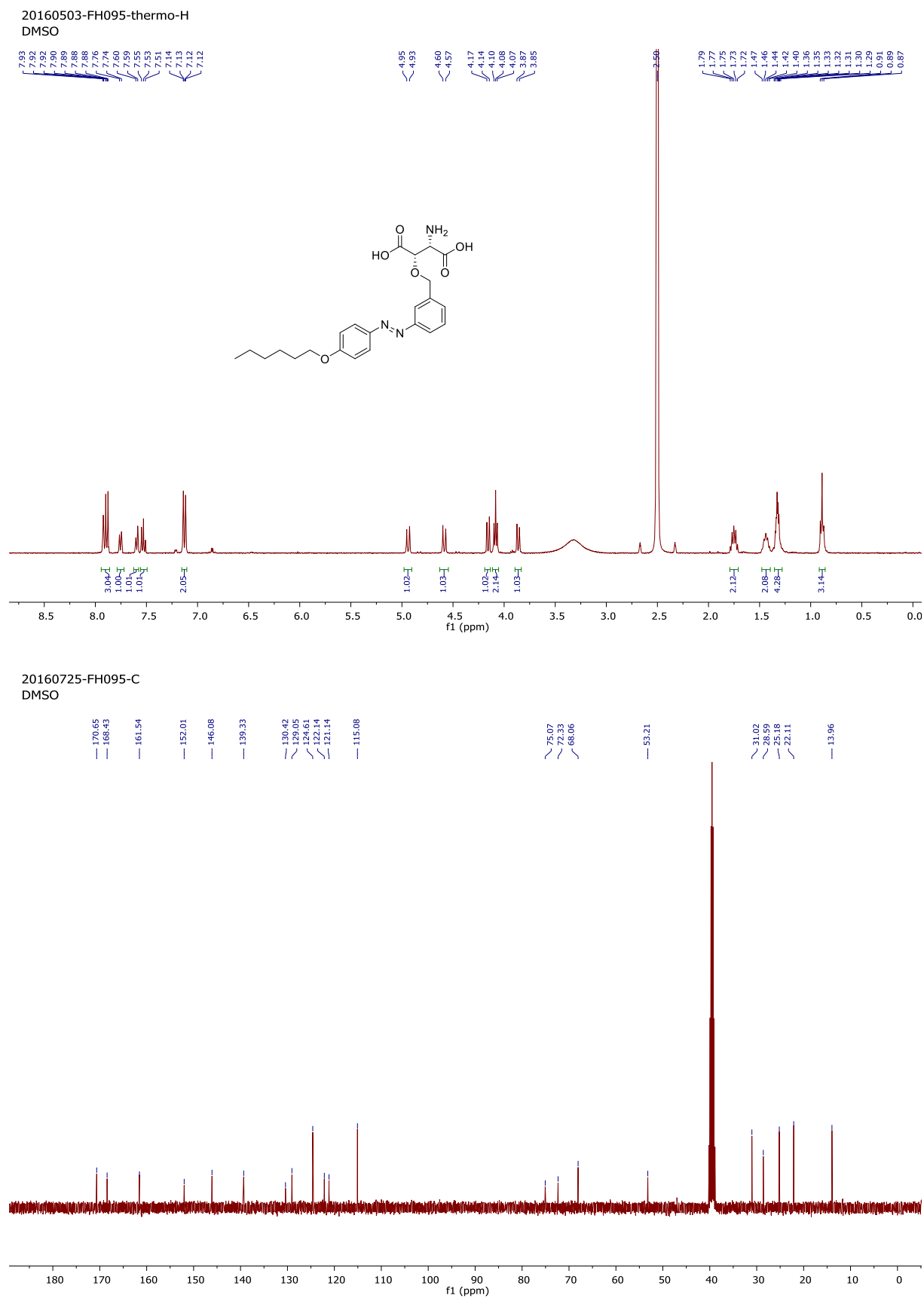


Figure S32: ¹H NMR spectrum and ¹³C NMR spectrum of compound 1c (p-HexO-azo-TBOA)

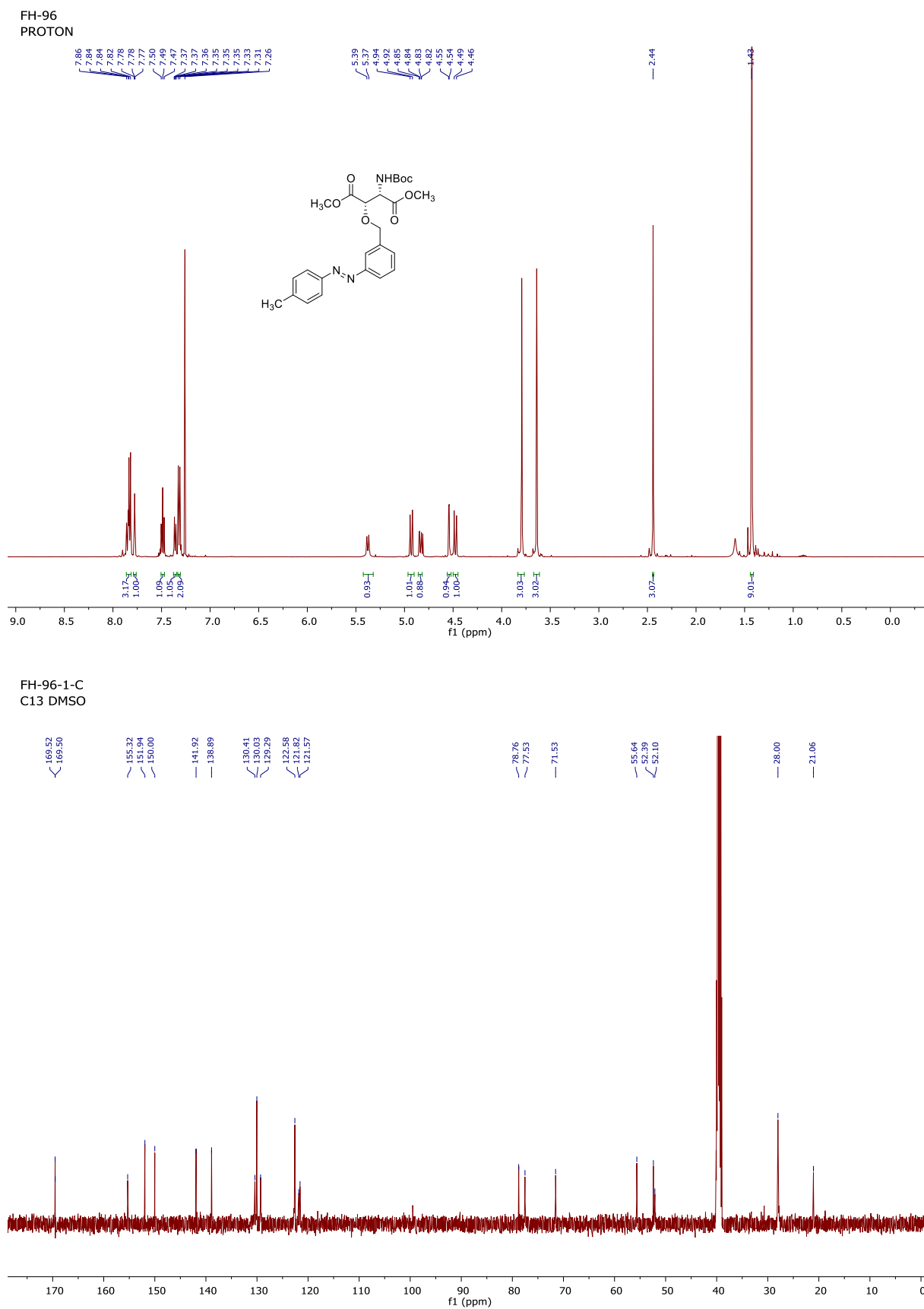


Figure S33: ¹H NMR spectrum and ¹³C NMR spectrum of compound 18d

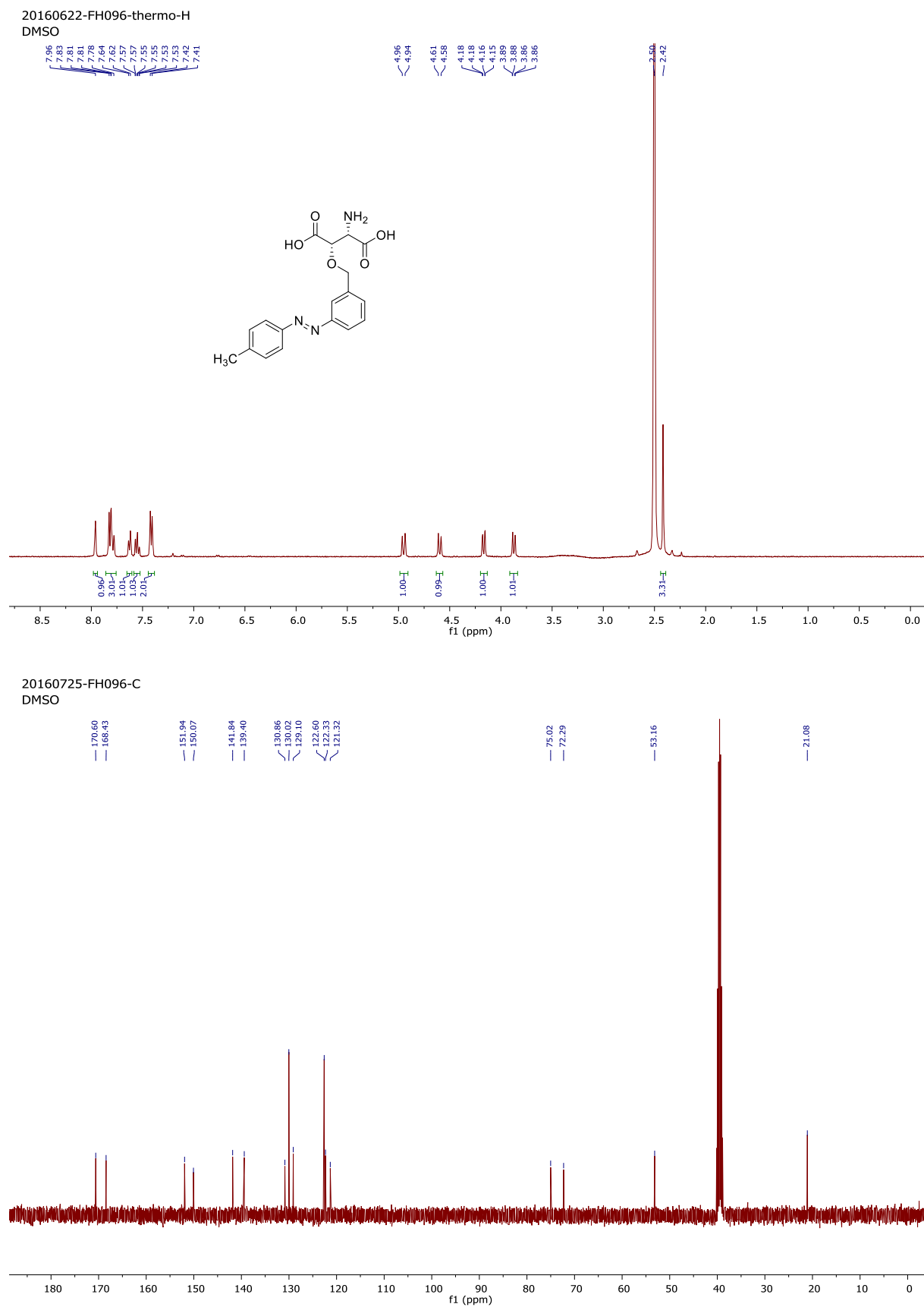
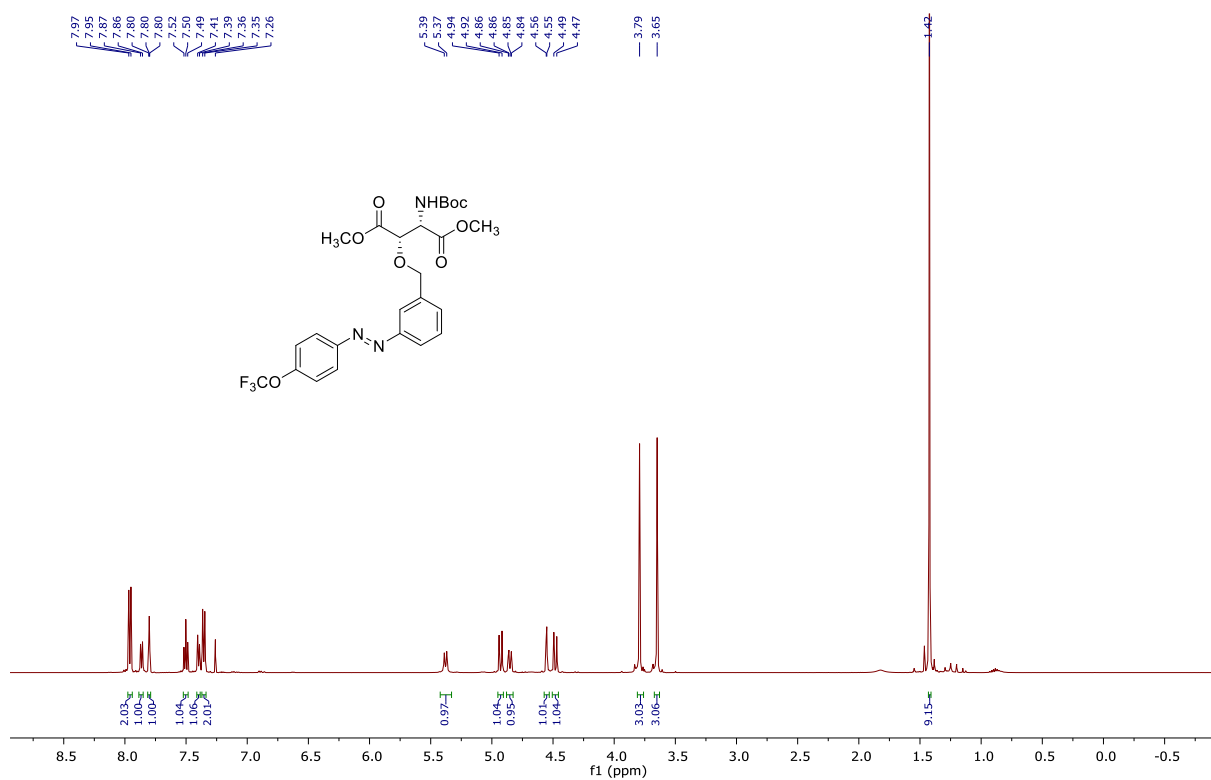


Figure S34: ^1H NMR spectrum and ^{13}C NMR spectrum of compound **1d** (*p*-Me-azo-TBOA)

FH-97-1
PROTON CDCl₃



FH-97-1
C13 CDCl₃

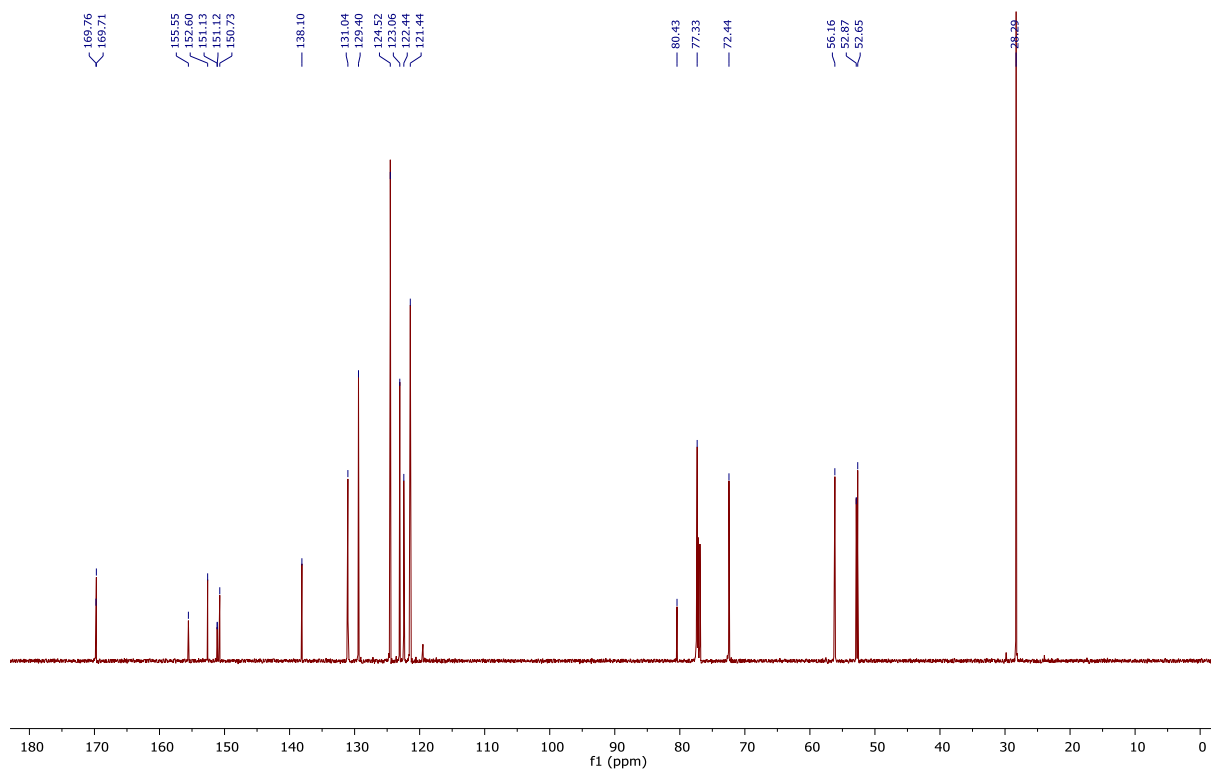
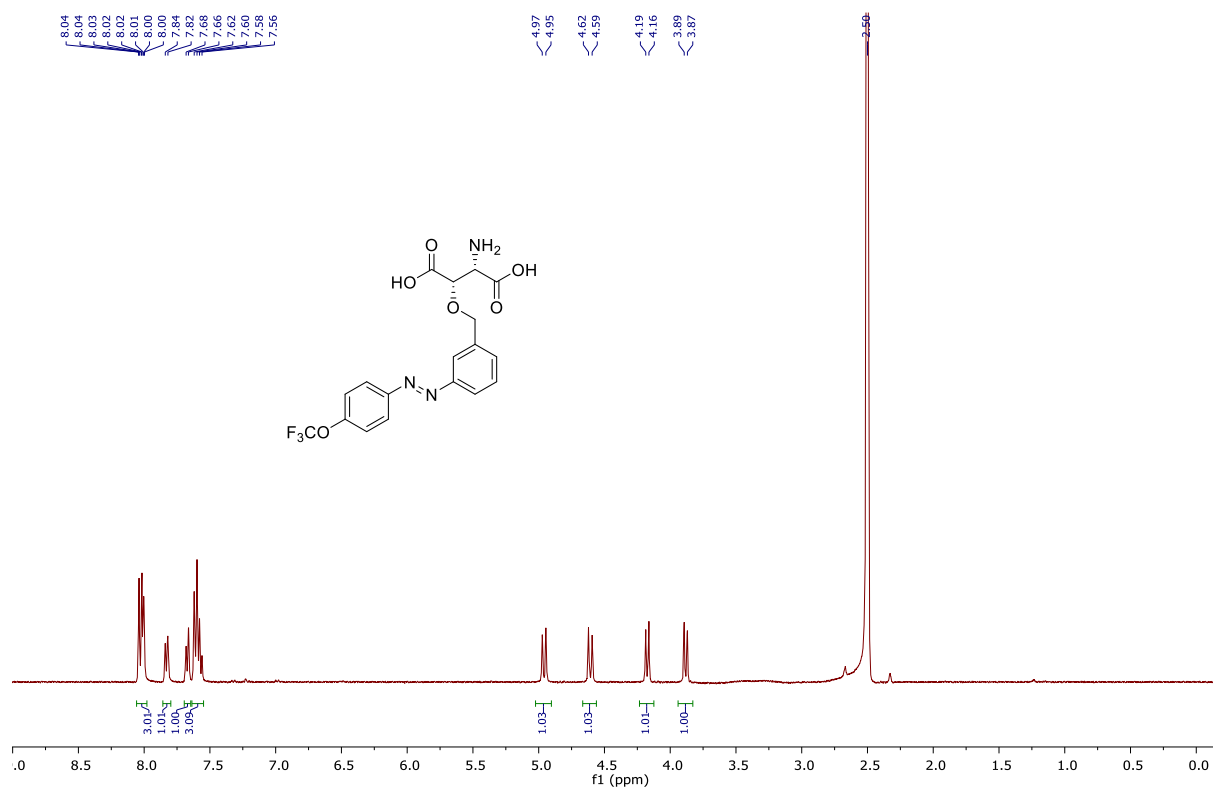


Figure S35: ¹H NMR spectrum and ¹³C NMR spectrum of compound 18e

20160627-FH097-thermo-H
DMSO



20160725-FH097-C
DMSO

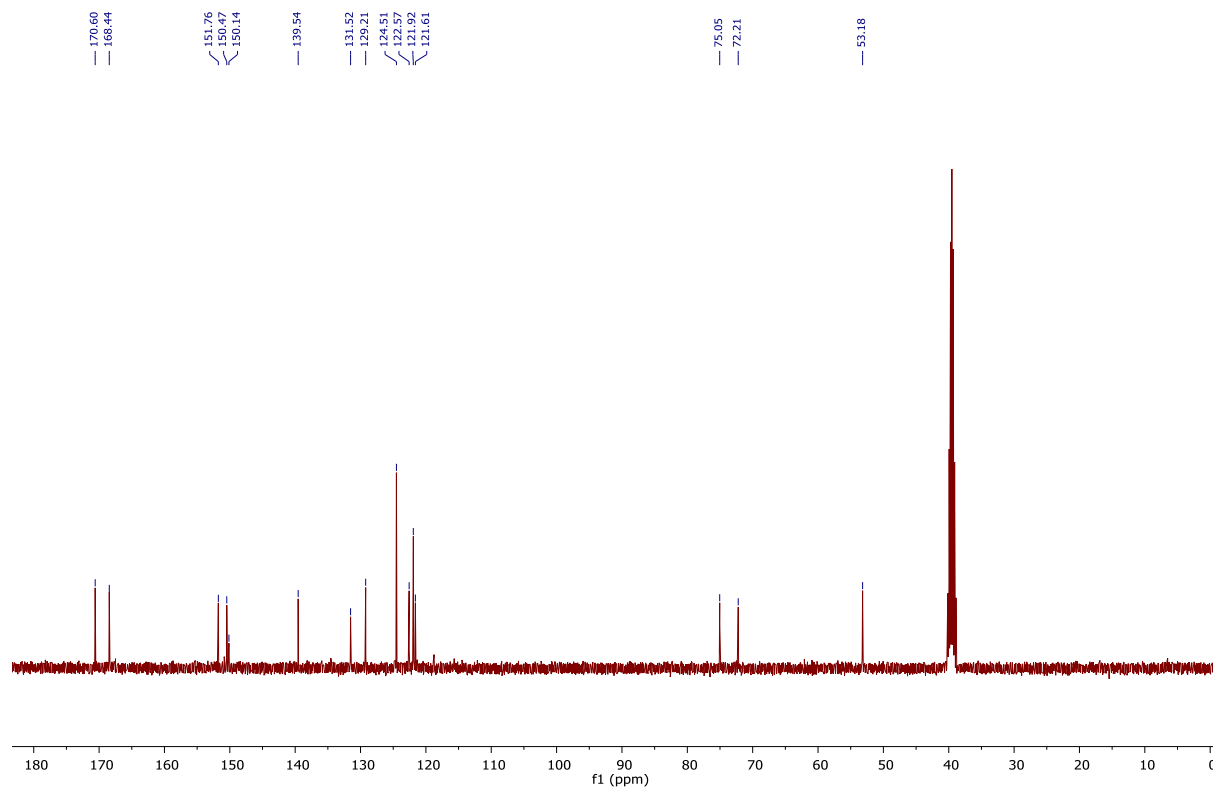
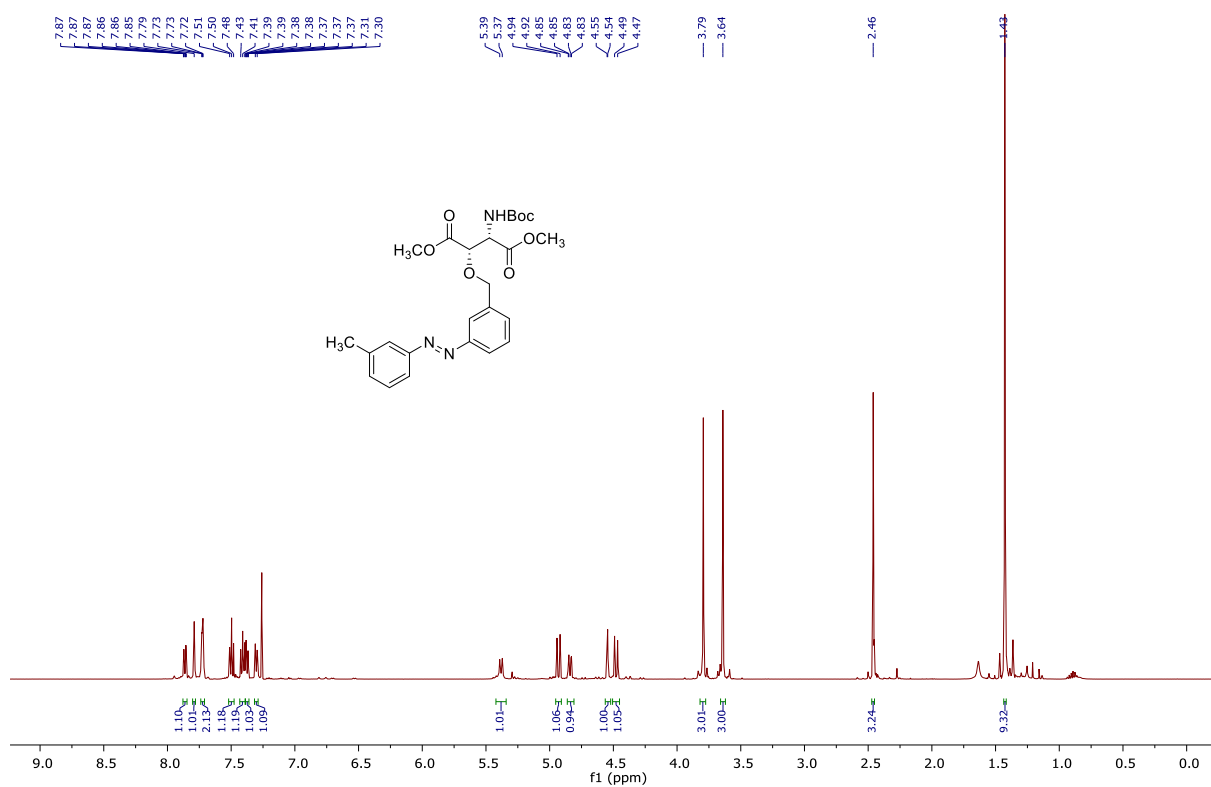


Figure S36: ¹H NMR spectrum and ¹³C NMR spectrum of compound **1e** (p-CF₃O-azo-TBOA)

FH-98-1
PROTON CDCl₃



FH-98-1
C13 DMSO

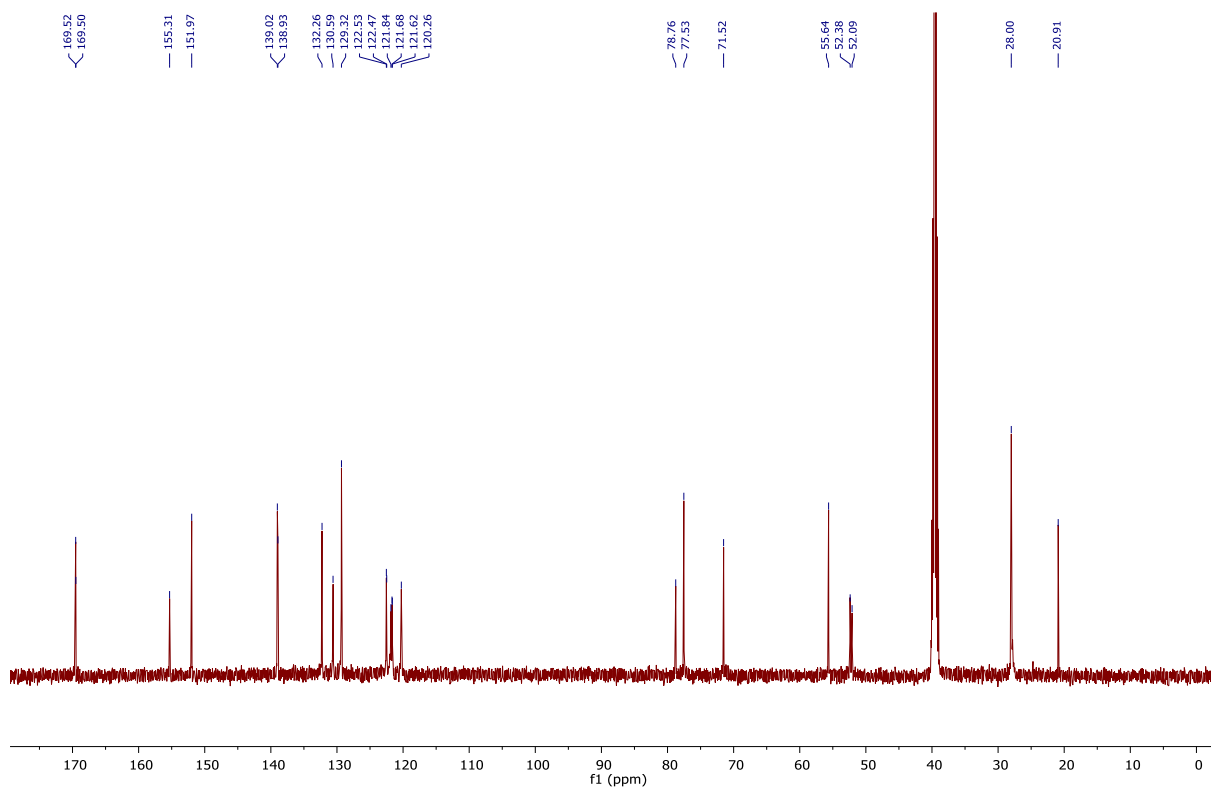
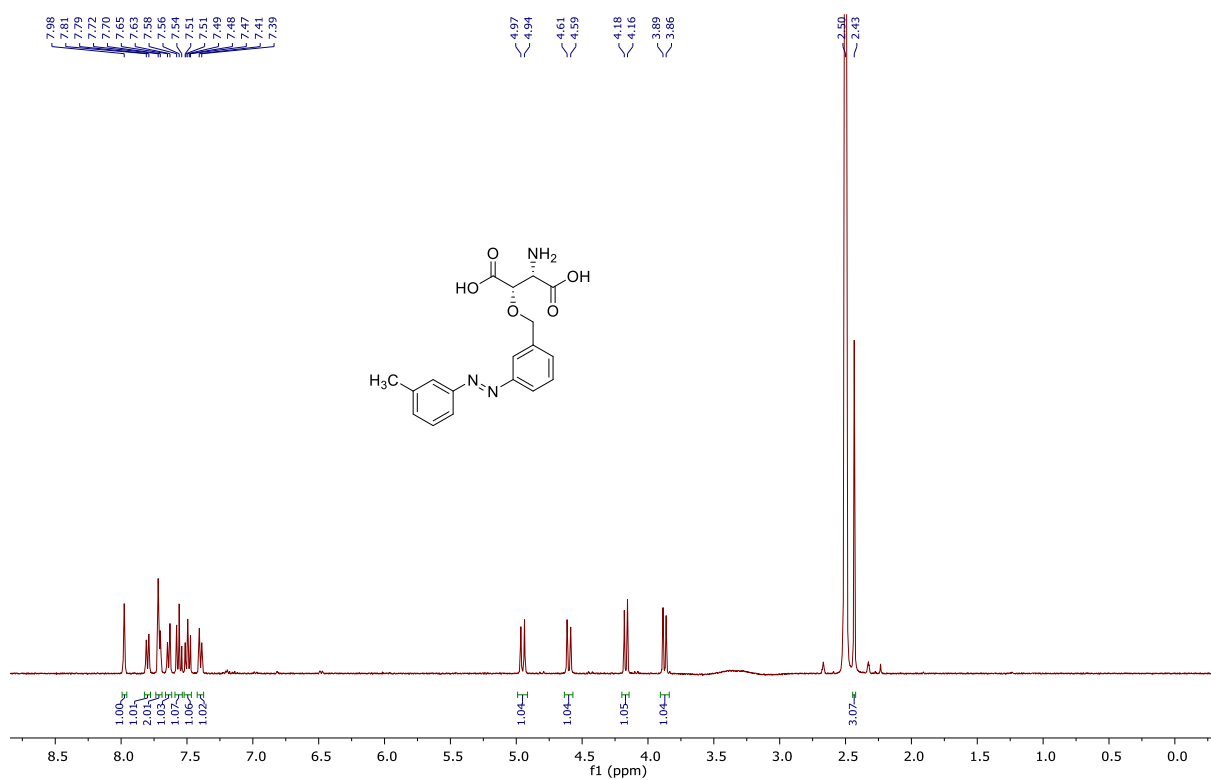


Figure S37: ¹H NMR spectrum and ¹³C NMR spectrum of compound 18f

20160622-FH098-thermo-H
DMSO



20160725-FH098-C
DMSO

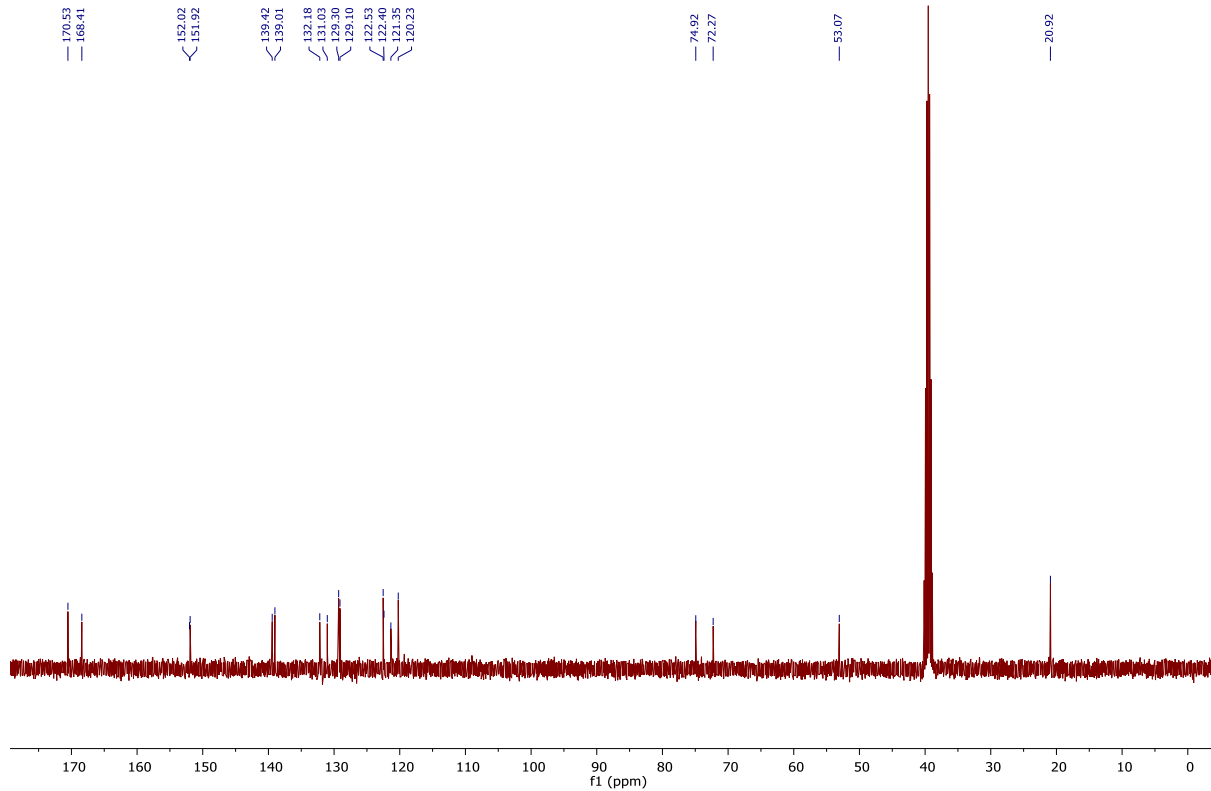


Figure S38: ¹H NMR spectrum and ¹³C NMR spectrum of compound 1f (*m*-Me-azo-TBOA)

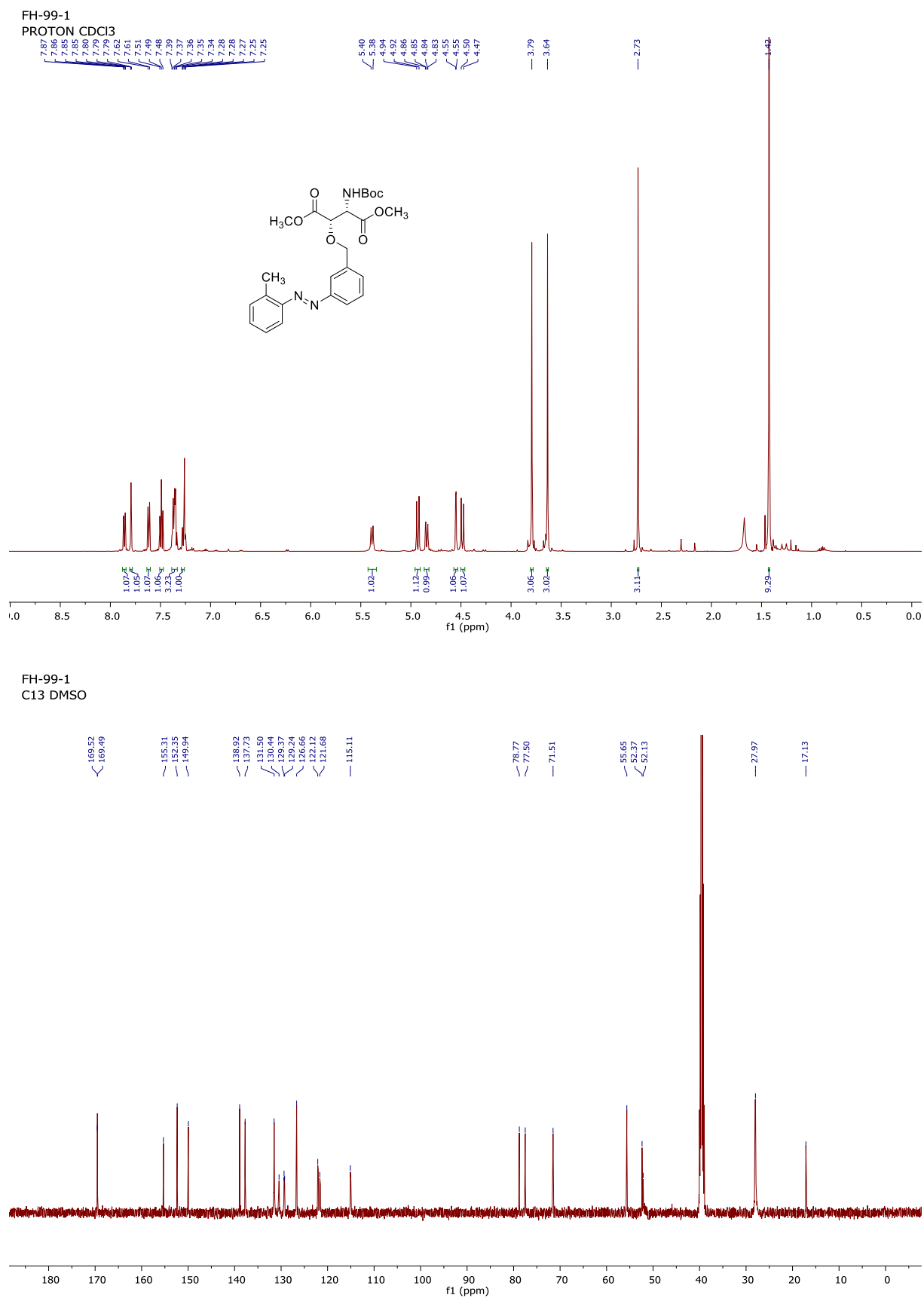


Figure S39: ¹H NMR spectrum and ¹³C NMR spectrum of compound 18g

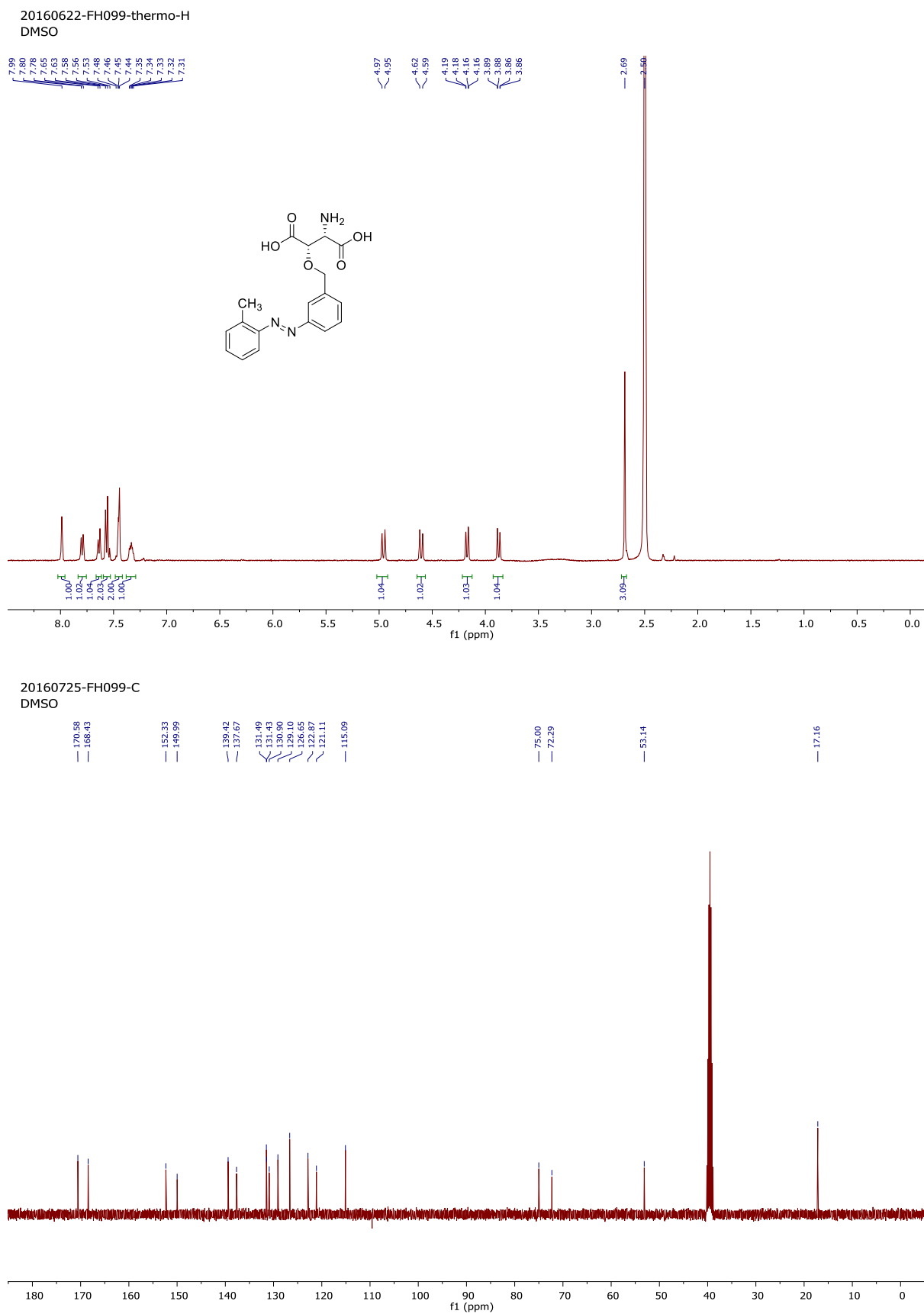


Figure S40: ¹H NMR spectrum and ¹³C NMR spectrum of compound **1g** (*o*-Me-azo-TBOA)

2. Photochemical data

Room temperature UV-Vis absorption spectra were recorded on an Agilent 8453 UV-Vis Spectrophotometer using Uvasol grade solvents. Irradiation experiments were performed: 312/365 nm: with a spectroline ENB - 280C/FE UV lamp; white light: Thor Labs OSL1 - EC Fiber Illuminator. Absorption for half-life were recorded on a in a microplate reader (Synergy H1, BioTek)

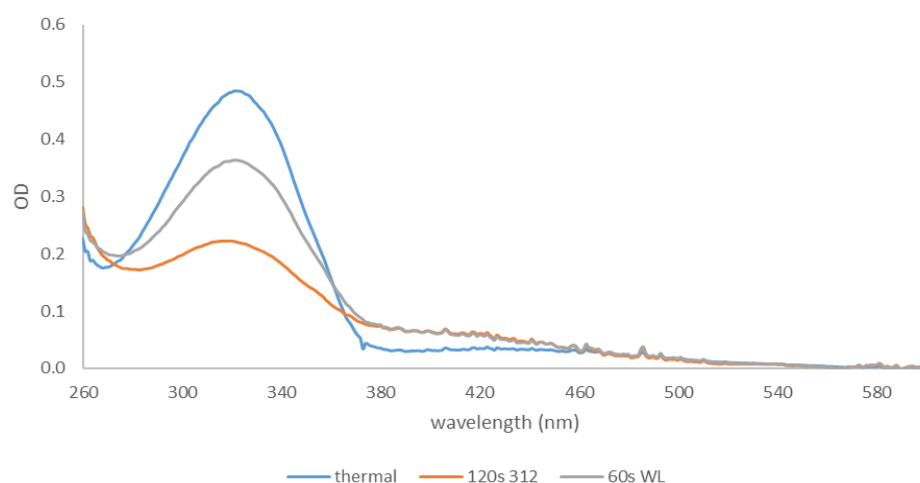


Figure S41: UV/VIS spectra of *p*-CF₃-azo-TBOA, 20 μM in DMSO, thermally adapted, irradiated with $\lambda = 312$ nm light for 120s and white light for 30s

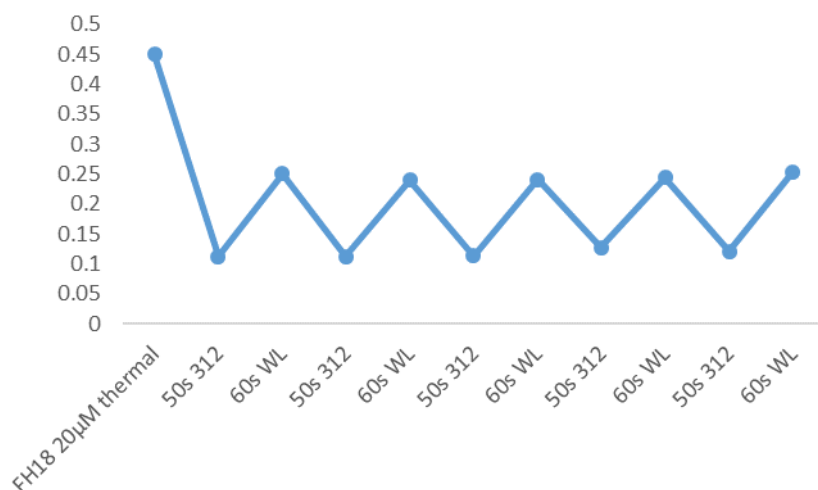


Figure S42: UV/VIS absorbance of *p*-CF₃-azo-TBOA at $\lambda = 317$ nm, 20 μM in DMSO, irradiated with 312 nm light and white light

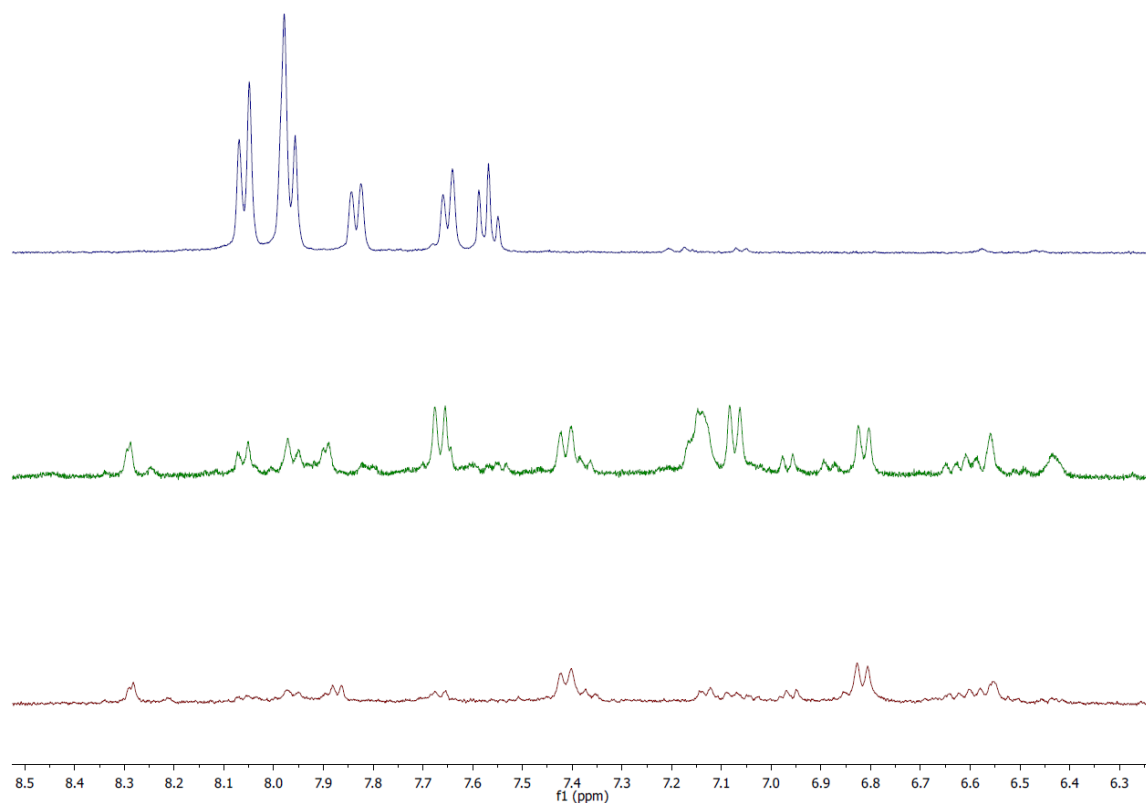


Figure S43: ^1H NMR spectrum of *p*- CF_3 -azo-TBOA, 1mg in 500 μl DMSO-d_6 . Top: thermal, middle: 30 min irradiation with 312 nm light, bottom, 60 min irradiation with 312 nm light

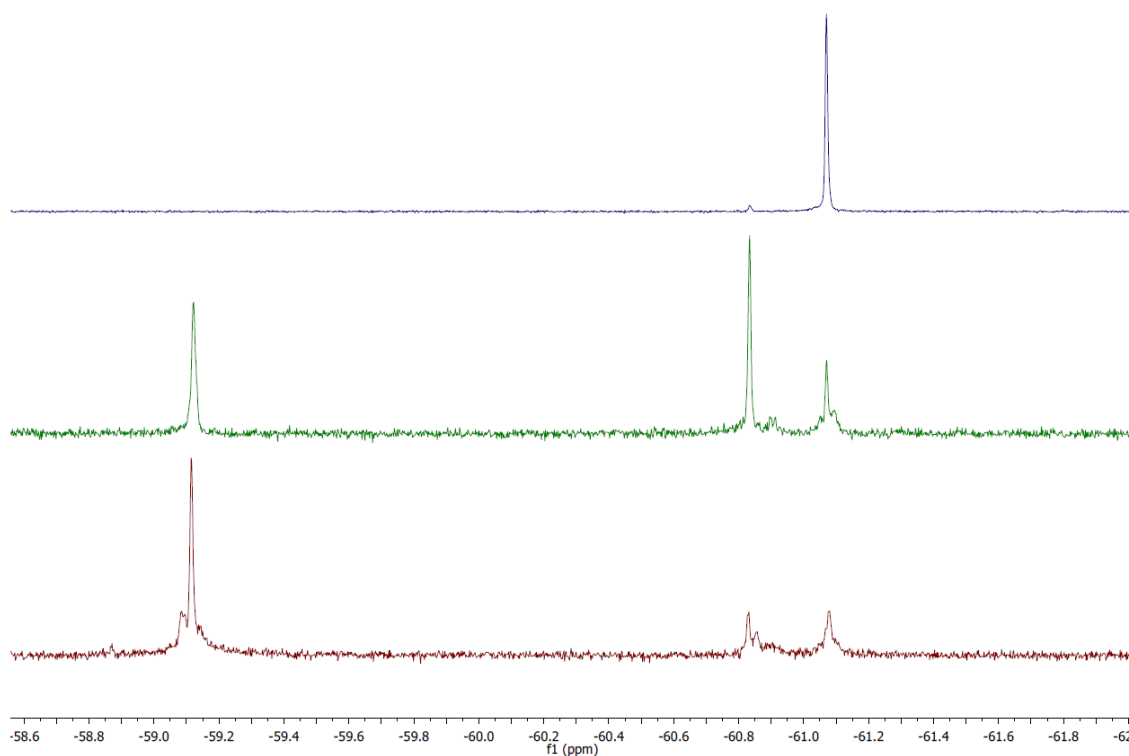


Figure S44: ^{19}F NMR spectrum of *p*- CF_3 -azo-TBOA, 1mg in 500 μl DMSO-d_6 . Top: thermal, middle: 30 min irradiation with 312 nm light, bottom, 60 min irradiation with 312 nm light

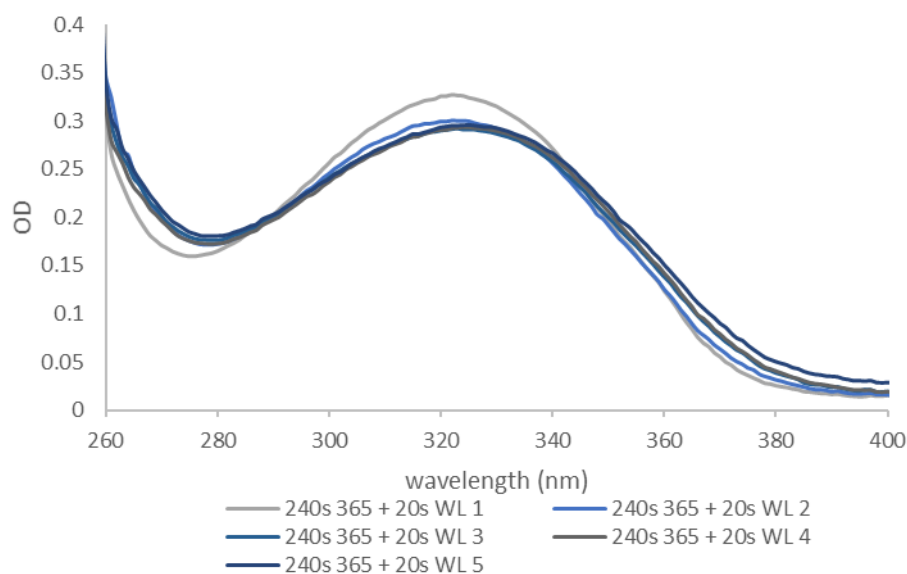


Figure S45: UV/VIS absorbance of *p*-CF₃-azo-TBOA, 20 μM in DMSO, irradiated with 365 nm light and white light.

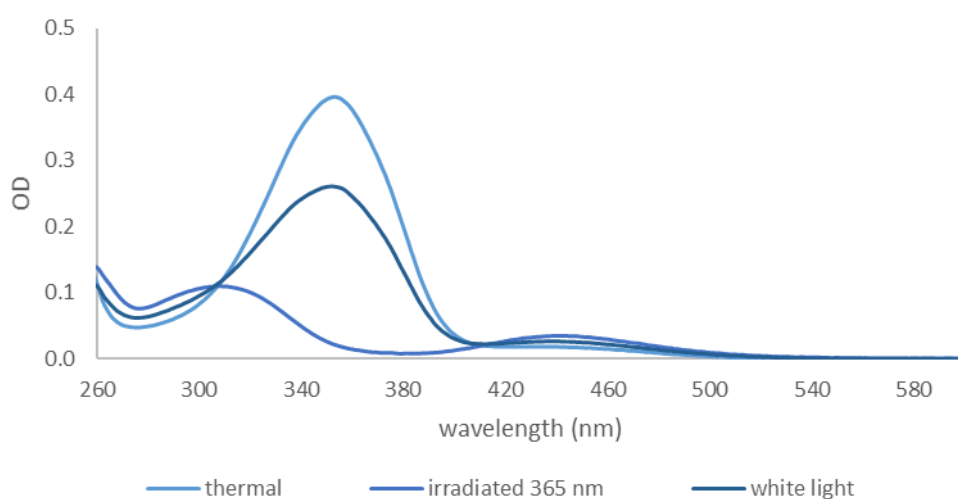


Figure S46: UV/VIS spectra of *p*-MeO-azo-TBOA 20 μM in DMSO, thermally adapted, irradiated with $\lambda = 365$ nm light for 40 s and white light for 20 s.

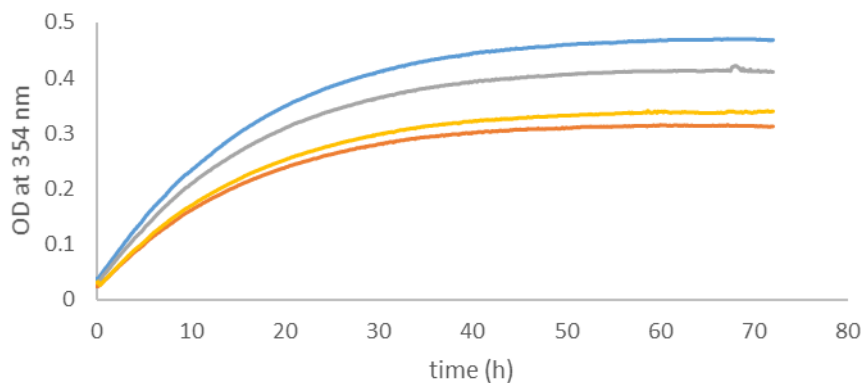


Figure S47: UV/VIS absorbance of *p*-MeO-azo-TBOA at $\lambda = 354$ nm, ~0.1 mM in DMSO in quadruplo, measured for thermal *cis-trans* isomerization at 37 °C.

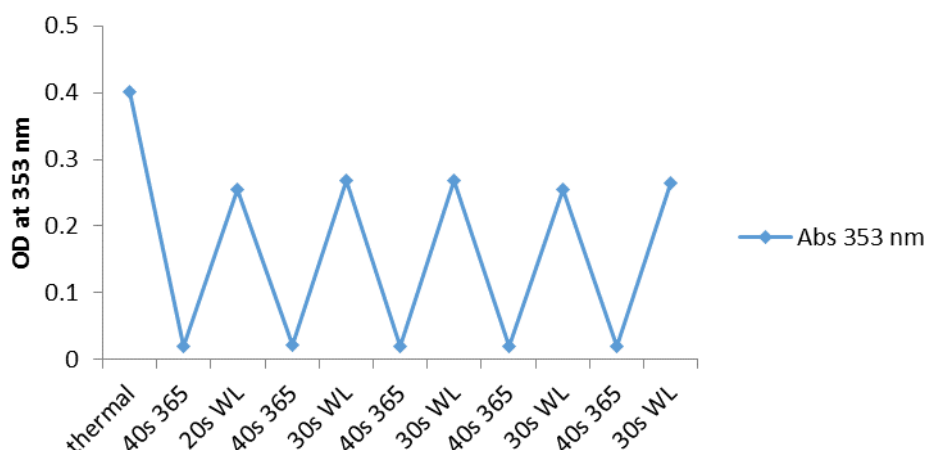


Figure S48: UV/VIS absorbance of *p*-MeO-azo-TBOA at $\lambda = 353$ nm, $20 \mu\text{M}$ in DMSO, irradiated with 365 nm light and white light

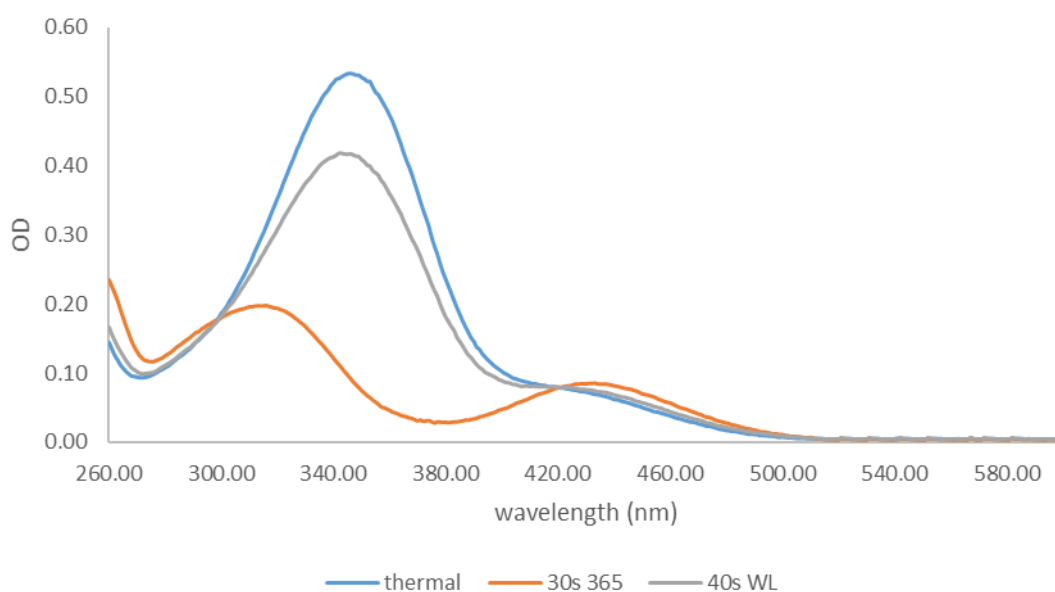


Figure S49: UV/VIS spectra of *p*-MeO-azo-TBOA $20 \mu\text{M}$ in $50 \mu\text{M}$ KPi pH = 7.4, 1% DMSO, thermally adapted, irradiated with $\lambda=365$ nm light for 40 s and white light for 20 s.

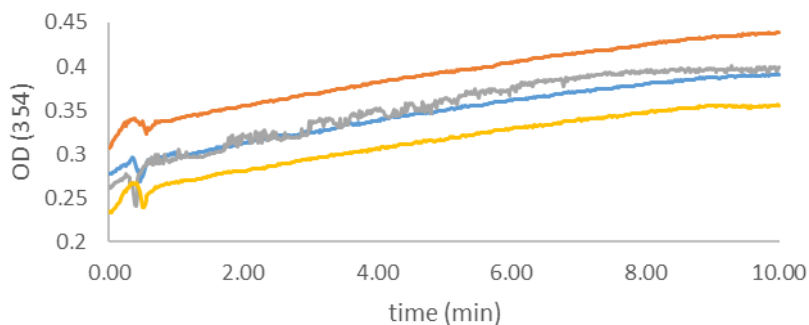


Figure S50: UV/VIS absorbance of *p*-MeO-azo-TBOA at $\lambda = 354$ nm, ~ 0.1 mM in KPi pH = 7.4, 1% DMSO in quadruplo, measured for thermal cis-trans isomerization at 37°C . The calculated half-life is 6 h.

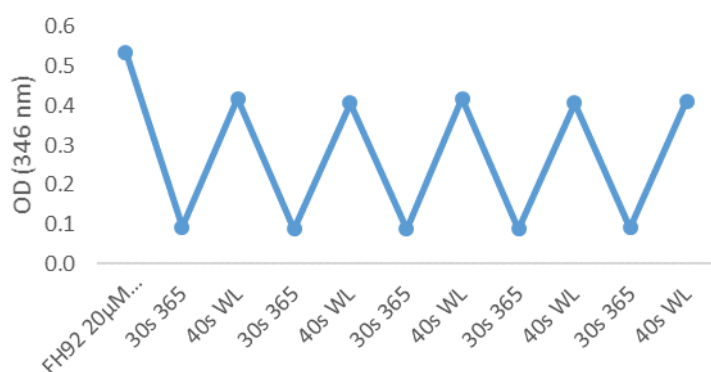


Figure S51: UV/VIS absorbance of *p*-MeO-azo-TBOA at $\lambda = 353$ nm, 20 μ M in KPi pH = 7.4, 1% DMSO, irradiated with 365 nm light and white light

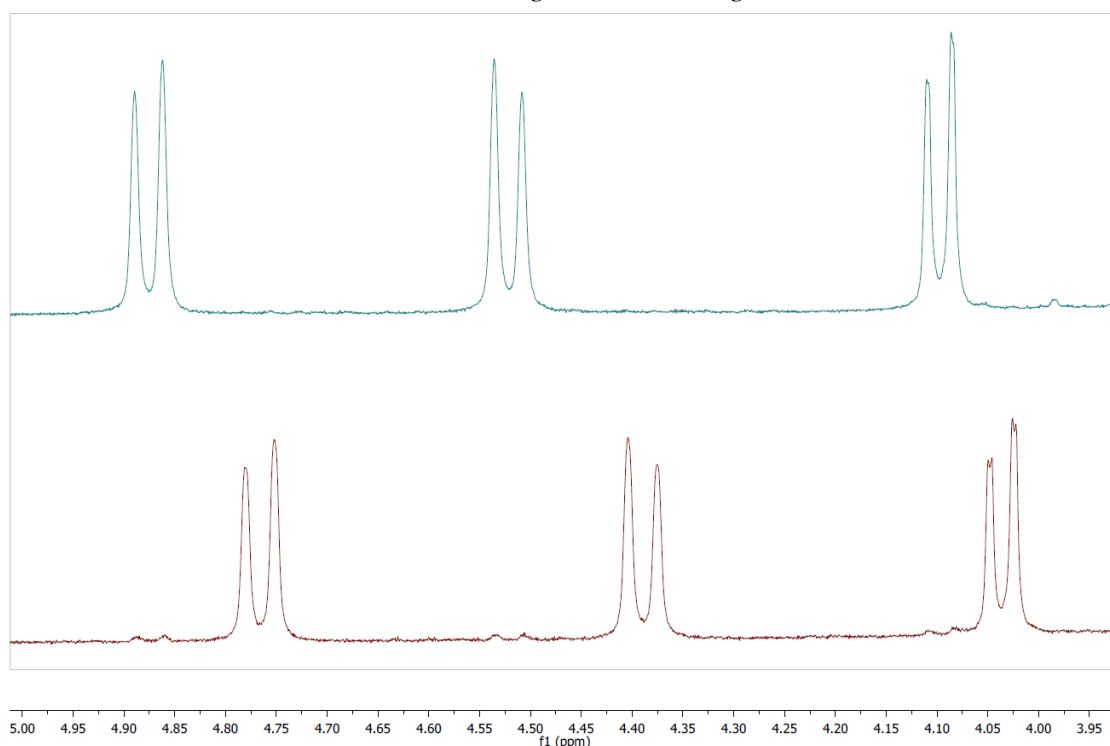


Figure S52: ^1H NMR spectrum of *p*-MeO-azo-TBOA 1mg in 500 μ l DMSO- d_6 , cis-trans ratio's calculated from the ^1H signals of Ar-CH₂-O and O-CH-R₂ protons. Top: thermal, cis-trans ratio 1:99. Bottom: irradiated with $\lambda = 365$ nm light, cis-trans ratio 96:4.

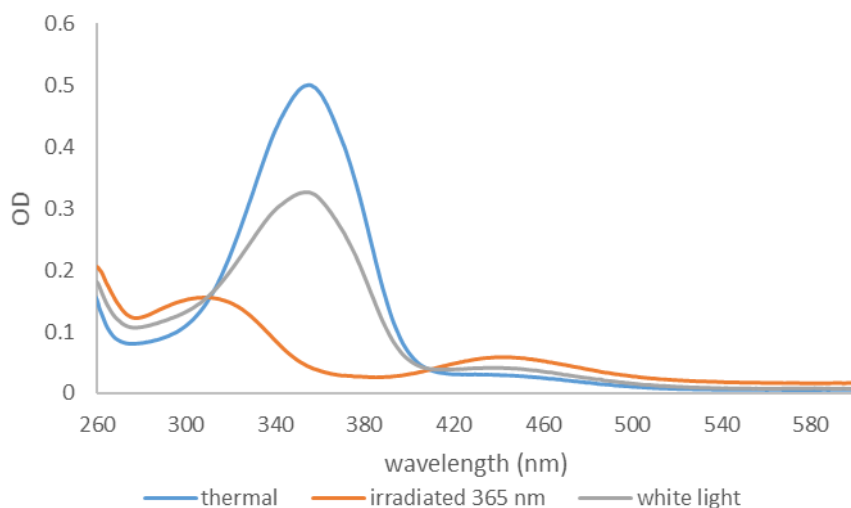


Figure S53: UV/VIS spectra of *p*-HexO-azo-TBOA, 20 μM in DMSO, thermally adapted, irradiated with $\lambda = 365$ nm light for 30 s and white light for 40 s.

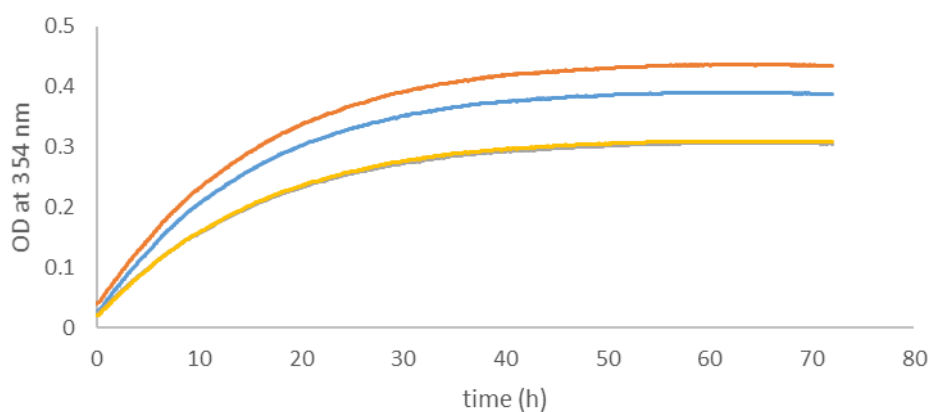


Figure S54: UV/VIS absorbance of *p*-HexO-azo-TBOA at $\lambda = 354$ nm, ~0.1 mM in DMSO, measured in quadruplo for thermal cis-trans isomerization at 37 °C.

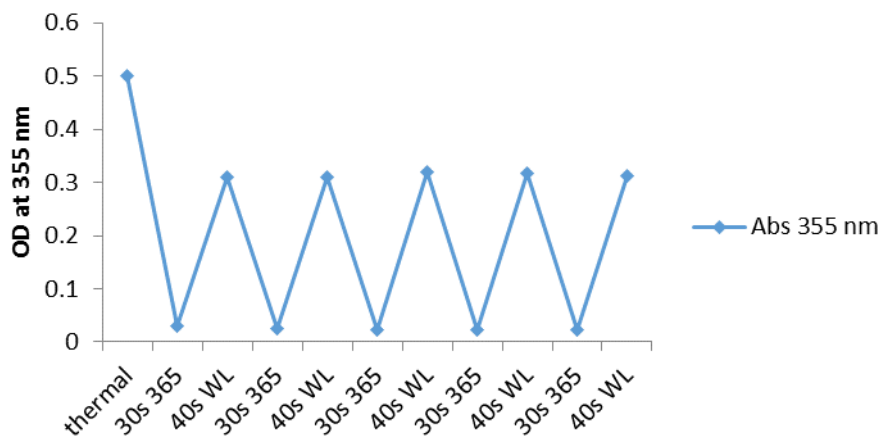


Figure S55: UV/VIS absorbance of *p*-HexO-azo-TBOA at $\lambda = 355$ nm, 20 μM in DMSO, irradiated with 365 nm light and white light

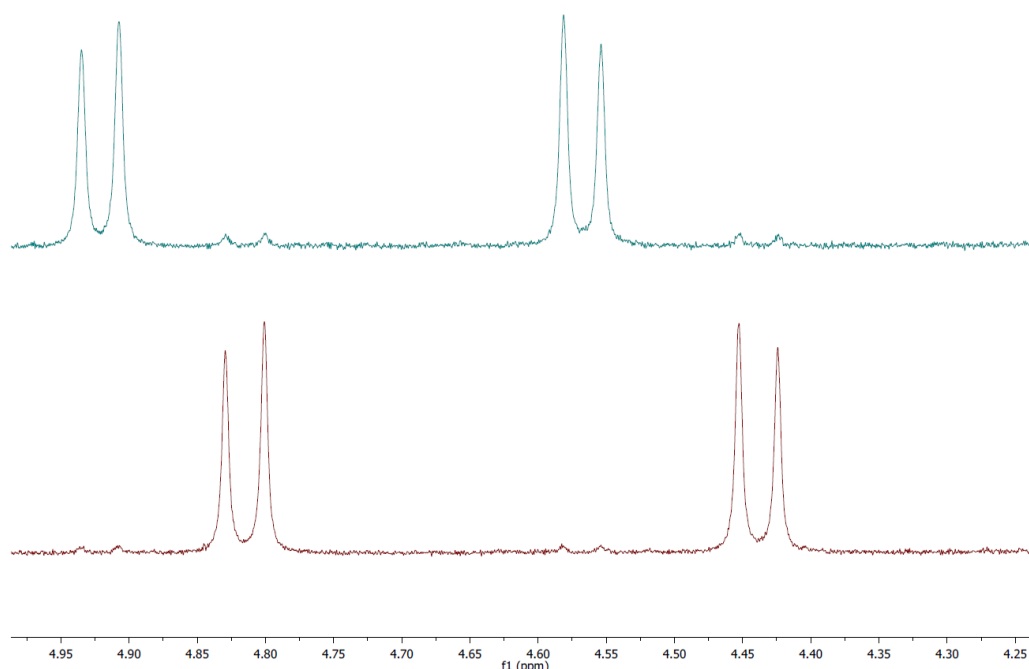


Figure S56: ^1H NMR spectrum of *p*-HexO-azo-TBOA, 1mg in 500 μl DMSO- d_6 , cis-trans ratio's calculated from the ^1H signals of Ar- $\text{CH}_2\text{-O}$ protons. Top: thermal, cis-trans ratio 2:98. Bottom: irradiated with $\lambda = 365$ nm light, cis-trans ratio 2:98.

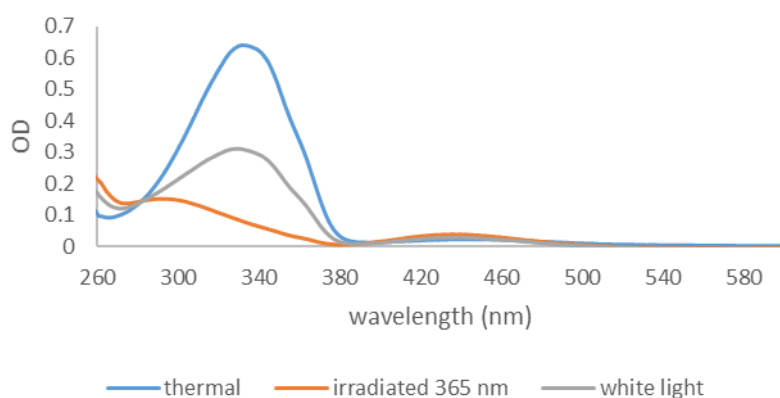


Figure S57: UV/VIS spectra of *p*-Me-azo-TBOA, 20 μM in DMSO, thermally adapted, irradiated with $\lambda = 365$ nm light for 80 s and white light for 80 s.

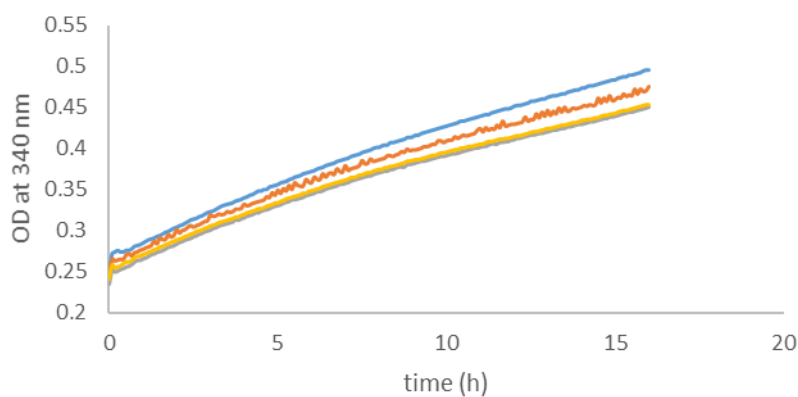


Figure S58: UV/VIS absorbance of *p*-Me-azo-TBOA at $\lambda = 340$ nm, ~ 0.2 mM in DMSO in quadruplo, measured for thermal cis-trans isomerization at 37 $^\circ\text{C}$.

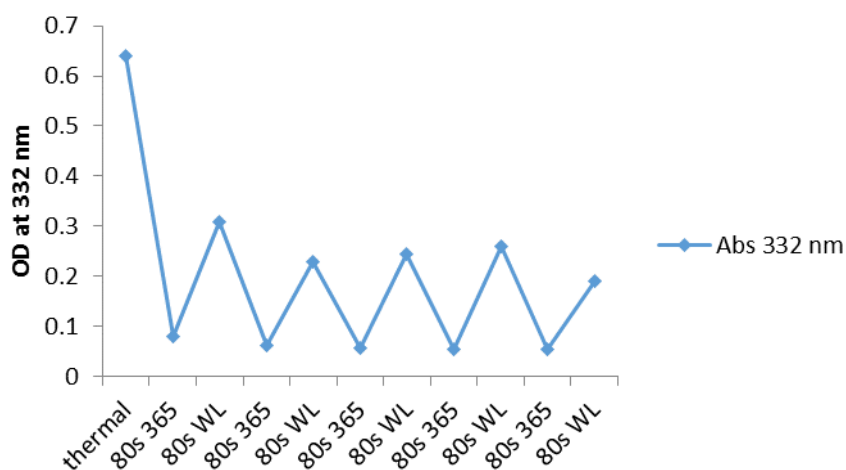


Figure S59: UV/VIS absorbance of *p*-Me-azo-TBOA at $\lambda = 332$ nm, 20 μ M in DMSO, irradiated with 365 nm light and white light

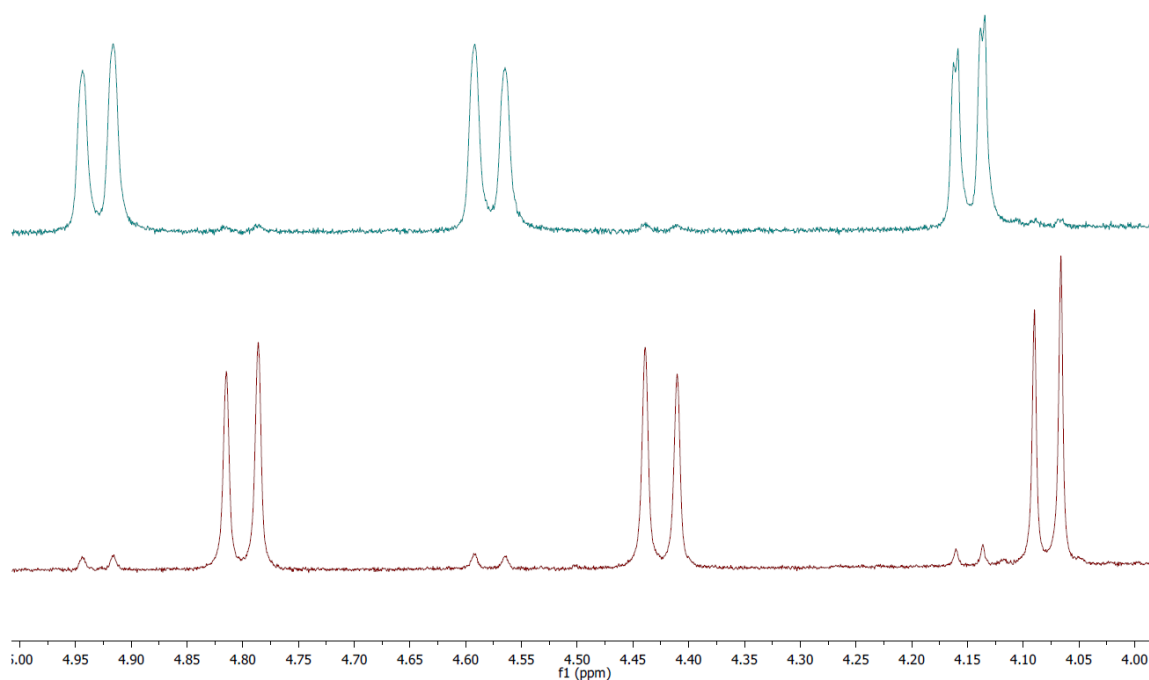


Figure S60: ^1H NMR spectrum of *p*-Me-azo-TBOA, 1mg in 500 μ l DMSO- d_6 , cis-trans ratio's calculated from the ^1H signals of Ar-CH₂-O and O-CH-R₂ protons. Top: thermal, cis-trans ratio 3:97. Bottom: irradiated with $\lambda = 365$ nm light, cis-trans ratio 93:7.

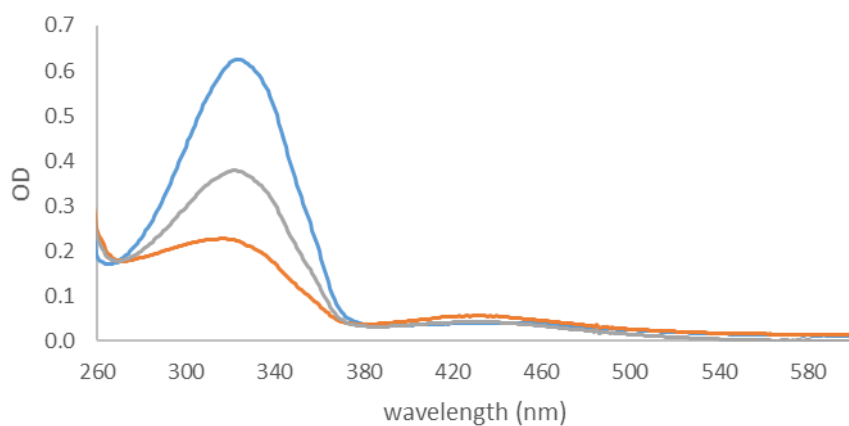


Figure S61: UV/VIS spectra of *p*-CF₃O-azo-TBOA, 20 μ M in DMSO, thermally adapted, irradiated with $\lambda = 312$ nm light for 60 s and white light for 90 s.

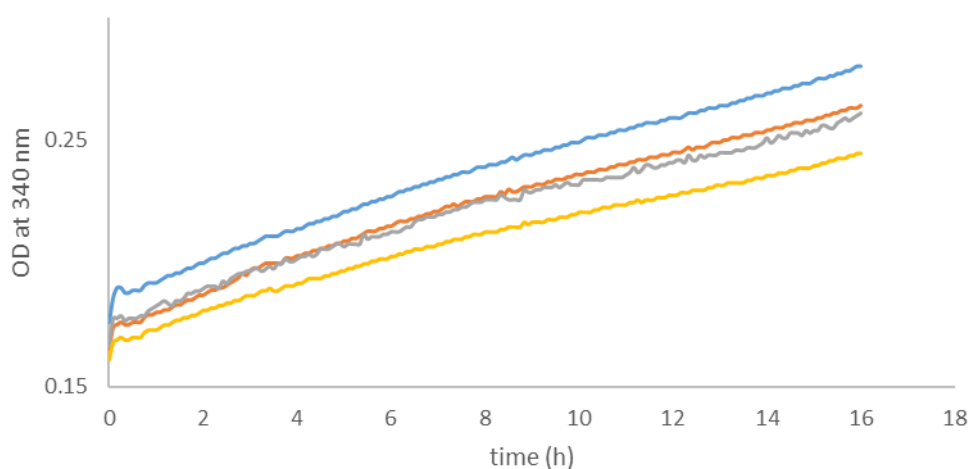


Figure S62: UV/VIS absorbance of *p*-CF₃O-azo-TBOA at $\lambda = 340$ nm, ~ 0.2 mM in DMSO in quadruplo, measured for thermal cis-trans isomerization at 37 °C.

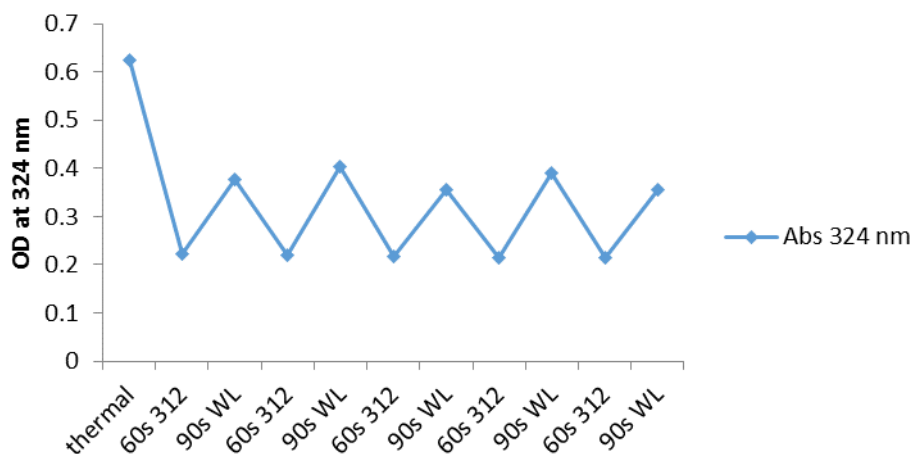


Figure S63: UV/VIS absorbance of *p*-CF₃O-azo-TBOA at $\lambda = 324$ nm, 20 μ M in DMSO, irradiated with 312 nm light and white light

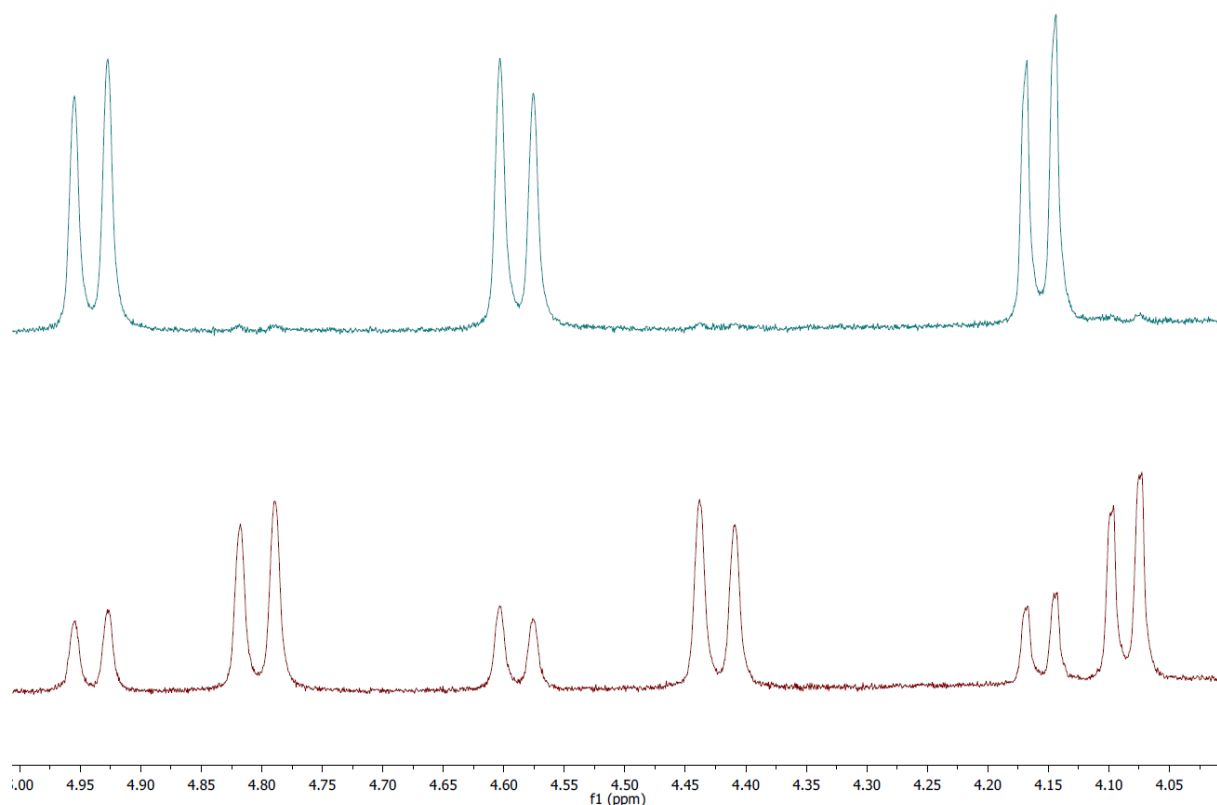


Figure S64: ^1H NMR spectrum of *p*- CF_3O -azo-TBOA, 1 mg in 500 μl DMSO- d_6 , cis-trans ratio's calculated from the ^1H signals of Ar- $\text{CH}_2\text{-O}$ and O- CH-R_2 protons. Top: thermal, cis-trans ratio 4:96. Bottom: irradiated with $\lambda = 365$ nm light, cis-trans ratio 71:29.

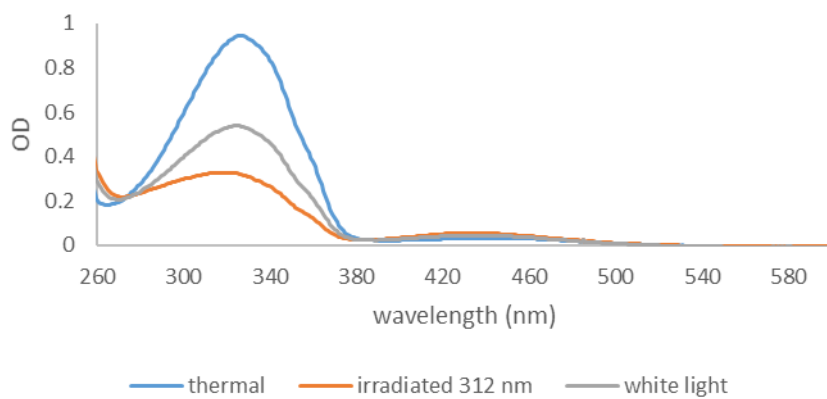


Figure S65: UV/VIS spectra of *m*-Me-azo-TBOA, 20 μM in DMSO, thermally adapted, irradiated with $\lambda = 365$ nm light for 90 s and white light for 70 s.

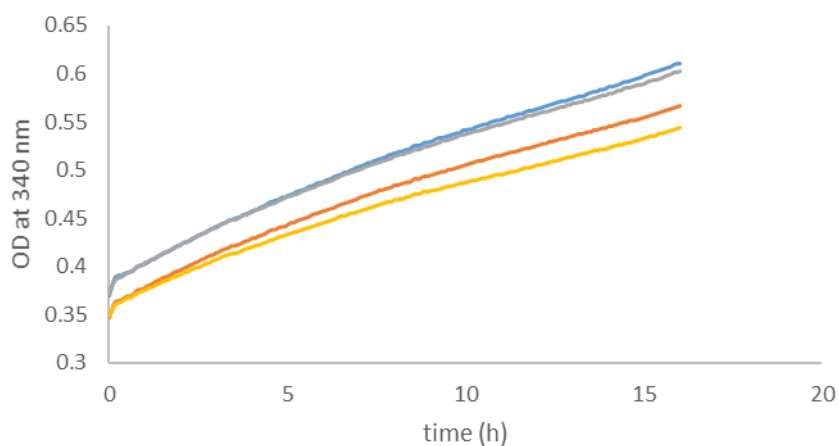


Figure S66: UV/VIS absorbance of *m*-Me-azo-TBOA at $\lambda = 340$ nm, ~ 0.2 mM in DMSO in quadruplo, measured for thermal cis-trans isomerization at 37 °C.

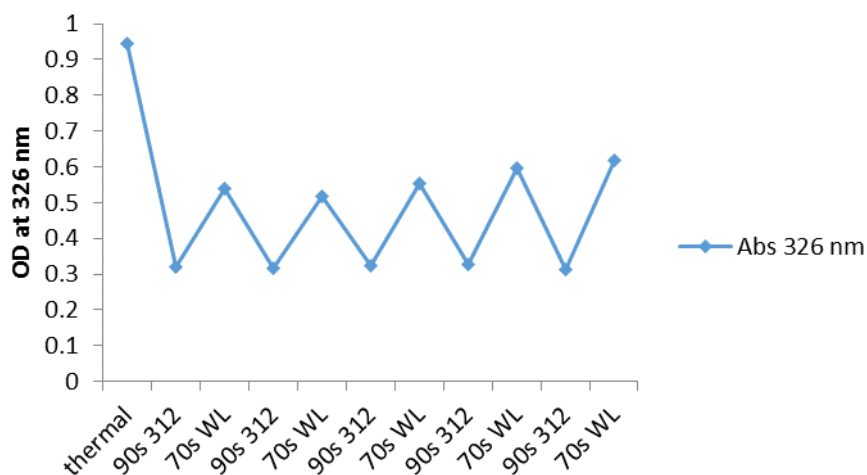


Figure S67: UV/VIS absorbance of *m*-Me-azo-TBOA at $\lambda = 326$ nm, $20 \mu\text{M}$ in DMSO, irradiated with 312 nm light and white light

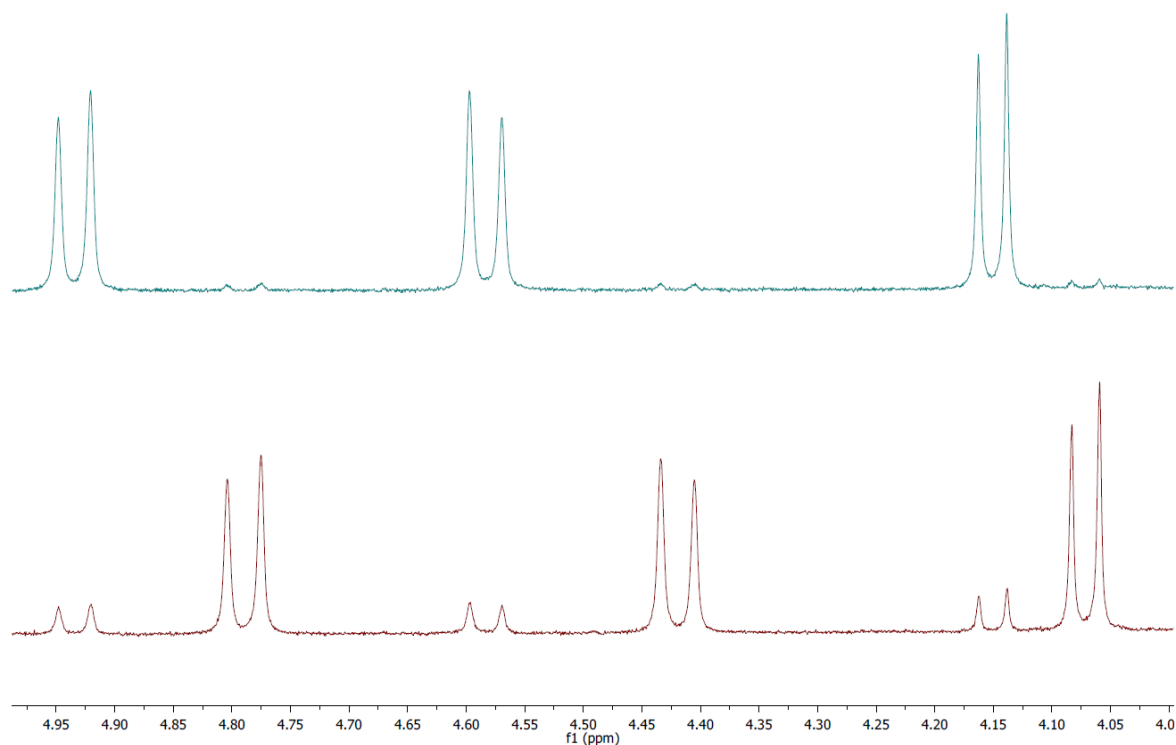


Figure S68: ^1H NMR spectrum of *m*-Me-azo-TBOA, 1 mg in 500 μl DMSO- d_6 , *cis-trans* ratio's calculated from the ^1H signals of Ar- $\text{CH}_2\text{-O}$ and O- CH-R_2 protons. Top: thermal, *cis-trans* ratio 3:97. Bottom: irradiated with $\lambda = 312$ nm light, *cis-trans* ratio 86:14.

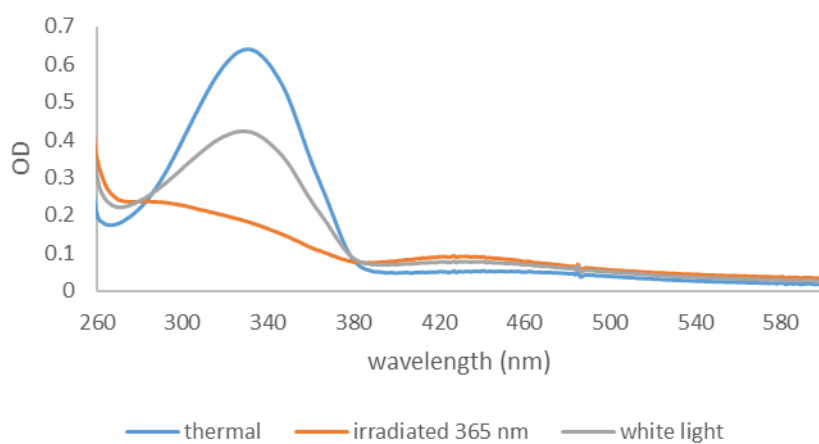


Figure S69: UV/VIS spectra of *o*-Me-azo-TBOA 20 μM in DMSO, thermally adapted, irradiated with $\lambda = 365$ nm light for 60 s and white light for 90 s.

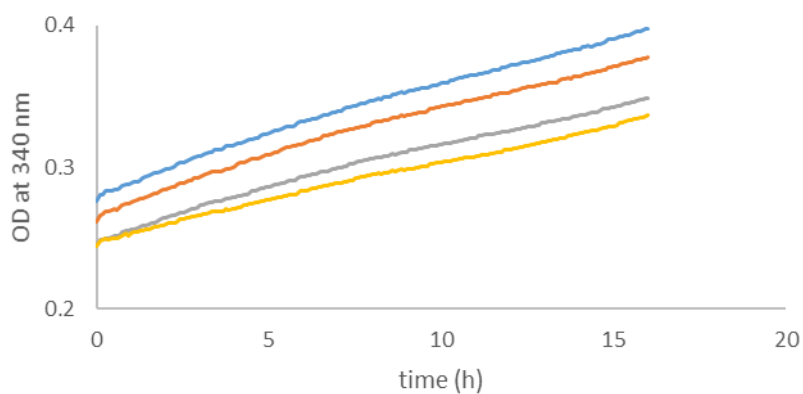


Figure S70: UV/VIS absorbance of *o*-Me-azo-TBOA at $\lambda = 340$ nm, ~ 0.2 mM in DMSO in quadruplo, measured for thermal *cis-trans* isomerization at 37°C .

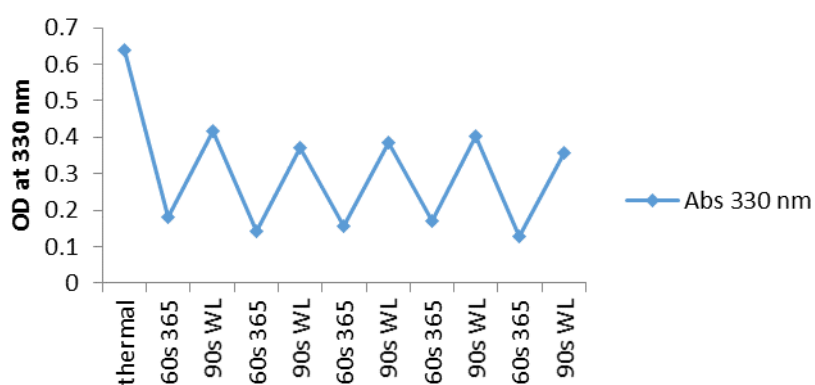


Figure S71: UV/VIS absorbance of *o*-Me-azo-TBOA at $\lambda = 330$ nm, $20\ \mu\text{M}$ in DMSO, irradiated with 365 nm light and white light

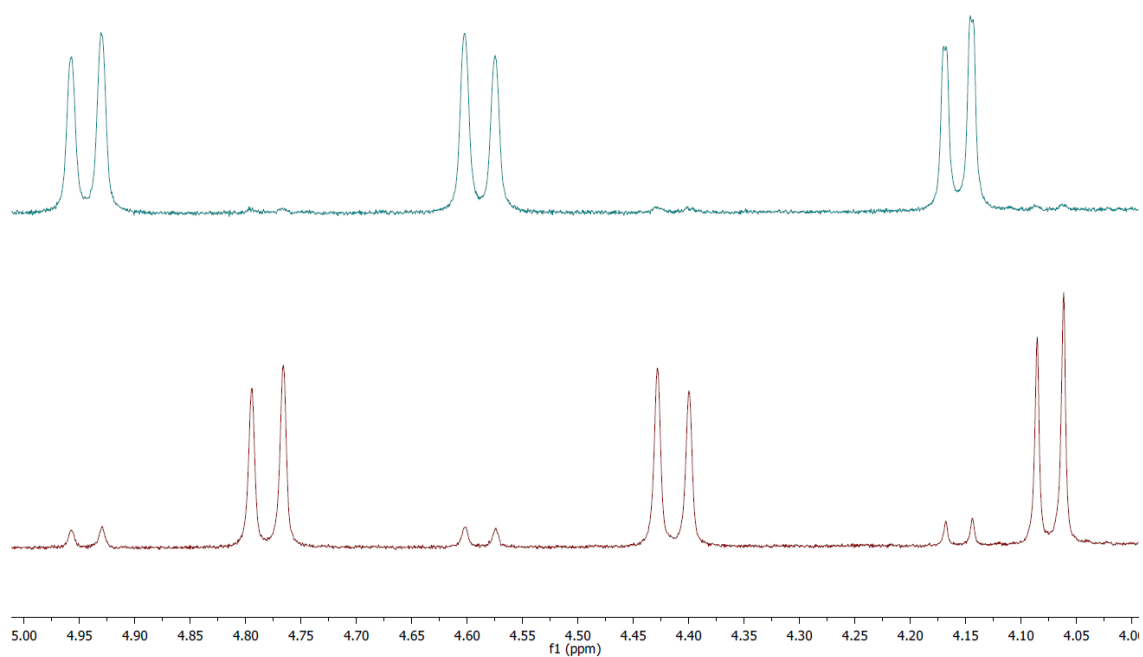


Figure S72: ^1H NMR spectrum of ***o*-Me-azo-TBOA**, 1mg in 500 μl DMSO- d_6 , *cis-trans* ratio's calculated from the ^1H signals of Ar- $\text{CH}_2\text{-O}$ and O- CH-R_2 protons. Top: thermal, *cis-trans* ratio 3:97. Bottom: irradiated with $\lambda = 365\text{ nm}$ light, *cis-trans* ratio 90:10.

3. Biological evaluation

3.1 DNA manipulation, protein purification and concentration determination.

As described in Jensen *et al.*,³

Proteoliposome preparation

E. coli total lipid extract was purified with acetone and diethylether, both with 1 mM DTT. The *E. coli* lipids was mixed with L-(α)-phosphatidylcholine Egg chicken in a ratio of 3:1. Finally they were dissolved in 50 mM KPi pH 7.0 (20 mg/ml) and frozen in liquid N₂. Subsequently the lipid mixture was extruded with a 400 nm filter 11 times and diluted with 50mM KPi (pH 7.0) to a final concentration of 4 mg/ml. The mixture was titrated with 10% triton X-100 until Rsat. 100 μ g of the purified protein and lipids was mixed in a ratio of 1:1600 (w:w) and incubated at room temperature for 30 minutes. Biobeads were added four times (200 mg for 5 mL 4 mg/ml lipid solution) for 0.5 h, 1 h, overnight and 2 h at 4 °C. The biobeads were removed by filtration. The proteoliposomes where spun down for 20 min at 80000 Cpm and subsequently resuspended in 50 mM KPi pH 7.0 at a concentration of 16.7 μ g protein per 500 μ L and freeze-thawed for four cycles. The proteoliposomes are stored in liquid N₂.

3.2 Uptake assay

The proteoliposomes were thawed, extruded with a 400 nm filter, spin down for 20 minutes at 80000 Cpm and subsequently resuspended in 50 mM KPi pH 7.0 at a concentration of 16.7 μ g protein per 120 μ L buffer. 1800 μ L of 50 mM NaPi pH 7.0, 1 μ M [¹⁴C]aspartic acid and 3 μ M Valinomycin was stirred in a tube at 30°C and to that the transport assay was started by the addition of 10 μ L proteoliposomes (1.39 μ g protein) and either pure DMSO or a DMSO solution of inhibitor (final DMSO concentration 1%). From this mixture, at several time points 100 μ L was taken and the transport was stopped by adding 2 mL cold 100mM LiCl and

subsequently filtering over a Protran BA 85-Whatman filter. The filter was washed by 2 mL cold 100 mM LiCl and transported to a cup. (Optionally the assay was irradiated with 365 nm UV light for 45 s to switch compounds ***p*-MeO-azo-TBOA** at a concentration of 50 mM from *trans* to *cis* or irradiated with white light using a Thor Labs OSL1 - EC Fiber Illuminator to switch compound ***p*-MeO-azo-TBOA** at a concentration of 50 mM from *cis* to *trans*). To the cup, 2 mL of scintillation liquid was added and the activity of the cup was measured with a PerkinElmer Tri-Carb 2800RT liquid scintillation counter.

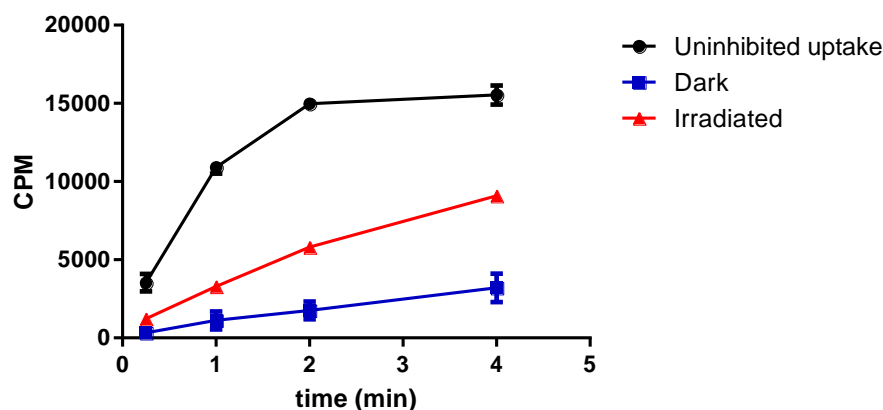


Figure S73: $[^{14}\text{C}]$ Aspartate uptake assay, with uninhibited uptake, 10 μM non-irradiated ***p*-CF₃-azo-TBOA** and 10 μM irradiated ***p*-CF₃-azo-TBOA**. All experiments were done in duplicate.

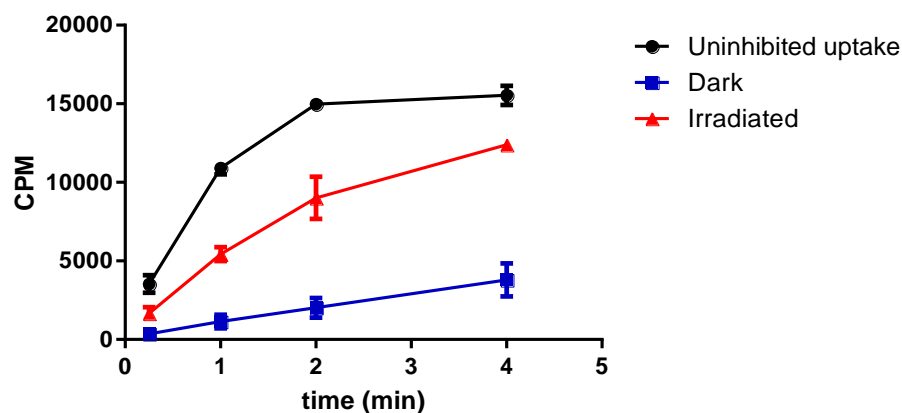


Figure S74: [^{14}C]Aspartate uptake assay, with uninhibited uptake, 10 μM non-irradiated *p*-MeO-azo-TBOA and 10 μM irradiated *p*-MeO-azo-TBOA. All experiments were done in duplicate.

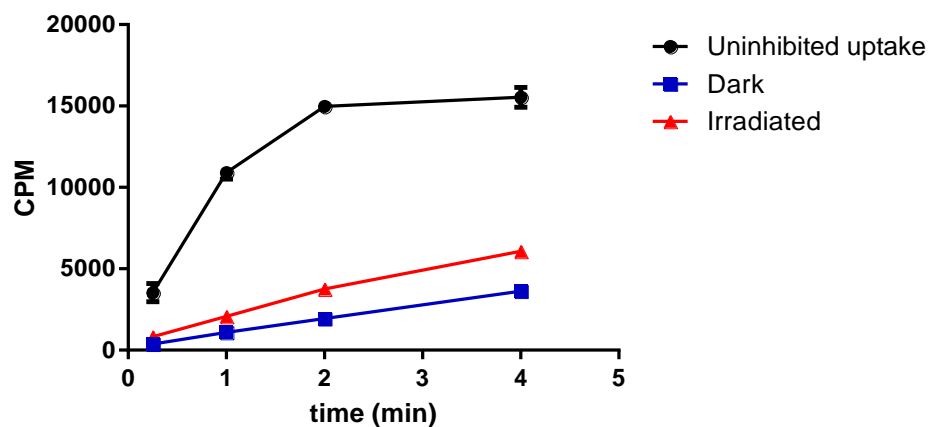


Figure S75: [^{14}C]Aspartate uptake assay, with uninhibited uptake, 10 μM non-irradiated *p*-HexO-azo-TBOA and 10 μM irradiated *p*-HexO-azo-TBOA. All experiments were done in duplicate.

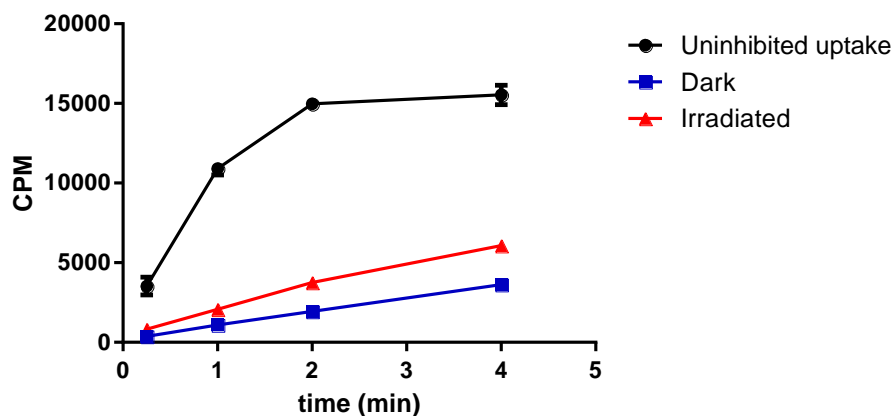


Figure S76: [^{14}C]Aspartate uptake assay, with uninhibited uptake, 10 μM non-irradiated *p*-Me-azo-TBOA and 10 μM irradiated *p*-Me-azo-TBOA. All experiments were done in duplicate.

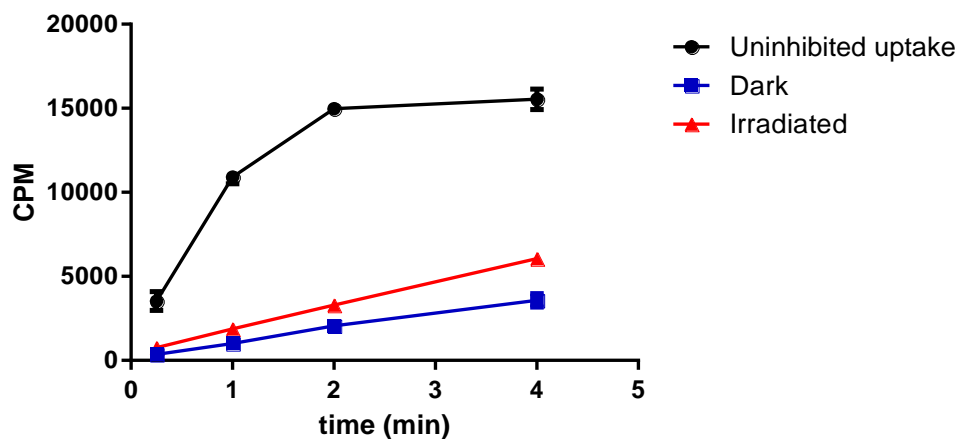


Figure S77: [^{14}C]Aspartate uptake assay, with uninhibited uptake, 10 μM non-irradiated *p*- CF_3O -azo-TBOA and 10 μM irradiated *p*- CF_3O -azo-TBOA. All experiments were done in duplicate.

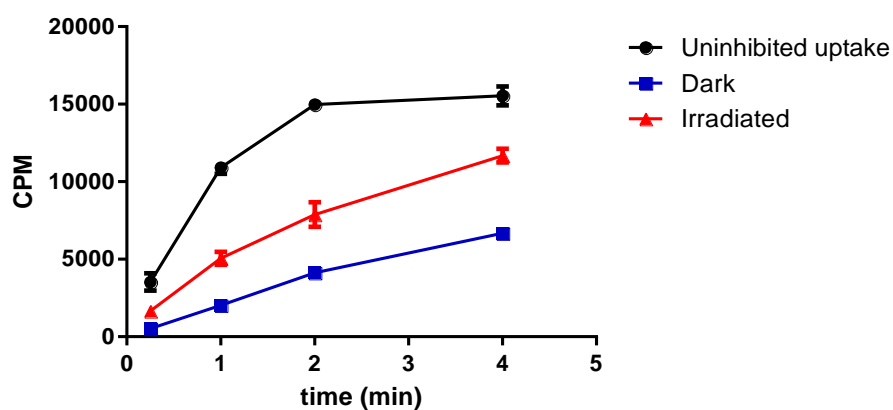


Figure S78: [^{14}C]Aspartate uptake assay, with uninhibited uptake, 10 μM non-irradiated *m*-Me-azo-TBOA and 10 μM irradiated *m*-Me-azo-TBOA. All experiments were done in duplicate.

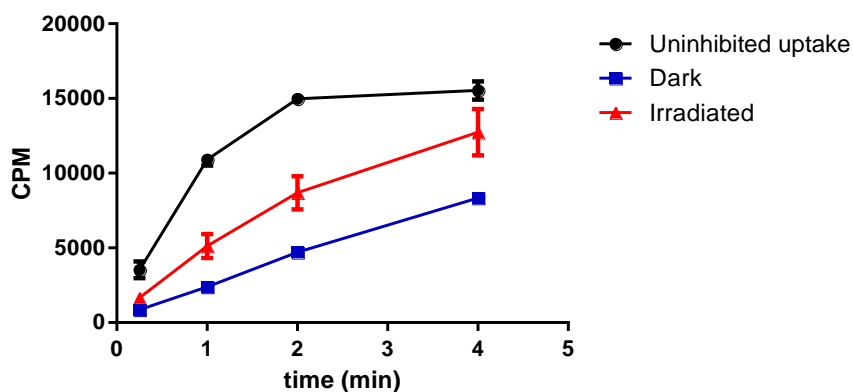


Figure S79: [^{14}C]Aspartate uptake assay, with uninhibited uptake, 10 μM non-irradiated *o*-Me-azo-TBOA and 10 μM irradiated *o*-Me-azo-TBOA. All experiments were done in duplicate.

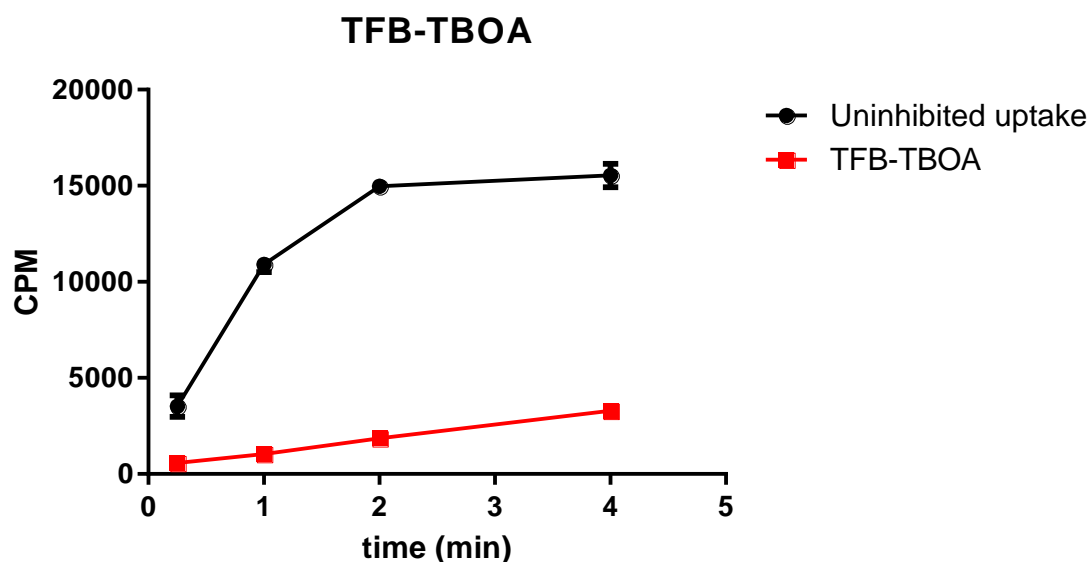


Figure S80: [^{14}C]Aspartate uptake assay, with uninhibited uptake and 10 μM TFB-TBOA. All experiments were done in duplicate.

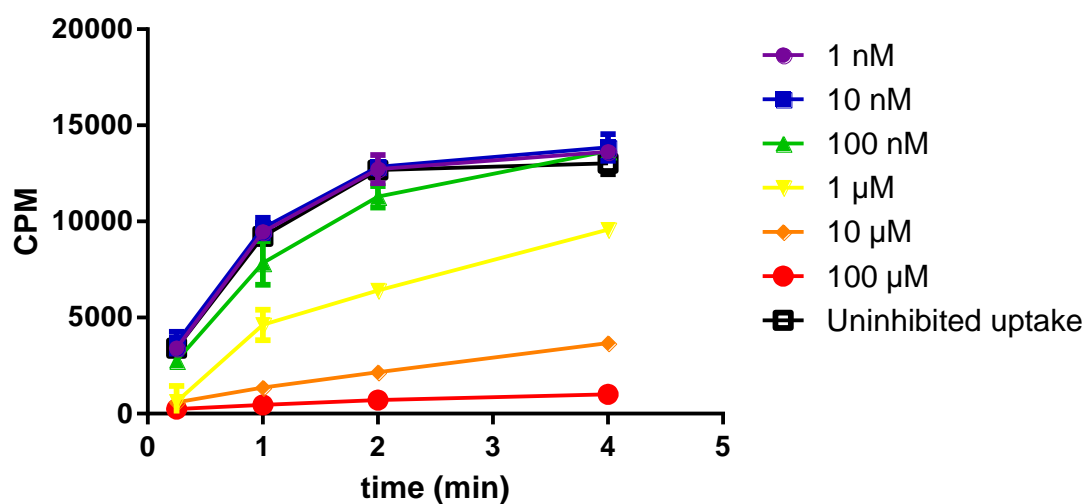


Figure S81: [^{14}C]Aspartate uptake assay, with uninhibited uptake and increasing concentrations of TFB-TBOA. All experiments were done in duplicate.

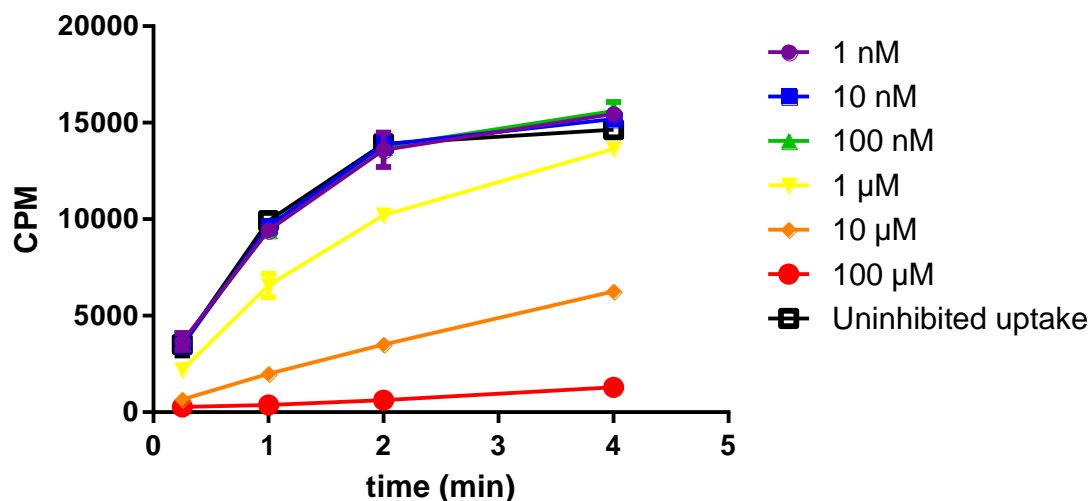


Figure S82: $[^{14}\text{C}]$ Aspartate uptake assay, with uninhibited uptake and increasing concentrations of *p*-MeO-azo-TBOA *trans*. All experiments were done in duplicate.

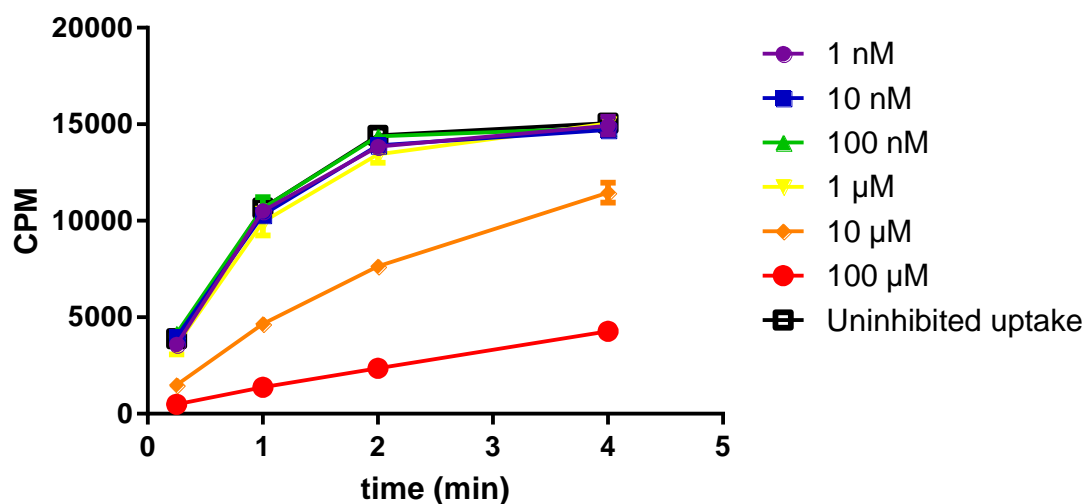


Figure S83: $[^{14}\text{C}]$ Aspartate uptake assay, with uninhibited uptake and increasing concentrations of *p*-MeO-azo-TBOA *cis*. All experiments were done in duplicate.

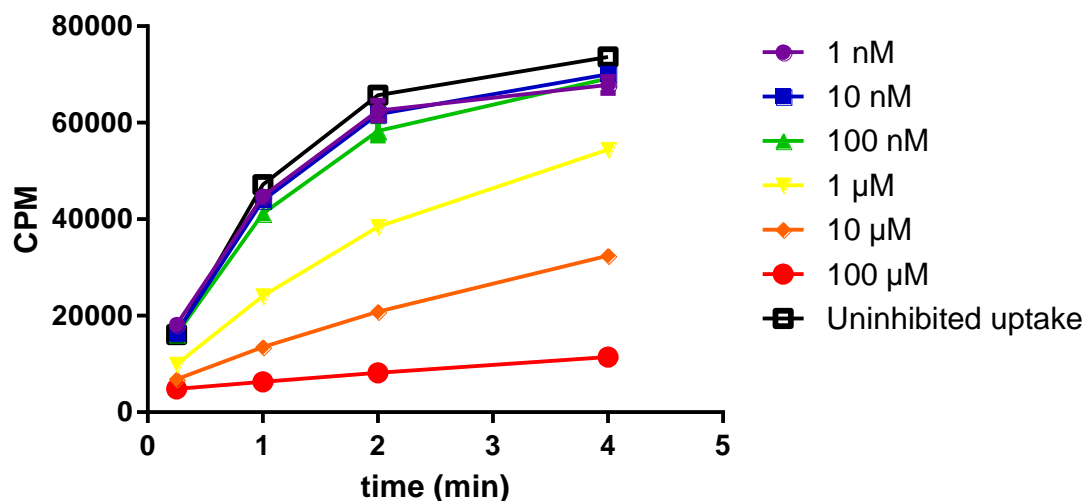


Figure S84: $[^{14}\text{C}]$ Aspartate uptake assay, with uninhibited uptake and increasing concentrations of *p*-HexO-azo-TBOA *trans*. All experiments were done in duplicate.

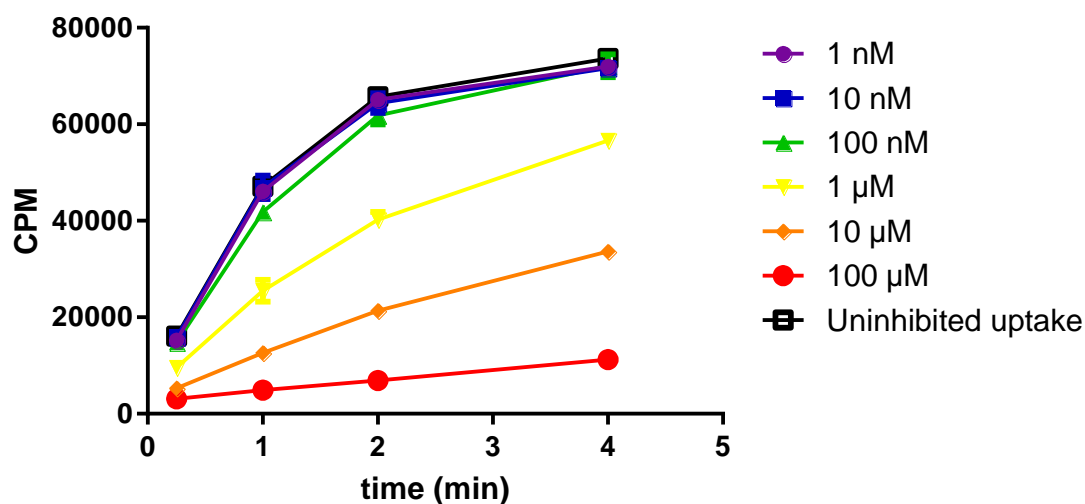


Figure S85: $[^{14}\text{C}]$ Aspartate uptake assay, with uninhibited uptake and increasing concentrations of *p*-HexO-azo-TBOA *cis*. All experiments were done in duplicate.

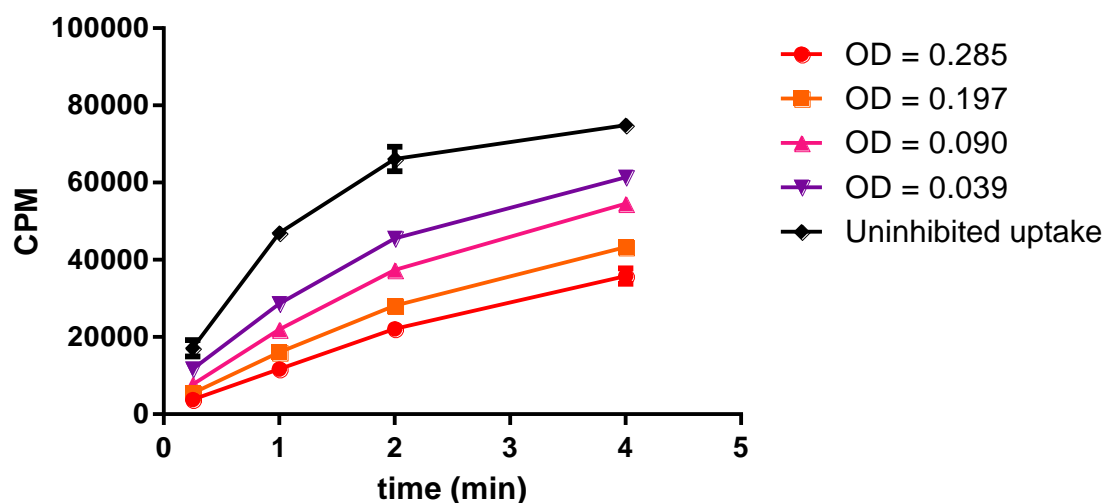


Figure S86: $[^{14}\text{C}]$ Aspartate uptake assay, with uninhibited uptake and several concentrations of $p\text{-MeO-azo-TBOA}$ in different trans-cis ratios. A 0.5 mM stock solution was irradiated and samples were removed at several timepoints. From the 0.5 mM solution, 20 μL was diluted 5 times in DMSO to a total volume of 100 μL and OD340 was recorded in a transparent 96 well plate. The 0.5 mM solution was diluted 50 times with buffer to a final concentration of 10 μM at which the uptake was measured. All experiments were done in duplicate.

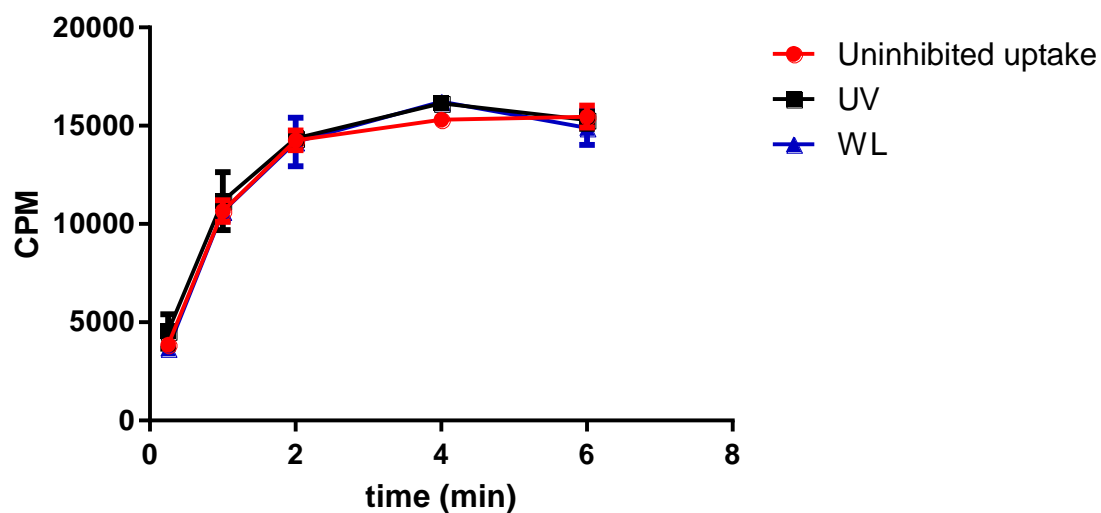


Figure S87: $[^{14}\text{C}]$ Aspartate uptake assay, with uninhibited uptake, continuously irradiated with UV light for 6 minutes and continuously irradiated with white light for 6 minutes. All experiments were done in duplicate.

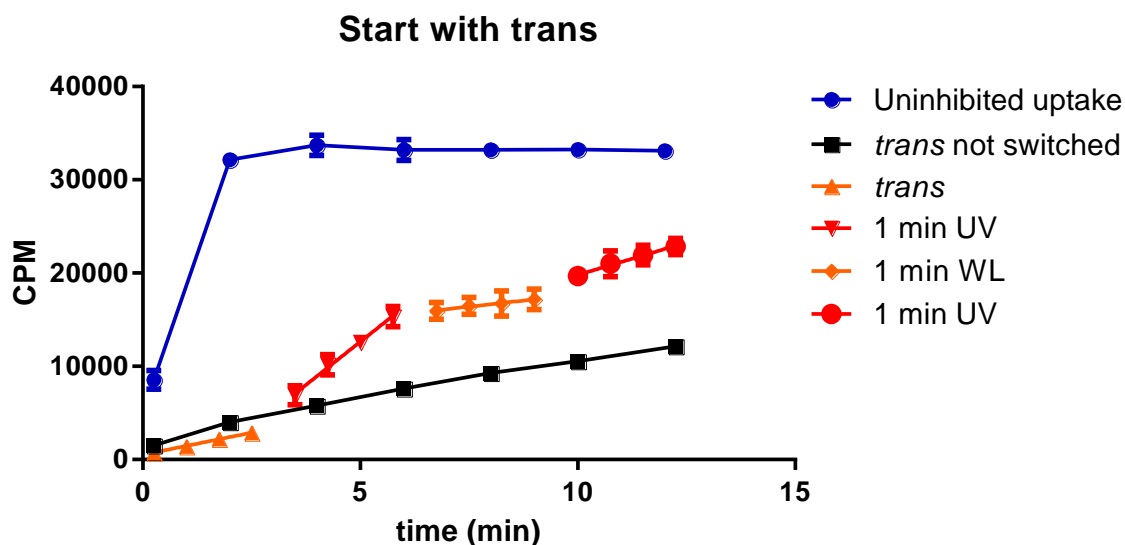


Figure S88: [^{14}C]Aspartate uptake assay, with uninhibited uptake and a control of $50\ \mu\text{M}$ *trans* *p*-MeO-azo-TBOA without further switching. Irradiation reversibly controls the transport, starting with *p*-MeO-azo-TBOA in *trans*, Irradiated for 45 s with UV light after 2.5 minutes, 45 s white light after 5.75 minutes and 45 s UV light after 9 minutes. All experiments were done in duplicate.

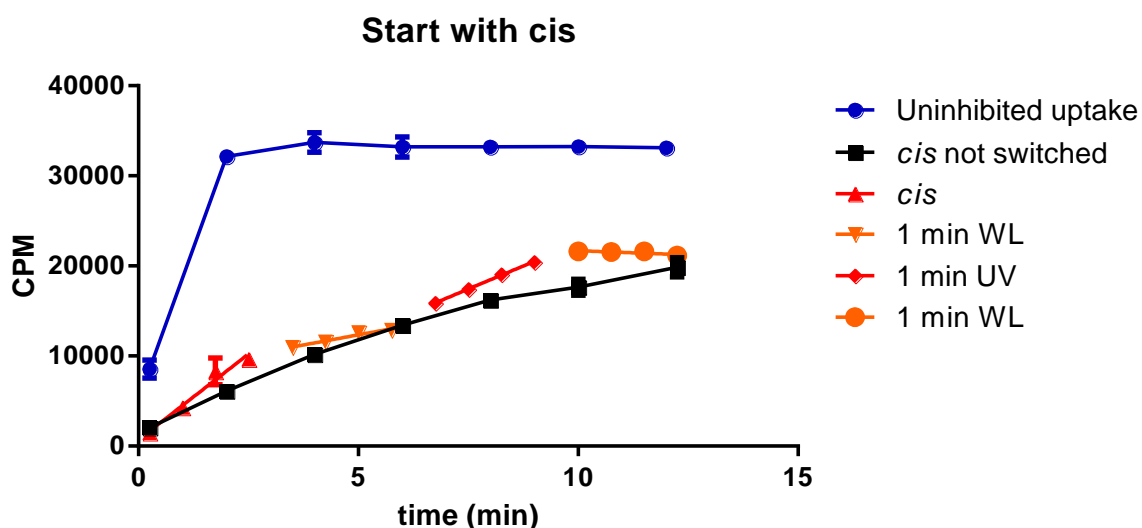


Figure S89: [^{14}C]Aspartate uptake assay, with uninhibited uptake and a control of $50\ \mu\text{M}$ *cis* *p*-MeO-azo-TBOA without further switching. Irradiation reversibly controls the transport, starting with *p*-MeO-azo-TBOA in *cis*, Irradiated for 45 s with white light after 2.5 minutes,

45 s UV light after 5.75 minutes and 45 s white light after 9 minutes. All experiment were done in duplicate.

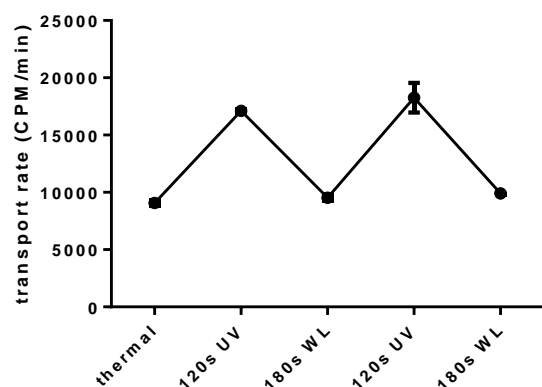


Figure S90: [^{14}C]Aspartate uptake assay of *p*-MeO-azo-TBOA. A 0.5 mM DMSO solution of *p*-MeO-azo-TBOA was irradiated with UV (120 s), white light (180 s), UV light (120 s) and white light (180 s) and after every irradiation step a samples was taken and diluted 50 times in the uptake assay to a concentration of 10 μM , all in duplicate.

Isothermal Titration Calorimetry

For the binding experiments, Glt_{TK} was purified as described above, using a buffer containing 10 mM HEPES pH 8.0, 100 mM KCl and 0.15% DM on the size exclusion column. The solution of purified protein was supplemented with 300 mM NaCl and 250 μ L of solution were loaded into the measuring cell of a small-volume NANO ITC (TA Instruments) at concentrations between 5 μ M and 15 μ M. L-Aspartate, **TFB-TBOA**, ***p*-MeO-azo-TBOA** and ***p*-HexO-azo-TBOA** were dissolved in purification buffer supplemented with 300 mM NaCl and loaded into the titration syringe at concentrations ranging from 100 μ M to 400 μ M. After equilibrating the cell at 25 °C, aliquots of 1 μ L were injected every 1.5 - 2.5 minutes depending on the time needed for the signal to return to the baseline value after each injection. The binding isotherms were analyzed with NanoAnalyze (TA Instruments) using the independent binding-site model. The K_d values obtained in different experiments were averaged and the standard error of the mean was calculated.

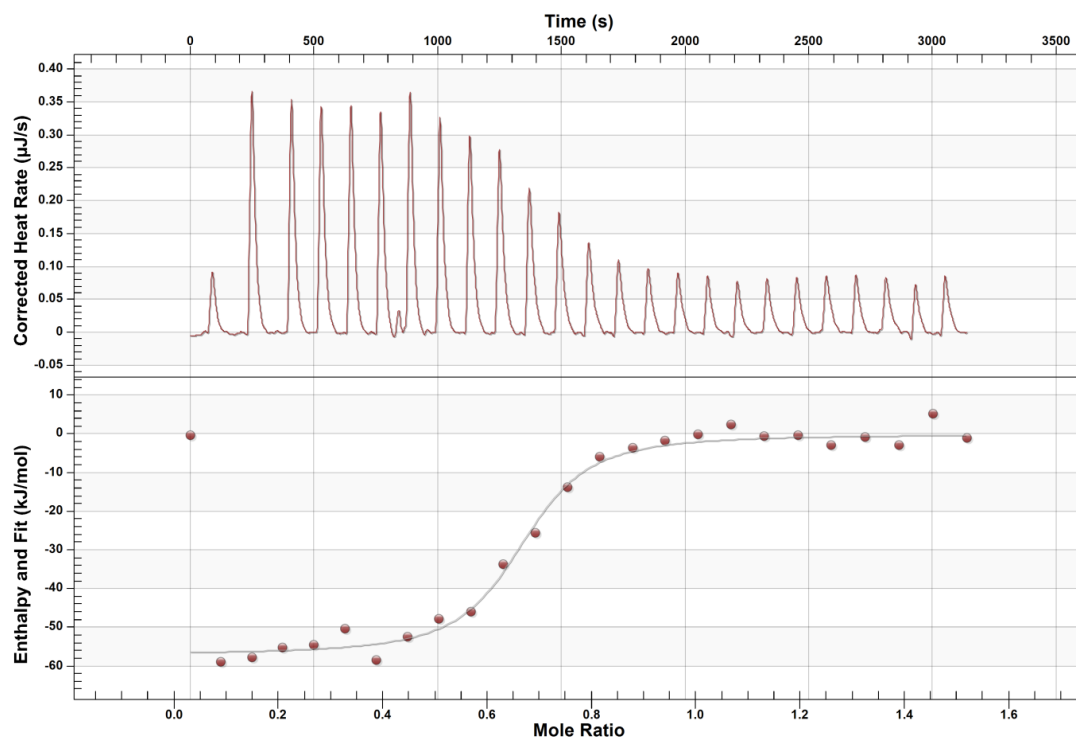


Figure S91: ITC measurement of *L*-Aspartate

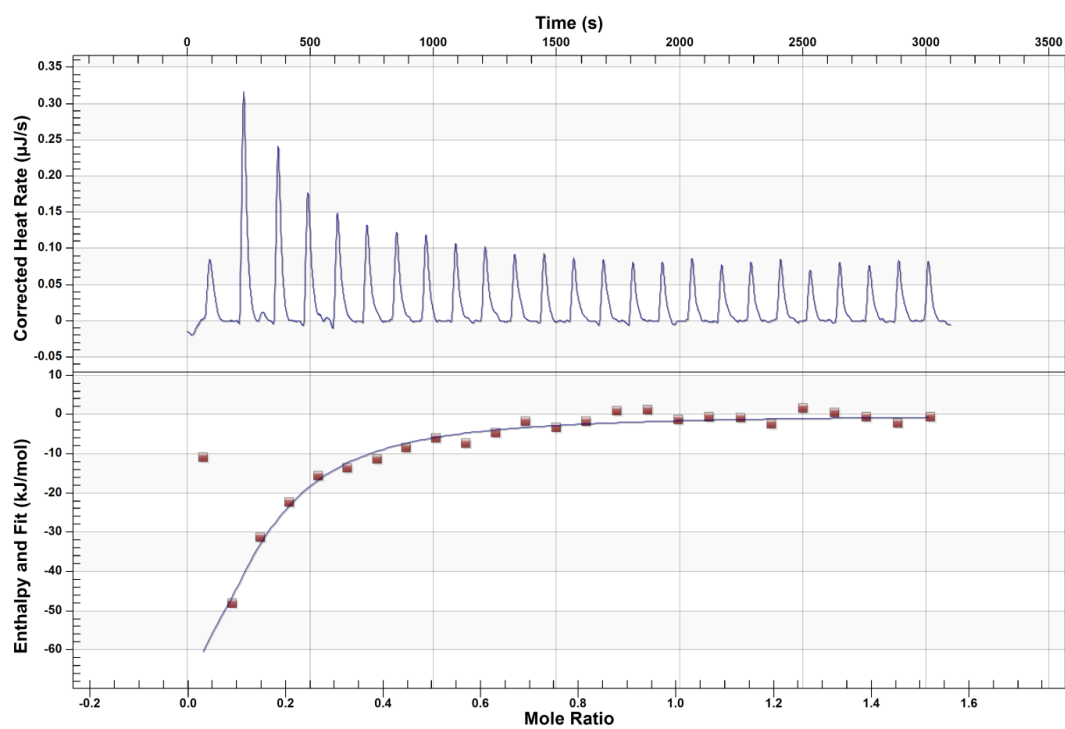


Figure S92: ITC measurement of TFB-TBOA

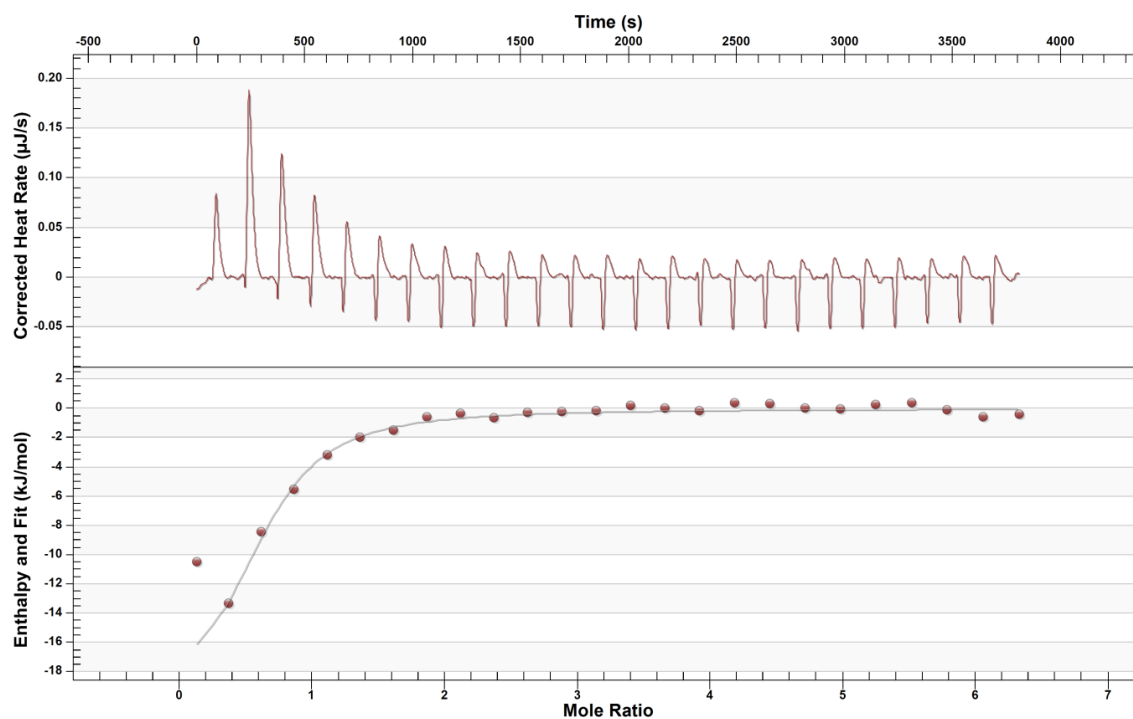


Figure S93: ITC measurement of *trans-p*-MeO-azo-TBOA

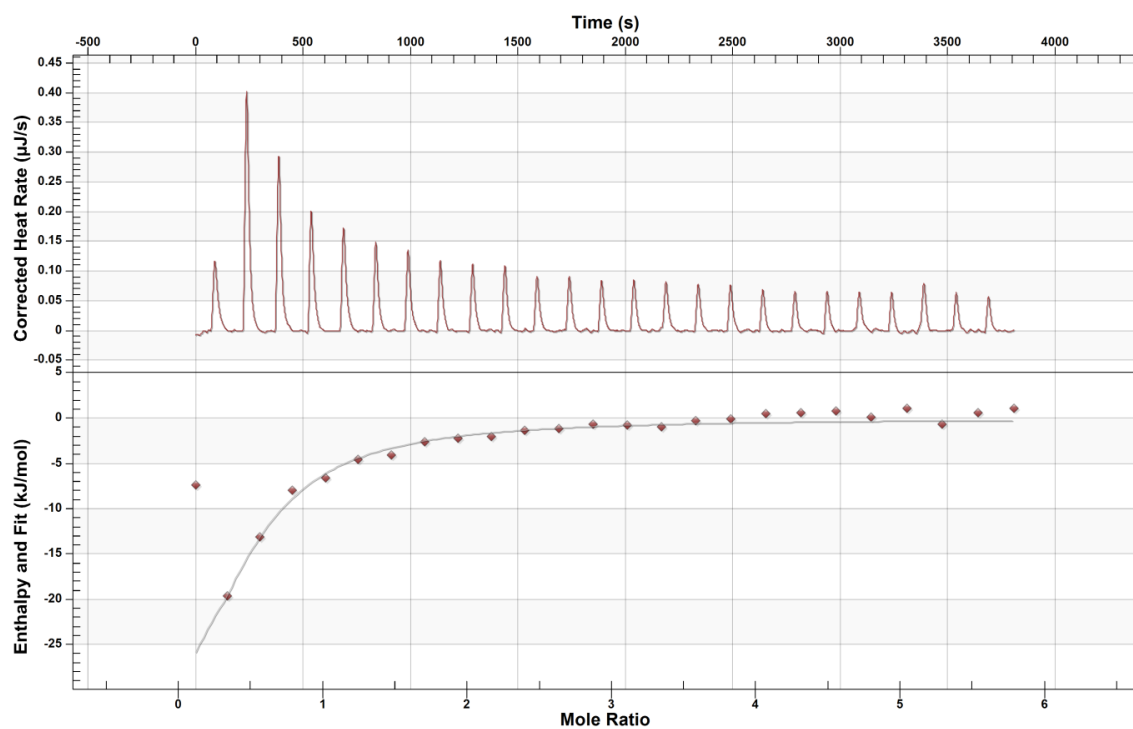


Figure S94: ITC measurement of *p*-MeO-azo-TBOA *cis*

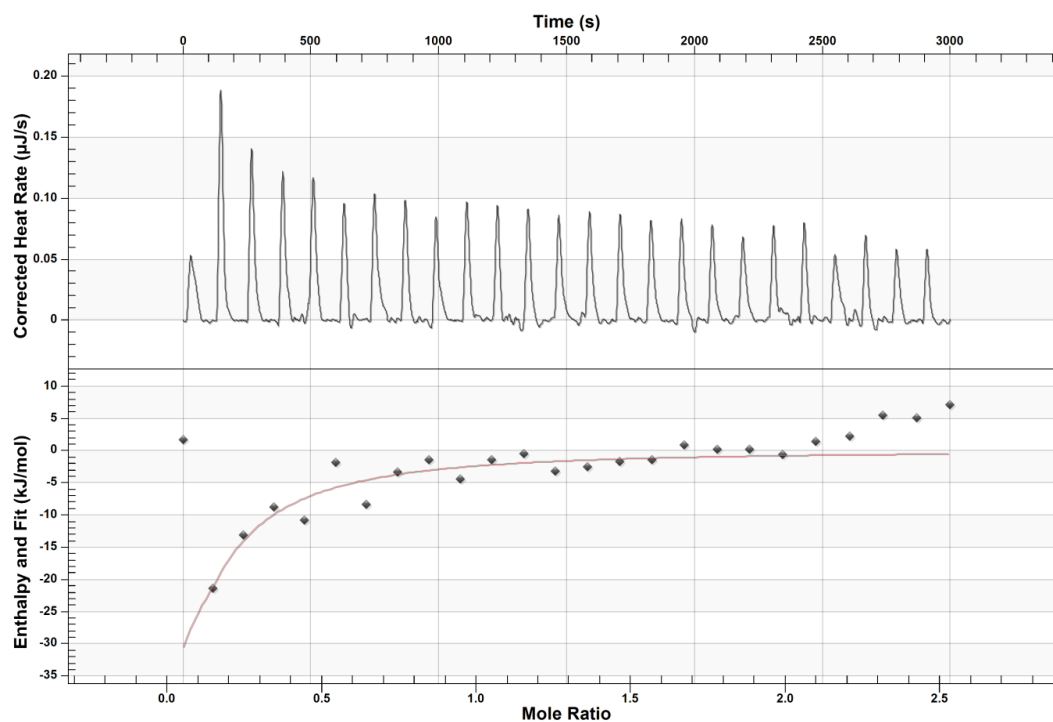


Figure S95: ITC measurement of *trans-p*-HexO-azo-TBOA

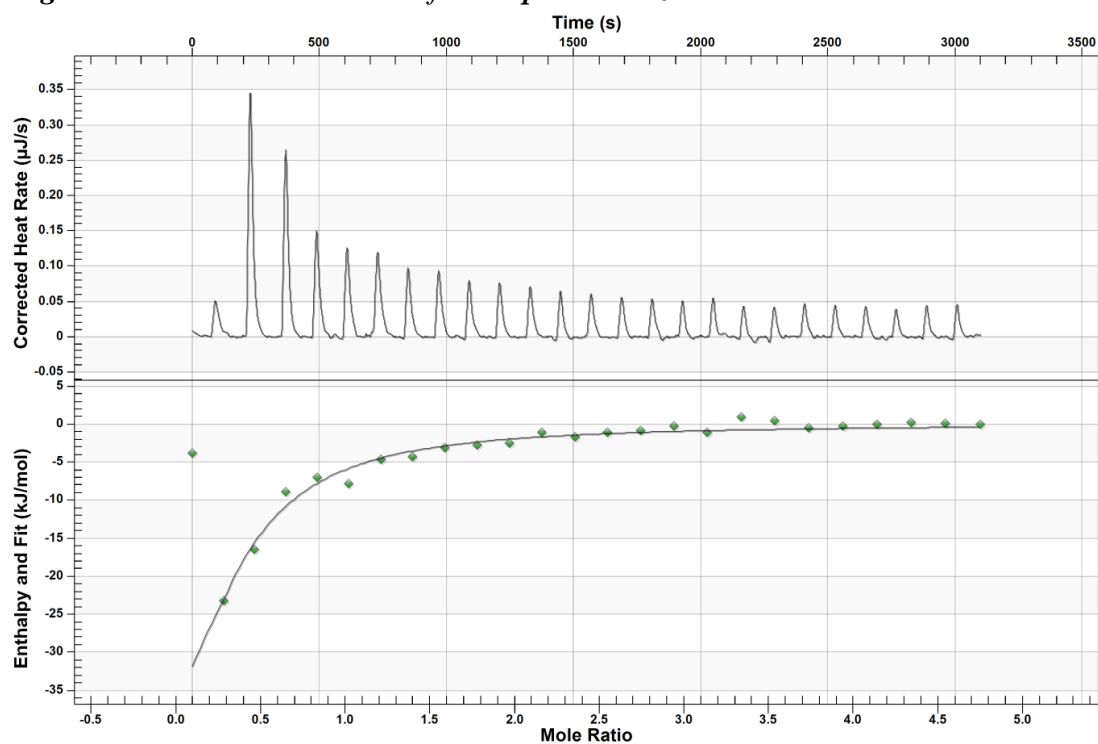


Figure S96: ITC measurement of *cis-p*-HexO-azo-TBOA

4 Statistical analysis

All data processing of the biological evaluation was done using Graphpad Prism 6 software.

Of the linear region of [^{14}C]aspartate uptake rates, slopes were calculated using the linear regression function and subsequently normalized to the uninhibited uptake rate, which was set at 100%. The calculation of IC_{50} values was performed using the non-linear regression function, without any constraints. Statistical significance was determined using a two-sided t-test, with $\alpha = 0.05$.

5 References

1. J. de Villiers, M. de Villiers, E. M. Geertsema, H. Raj, G. J. Poelarends, *Chem. Cat. Chem.* **2015**, 7, 1931.
2. Fu, H., Younes, S.H., Saifuddin, M., Tepper, P.G., Zhang, J., Keller, E., Heeres, A., Szymanski, W., Poelarends, G.J., *Org. Biomol. Chem.* **2017**, 15, 2341.
3. S. Jensen, A. Guskov, S. Rempel, I. Hänelt, D. J. Slotboom, *Nat. Struct. Mol. Biol.* **2013**, 20, 1224.